

**Funktionelle Charakterisierung von Aquaporinen aus *Plasmodium falciparum*,
Toxoplasma gondii und *Trypanosoma brucei***

**Functional characterisation of aquaporins from *Plasmodium falciparum*, *Toxoplasma*
gondii und *Trypanosoma brucei***

DISSERTATION

**der Fakultät für Chemie und Pharmazie
der Eberhard-Karls-Universität Tübingen**

**zur Erlangung des Grades eines Doktors
der Naturwissenschaften**

2006

vorgelegt von

Slavica Pavlovic-Djuranovic

Tag der mündlichen Prüfung:

10. März 2006

Dekan:

Prof. Dr. S. Laufer

1. Berichterstatter:

Priv. Doz. E. Beitz

2. Berichterstatter:

Prof. Dr. J. E. Schultz

The experimental part of this work was done between October 2002 and October 2005 at the Institute for Pharmaceutical Chemistry, the University of Tübingen under the supervision of PD Dr. Eric Beitz and Prof. Dr. J.E. Scultz.

I would like to thank to PD Dr. Eric Beitz Prof. and Dr. J.E. Scultz for giving me the possibility to work on this interesting theme and for constructive discussions which resulted in my PhD thesis.

I would like to thank to Prof. Dr. O. Werz and Prof. Dr. L. Heide for taking a part on my finale exam.

Thank you, dear colleagues in the lab, at the Institute for Tropical Medicine and the Prof. Dr. M. Duszenko's working group.

Special thanks to my husband Sergej, for support and constructive discussions during my work, to my family and to my dear friends.

Table of contents

1 Introduction	1
1.1 Aquaporins	1
1.1.1 Discovery of aquaporins	1
1.1.2 Structural organisation of aquaporins	2
1.1.3 Parasite aquaporins	7
1.2 Plasmodium falciparum	8
1.2.1 GAPDH enzyme, possible roles in the cell	11
1.3 Toxoplasma gondii	13
1.4 Trypanosoma brucei	13
2 Materials	15
2.1 Enzymes, kits and chemicals	15
2.2 Equipment and materials	16
2.3 Buffers and solutions	18
2.3.1 Molecular biology	18
2.3.1.1 DNA electrophoresis	18
2.3.1.2 Reaction buffers	18
2.3.1.3 Media for <i>E. coli</i> cultures	19
2.3.1.4 Transformation of <i>E. coli</i>	19
2.3.1.5 DNA precipitation and purification	19
2.3.2 Protein chemistry	19
2.3.2.1 Protein purification	19

2.3.2.2 SDS-Polyacrylamide gel electrophoresis.....	20
2.3.2.3 Western blot.....	21
2.3.2.4 Medium for <i>Xenopus</i> oocytes	21
2.3.3 Media for <i>Plasmodium falciparum</i> cultures.....	21
2.3.3.1 Complete RPMI 1640 medium with glucose.....	22
2.3.3.2 Complete RPMI 1640 medium without glucose.....	22
2.3.3.3 Albumax II (10× concentrate).....	22
2.3.3.4 Solution for parasite synchronization	23
2.3.3.5 Giemsa staining of thin blood films.....	23
2.3.4 Buffers and solutions for enzyme assays.....	23
2.3.4.1 GAPDH enzyme assay.....	23
2.3.4.2 Assay for ammonia determination.....	23
2.4 Primer list	24
3 Methods.....	25
3.1 Molecular biology methods	25
3.1.1 Polymerase chain reaction (PCR)	25
3.1.2 DNA agarose gel electrophoresis	26
3.1.3 Plasmid isolation.....	27
3.1.4 Photometric determination of DNA concentration.....	27
3.1.5 DNA digestion with restriction enzymes.....	27
3.1.6 DNA extraction from agarose gels	28
3.1.7 Generation of DNA blunt ends	28
3.1.8 5'-DNA-phosphorylation.....	28
3.1.9 5'-DNA-dephosphorylation.....	29
3.1.10 Ligation of DNA fragments.....	29
3.1.11 Purification of DNA by precipitation with ethanol.....	29
3.1.12 DNA Sequencing.....	30
3.2 Cloning strategies.....	31

3.2.1 Vectors used	31
3.2.1.1 pBluescriptII SK (-) vector	31
3.2.1.2 pOG1/2 vectors	31
3.2.1.3 myc-pOG2 vectors	32
3.2.1.4 pQE-30 vector	32
3.2.2 Cloning strategy of the PfAQP E₁₂₅S/F₁₉₀Y mutant	33
3.2.3 Cloning of the PfGAPDH open reading frame into the pQE-30 expression vector	34
3.2.4 Cloning strategy of the <i>Toxoplasma gondii</i> aquaporin	37
3.3 Microbiological methods	39
3.3.1 Competent cells	39
3.3.2 Transformation of competent <i>E. coli</i> cells	39
3.4 Protein expression in <i>Xenopus laevis</i> oocytes	40
3.4.1 Oocyte preparation	40
3.4.2 cRNA synthesis	40
3.4.3 Oocyte injection	41
3.4.4 Standard oocyte swelling assay	41
3.5 Protein chemistry methods	42
3.5.1 Protein expression in <i>Xenopus laevis</i> oocytes	42
3.5.2 Membrane protein preparation from <i>Xenopus laevis</i> oocytes	43
3.5.3 <i>Plasmodium falciparum</i> glyceraldehyde-3-phosphate dehydrogenase (PfGAPDH) expression in <i>E. coli</i>	43
3.5.4 Purification of PfGAPDH	44
3.5.5 Determination of protein concentration using the Bradford method	44
3.5.6 Preparation of membrane proteins from <i>Plasmodium falciparum</i> blood culture	45
3.5.7 SDS-polyacrylamide gel electrophoresis (SDS-PAGE)	45
3.5.8 Western blot	46
3.6 Culture of blood stage <i>Plasmodium falciparum</i> and purification of genomic DNA	47
3.6.1 Synchronisation of erythrocytic stage of <i>Plasmodium falciparum</i> parasites	48

3.6.2 Giemsa staining of thin blood films from parasite cultures	48
3.6.3 <i>Plasmodium falciparum</i> culture in medium supplemented with glycerol.....	49
3.7 Monitoring of <i>Plasmodium</i> proliferation by ELISA	49
3.8 GAPDH enzyme assay	50
3.9 Quantification of ammonia in the culture medium.....	50
4 Results.....	51
4.1 Modulation of water and glycerol permeability of the <i>Plasmodium falciparum</i> aquaglyceroporin by introducing a mutation in the pore constriction region	51
4.1.1 Expression and characterisation of PfAQP E ₁₂₅ S/F ₁₉₀ Y.....	52
4.1.2 pH dependency of water permeability in PfAQP.....	54
4.2 Glycerol induction of PfAQP expression in <i>Plasmodium falciparum</i> blood culture.....	55
4.2.1 Ammonia permeability of PfAQP	58
4.2.2 Ammonia production in <i>Plasmodium falciparum</i> parasites	59
4.2.3 Effect of ammonia on growth of <i>Plasmodium falciparum</i> parasites	60
4.3 Dihydroxyacetone and methylglyoxal permeability of PfAQP and AQP3	61
4.4 Influence of dihydroxyacetone and methylglyoxal on parasite growth	63
4.5 Co-treatment of <i>Plasmodia</i> with dihydroxyacetone plus chloroquine and fosmidomycin .	67
4.6 Cloning and characterisation of PfGAPDH from <i>Plasmodim falciparum</i> strain Binh1	69
4.6.1 Expression and purification of PfGAPDH	69
4.6.2 GAPDH inhibition assay with dihydroxyacetone and methylglyoxal	70
4.7 <i>Toxoplasma gondii</i> aquaporin (TgAQP).....	72
4.7.1 Identification of TgAQP.....	72
4.7.2 Expression and functional characterisation of TgAQP transcripts	74
4.7.2.1 Optimisation of cRNA amount and incubation time.....	75
4.7.3 Water and glycerol permeability of TgAQP M1 and TgAQP M39.....	76

4.7.4 Solute permeability of TgAQP	77
4.8 <i>Trypanosoma brucei</i> aquaporins (TbAQPs).....	79
4.8.1 Identification of <i>Trypanosoma brucei</i> aquaporins.....	79
4.8.2 Water and glycerol permeability of TbAQPs.....	81
4.8.3 Solute permeability profile of TbAQPs	82
5 Discussion.....	84
5.1 Importance of the C-loop in water permeability.....	84
5.2 The influence of different pH values on water and glycerol permeability.....	85
5.3 PfAQP as a conductor for dihydroxyactone and methylglyoxal.....	85
5.4 Characterisation of the <i>Toxoplasma gondii</i> aquaglyceroporin	88
5.5 Characterisation of <i>Trypanosoma brucei</i> aquaglyceroporin	89
5.6 Comparison of the constriction regions of parasite aquaporin pores	90
5.7 Possible physiological functions of protozoan aquaporins	92
5.8 Remaining questions.....	95
6 Summary.....	96
7 Zusammenfassung.....	98
8 References.....	100

List of abbreviations

BSA	Bovine serum albumin
dNTPs	Desoxynucleoside triphosphates
DTT	Dithiotreitol
EtOH	Ethanol
HEPES	N-2-hydroxyethyl piperazine-N'-2-ethanesulphonic acid
IPTG	Isopropyl- β -D-thiogalactoside
LB-broth	Luria-Bertani bacterial growth medium
MCS	Multiple cloning site
Ni-NTA	Nickel-nitrilotriacetic acid-agarose
ORF	Open reading frame
PVDF	Polyvinylidene difluoride
TEMED	N, N, N', N'-Tetramethylethylene diamine
X-Gal	5-bromo-4-chloro-3-indolyl- β -D-galactoside

1 Introduction

1.1 Aquaporins

1.1.1 Discovery of aquaporins

The cell, the basic unit of life, is essentially defined by its plasma membrane. The cell plasma membrane is a major barrier for the free movement of solvents. Its main purpose is to divide the intracellular content from the extracellular fluid. During cell evolution, specific channels evolved to transport nutrients, metabolic products etc. in and out of the cell.

The major component of a cell is water. The hydrophobic plasma membrane presents a significant energy barrier for water movement into and out of the cells. Water can diffuse across lipid bilayer membranes, although the activation energy (E_a) required for this process to occur is much greater than for diffusion (10-20 vs. 5 kcal mol⁻¹; Heymann et al., 1999).

However, studies on water flow through mammalian red blood cell membranes demonstrated that it occurs with an E_a of <5 kcal/mol whereas diffusion of water through pure lipid membranes occurs with a higher activation energy (E_a >10 kcal/mol; Engel et al., 2001). Furthermore, the high water permeability of mammalian red blood cells to water is strongly inhibited by mercuric chloride (HgCl₂). In addition, experiments with amphibian skin have shown that some epithelia are extremely “leaky” to water.

All together, these findings led to early speculations that beside simple diffusion water may enter the cell in an assisted manner probably through proteins that conduct water.

About one decade ago, Peter Agre showed that specific water channels (aquaporins) are indeed present in erythrocytes. Originally, this channel protein was named CHIP28. It was the first member of the aquaporin (AQP) family and was subsequently renamed to AQP1 (Preston et al., 1992).

To date the aquaporin family comprises more than 450 members (Zardoya et al., 2005) from all kingdoms of life e.g. from bacteria, protozoa, plants and animals. Thirteen aquaporins have been identified in humans designated as AQP0-12.

The aquaporin family consists of two major subfamilies: water specific channels (orthodox aquaporins) and channels which are permeable for glycerol, water and other small molecules (aquaglyceroporins).

AQP1 is the prototype of the orthodox aquaporins and it is exclusively permeable for water molecules (Sui et al. 2001). The *E. coli* GlpF, a prototypical aquaglyceroporin, has high permeability to glycerol, but low permeability to water (Fu et al., 2000).

1.1.2 Structural organisation of aquaporins

Initial inspection of the primary sequence of aquaporin AQP1 suggested that the protein consists of six α -helical transmembrane domains with an inverted symmetry between the first three and last three domains. The two loops between helix 2-3 and helix 5-6 contain an amino acid triplet Asn-Pro-Ala (NPA motif) which is highly conserved across the members of the aquaporin family (Fig. 1.1. A).

It was thought, that the six bilayer spanning helices surround a water pore with two conserved NPA motifs in the middle (Fig. 1.1. B; Preston et al., 1992; Jung et al., 1994; Borgnia et al., 1999). This topology was named “hour glass” model. This “hour glass” conformation was later confirmed using X-ray crystallography (Sui et al., 2001). The functional unit of aquaporins is a tetramer with an independent water pore in each subunit.

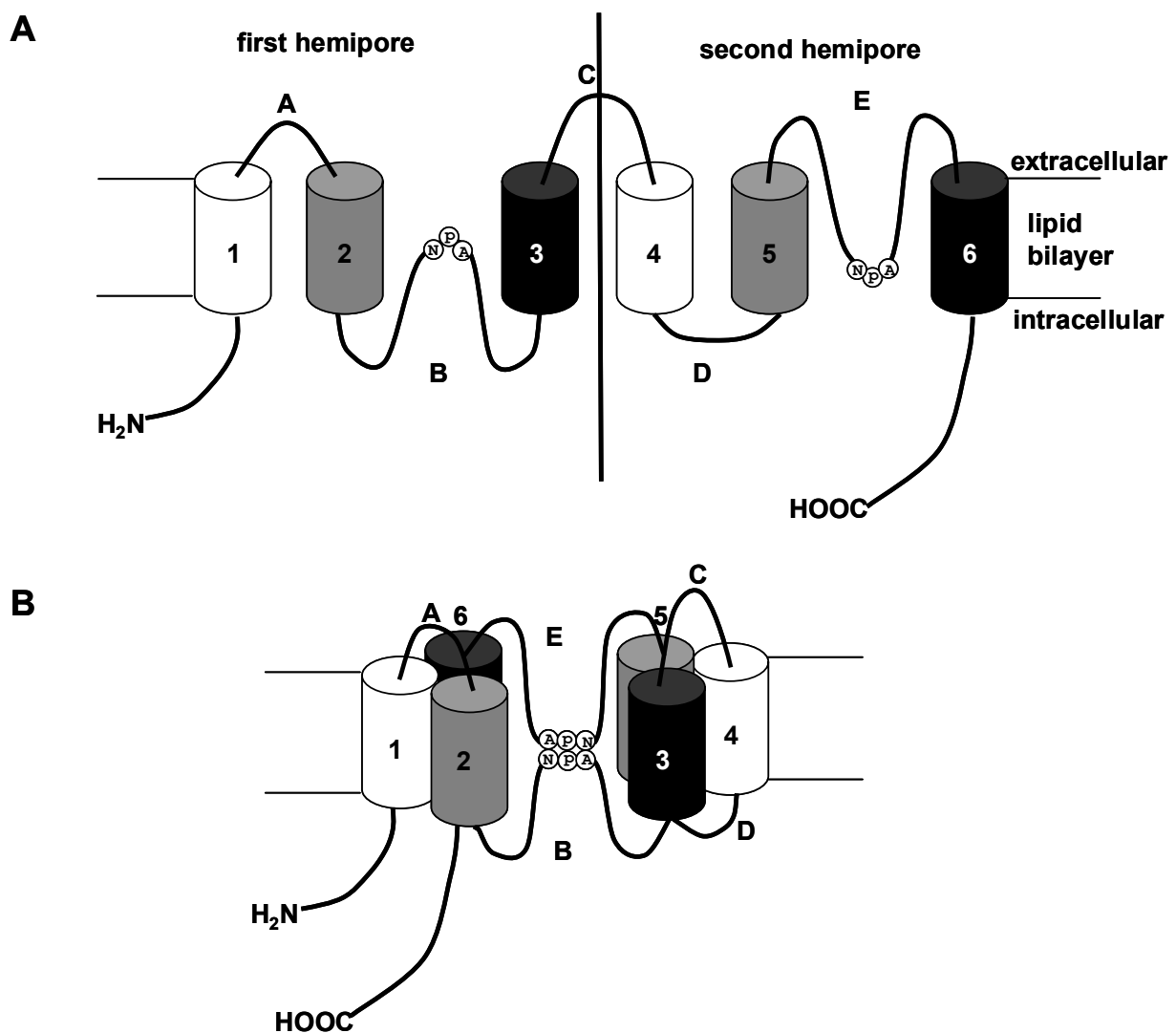


Fig. 1.1. Aquaporin-1 membrane topology and hourglass model. A: Aquaporin-1 contains six bilayer-spanning domains composed of two inversely symmetrical structures (first hemipore and second hemipore) and five loops (A, B, C, D, E) where loops A and C are extracellular, D is intracellular and B and E fold back into the membrane. N and C termini are intracellular. B: The NPA triads in loops B and E form a single aqueous pathway through the membrane.

Primary sequence analysis showed specific differences between aquaglyceroporins and orthodox aquaporins, such as the motive GLYY (Fig. 1.2., shaded in green) in the C-loop and an aspartate residue after the second NPA motif (NPARD) which are typical for aquaglyceroporins. In orthodox aquaporins the second NPA motif is followed by a serine (NPARS) (Fig. 1.2., shaded in yellow; Borgnia et al., 1999).

Another discrimination between aquaporins and aquaglyceroporins is the length of the extracellular C-loop which is about 15 amino acids longer in aquaglyceroporins (Engel et al., 2000; Beitz et al., 2004). Furthermore, the C-loop amino acid triad F[A/S]T is highly conserved in aquaglyceroporins (Beitz et al., 2004; Fig. 1.2. shaded in violet). In PfAQP this triad corresponds to a WET triplet with a highly conserved Thr. A marked difference between the WET and F[A/S]T motifs is the presence of a negatively charged Glu at the second position which might interact with a positively charged Arg in the pore constriction region. When the atomic structures of both, human orthodox aquaporin AQP1 and bacterial aquaglyceroporin GlpF, were reported, they revealed a surprising structural similarity (Beitz et al., 2004).

A few years ago, our group identified a single aquaglyceroporin in *Plasmodium falciparum* parasites (PfAQP; Hansen et al., 2002). The primary sequence suggested that the newly identified protein is an aquaglyceroporin with close a relationship to the *E. coli* GlpF. However, the characteristic NPA motifs are changed to NLA and NPS in the *P. falciparum* aquaporin (Fig. 1.2. shaded in red). Functional characterisation showed that this aquaporin has high water and glycerol permeability (Hansen et al., 2002).

Based on the GlpF structure PfAQP was modelled revealing that the amino acids of the pore constriction are identical to those of GlpF (Fig. 1.3.). Furthermore, the RD after NPS and

GLYY motifs which are characteristic for aquaglyceroporins, are present in PfaQP (Fig. 1.2.). However, the C-loop is shorter in PfaQP (13 aa) than in GlpF which is reminiscent of orthodox aquaporins.

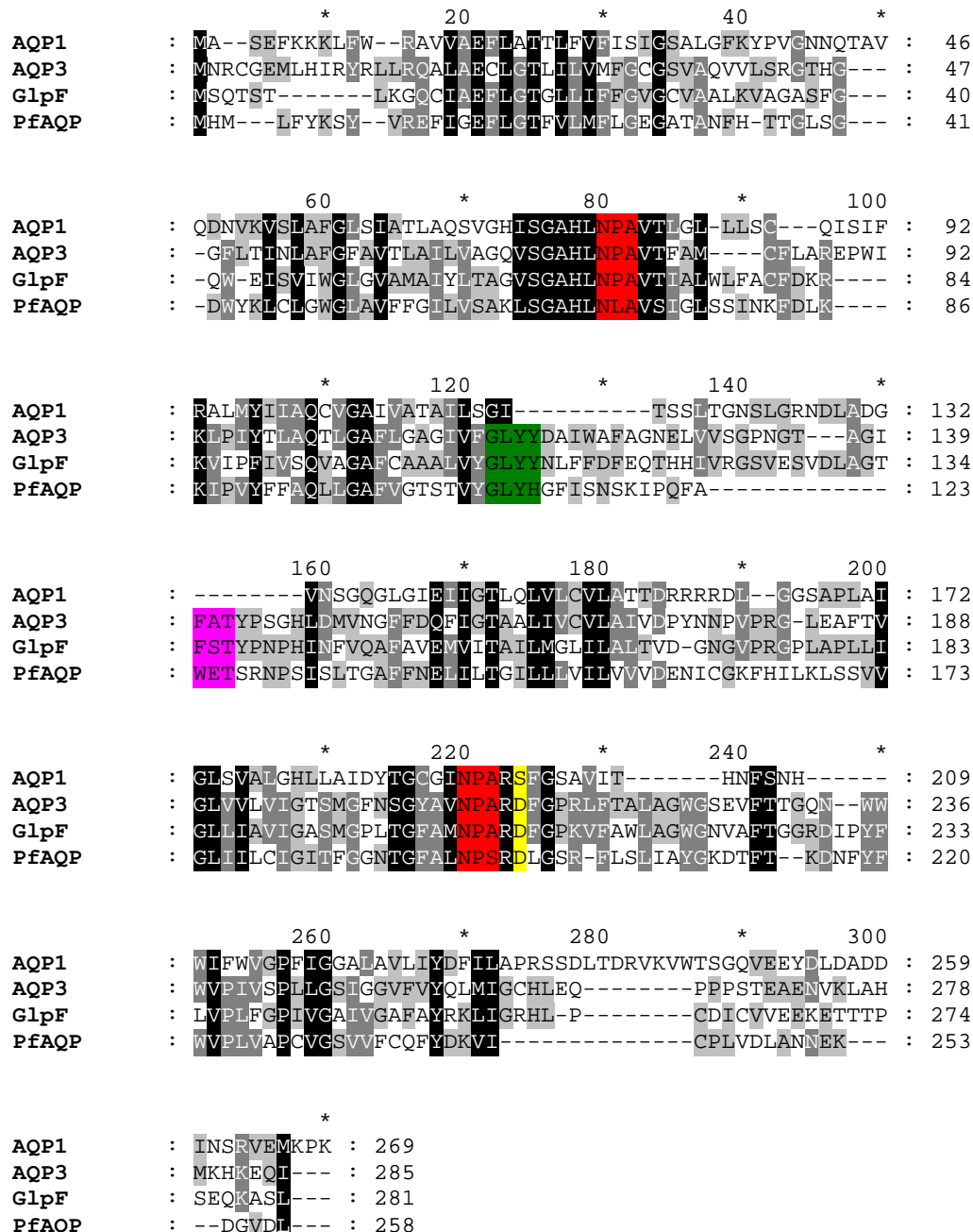


Fig. 1.2. Sequence alignment of human aquaporin-1 (AQP1), human aquaglyceroporin-3 (AQP3), *E. coli* aquaglyceroporin (GlpF) and *P. falciparum* aquaglyceroporin (PfaQP). The NPA motifs are coloured in red, F[A/S]T-WET triad is coloured in pink, GLYY is coloured in green and D or S after the second NPA motif is coloured in yellow. The alignment was generated using ClustalV.

It was shown that the C-loop has an important role in water permeability in PfAQP (Beitz et al., 2004). Introduction of a mutation into the WET triad which is an analogue to FST in the GlpF C-loop, (glutamate to serine, PfAQP E₁₂₅S), resulted in a high reduction of water permeability (Fig. 1.3.). A possible explanation may be that Glu125 interacts with Arg196 and interruption of this interaction influences on water permeability.

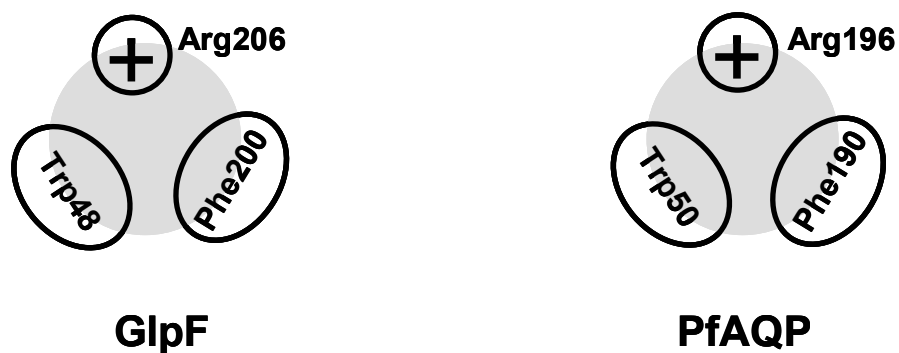


Fig. 1.3. Schematic presentation of the outer pore constriction in *E. coli* GlpF and PfAQP as viewed from the extracellular side.

1.1.3 Parasite aquaporins

Malaria, toxoplasmosis and Chagas' disease are infectious diseases caused by protozoa that affect more than 300-400 million people around the world and represent a major health problem in developing countries (Gelb et al., 2002). Because of the high infection rate and rapid development of drug resistant parasite strains, new strategies for drug development are needed.

Parasites from the phylum *Apicomplexa* and *Euglenozoa* (genus *Kinetoplastida*) are particular human pathogenic (Baldauf et al. 2000; Beitz et al., 2005).

The phylum *Apicomplexa* includes a large number of obligate intracellular parasites, among which are the human pathogens *Plasmodium* (malaria), *Toxoplasma* (AIDS related encephalitis), *Cryptosporidium* and *Cyclospora* (severe enteritis) as well as many parasites of veterinary importance (*Eimeria*, *Theileria*, *Sarcocystis* and *Babesia*).

The parasite life cycles can be relatively simple, involving only a single host (*Cryptosporidium*), whereas the others require interspecies transmission often between an insect and a mammal (Beitz et al., 2005, Roos et al., 2005). Some parasites are specialists, restricted to special species and tissues, e.g. *Plasmodium falciparum*, the others are more general and can infect almost any tissue of warm blooded animals, e.g. *Toxoplasma gondii*.

A characteristic organelle for all apicomplexan parasites is the apicoplast. It is postulated that apicomplexan parasite have acquired this organelle by the ingestion of an eucaryotic plastid containing alga (plastid of red alga and euglenoids; Dziarszinski et al., 1999).

Genome analysis showed that *P. falciparum* expresses only one aquaporin whereas *Kinetoplastida* parasites (*Trypanosoma cruzi*, *Trypanosoma brucei* and *Leishmania major*)

express from 3 to 5 aquaporins. Interestingly in the *Cryptosporidium parvum* genome no aquaporin gene was found at all (Beitz et al., 2005).

1.2 *Plasmodium falciparum*

It is estimated that there are around 300 million cases of malaria world-wide and up to 2.7 million deaths from malaria each year. Four species of malaria are infectious for humans: *P. falciparum*, *P. vivax*, *P. malariae* and *P. ovale*. *P. falciparum* is the most lethal species for humans.

Malaria parasites enter their vertebrate host via the bite of an infected *Anopheles* mosquito. Via the blood stream the parasites (sporozoites) first invade liver cells. Within two days, up to 32 new merozoites are released into the blood stream, where they are about to invade the red blood cells of their host.

The different stages of the asexual intra-erythrocytic phase of the parasite life cycle are schematically represented in Fig. 1.3. First, the malaria parasite invades an erythrocyte and during this process the parasite is being enclosed with a so-called parasitophorus vacuole membrane (PVM) (Fig. 1.3. a). Approximately, during the initial 15 hours after invasion (the so-called “ring” stage) the parasite presumably lies dormant (Fig. 1.3. b). There is a progressive increase in metabolic activity 15 h after invasion when parasites enter the trophozoite stage (Fig. 1.3. c).

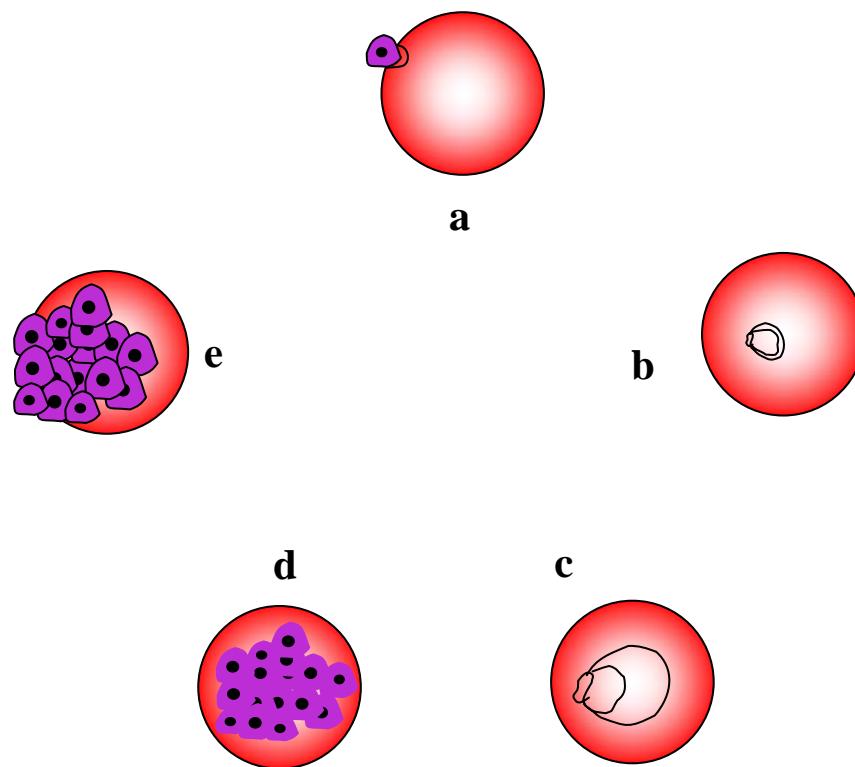


Fig. 1.4. Schematic representation of the different stages of the asexual erythrocyte phase of the life cycle of the malaria parasite *P. falciparum*. a: invasion a merozoite. b: represents "ring" stage. c: trophozoite stage. d: schizont stage. e: the host erythrocyte bursts and releases merozoites and a new cycle begins.

Protein, RNA and DNA synthesis is extensive in this stage of intra-erythrocytic development. Due to the fact that malaria parasites lack a functional citric acid cycle, their energy supply is fully dependent on glycolysis. During parasite growth glucose utilisation and lactate production is increased by up to 100 times the rate of uninfected erythrocytes (Roth et al., 1988).

Through the process of endocytosis, host proteins, especially haemoglobin, are internalised and further digested to small peptides and amino acids in the food vacuole and subsequently used for protein synthesis.

Protein degradation is accompanied by ammonia production. Due to the high level of haemoglobin degradation toxic ammonia has to be released or converted into a less toxic compound like urea. Inspection of the *P. falciparum* genome did not reveal sequences of any enzyme involved in the urea cycle except for arginase. From this information the question arose at which rate ammonia is produced during the erythrocytic stage of parasite development and how it is released.

About 36 h post invasion the parasite occupies approximately one third of the total volume of the host cell. Approximately 40 h after the trophozoite stage the parasite enters the “schizont” stage (Fig. 3 d).

At this stage, the parasite subdivides into 20-32 daughter merozoites. At “schizogony” the host cell ruptures and parasites are released (Fig. 3 e). This happens 48 h after invasion of the host erythrocyte.

During its life cycle the malaria parasite faces drastic osmotic changes during kidney passages. Further, there is the need for massive biosynthesis of glycerolipids during development in the blood stage because of fast growth and division (Hansen et al., 2002). PfAQP may facilitate rapid water movement during kidney passage and thus protect the parasite’s membrane integrity. It may further provide access to the serum glycerol as a precursor for lipid biosynthesis during the parasite development in the intraerythrocytic stage. Channels and transporters play a central role in parasite survival within the host organism. Hence, they are interesting as potential drug targets or may be used as uptake routes of cytotoxic drugs into the parasite cell.

The physiological function of PfAQP is unknown. One aim of this work is to characterise its permeability properties which may give hints on its physiological function.

1.2.1 GAPDH enzyme, possible roles in the cell

Glucose is the sole energy source of malaria parasites. Ten catalytic steps convert glucose to pyruvate to produce 2 mols ATP per mol of glucose. Conversion of glyceraldehyde-3-phosphate to 1,3-bisphosphoglycerate in the presence of NAD^+ and inorganic phosphate is catalyzed by glyceraldehyde-3-phosphate dehydrogenase (GAPDH). The GAPDH enzyme is a homotetramer with a molecular mass of approximately 150 kDa (Fig. 1.5). Each subunit is composed of an N-terminal NAD^+ binding domain and a C-terminal catalytic domain (Cown-Jacob et al., 2003). The NAD^+ binding domain is conserved among various dehydrogenases (Rossmann fold), but the structural changes in the adenosine binding pocket of *Leishmania mexicana* GAPDH can be used as a specific drug target (Bressi et al., 2001; Suresh et al., 2001).

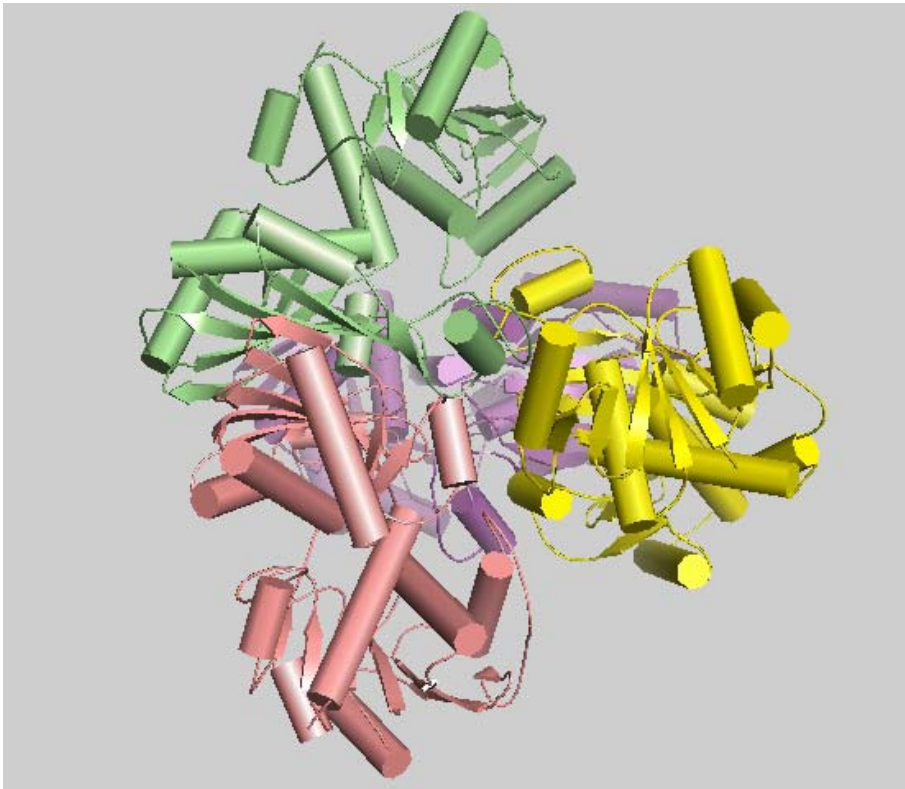


Fig. 1.5. Structure of the GAPDH homotrimer. (This was prepared using PyMOL). GAPDH is a tetramer composed of four identical polypeptide chains which are coloured in pink, violet, green and yellow.

Besides numerous other GAPDH structures from various species, the *P. falciparum* GAPDH structure has recently been resolved (Satchell et al., 2005).

Historically, mammalian GAPDH was considered as an enzyme involved in glycolysis with its main role in energy metabolism. Expression levels of the GAPDH remain constant under most experimental conditions and it has been frequently used as an internal control for studying the regulation of expression of other genes.

Independent from the traditional role in glycolysis, GAPDH is a protein with multiple intracellular localisations and diverse activities (Sirover et al., 1999). These new activities include regulation of the cytoskeleton, membrane fusion and function, export of nuclear RNA, DNA repair and, particularly intriguing, apoptosis. It is not clear whether PfGAPDH has additional functions in parasites besides in glycolysis.

1.3 *Toxoplasma gondii*

Toxoplasmosis is an infectious disease caused by the protozoan *T. gondii* which is, as *Plasmodium*, a member of the protozoan phylum *Apicomplexa*. Infections by *T. gondii* infect humans and animals world wide. Under certain conditions, toxoplasmosis can cause serious pathology; especially in individuals whose immune systems are compromised, e.g., AIDS patients.

While *Plasmodium* parasites multiply exclusively in the erythrocytes and liver cells, *Toxoplasma gondii* invades various cell types. The *T. gondii* genome is sequenced (www.tigr.org).

1.4 *Trypanosoma brucei*

Trypanosomatids like *Apicomplexan* parasites are frequent topics of research for two reasons: their pathogenicity and divergent biology. Among others, tripanomatids include African Trypanosomes (*T. brucei*), American trypanosomes (*T. cruzi*), and *Leishmania* spp. which cause chronic, often fatal diseases in humans.

The life cycle of *T. brucei* parasites includes two different stages: i.e., the long slender form in the blood, lymphatic fluids and in the cerebrospinal fluid of its mammalian host and the procyclic form in the mid gut of the tsetse fly.

In the mammalian bloodstream *T. brucei* has neither a functional Krebs cycle nor oxidative phosphorylation nor does it store any carbohydrates. Consequently, the energy metabolism of

T. brucei depends totally on glycolysis with glycerol as an alternative substrate (Bakker et al., 1997). It was reported that due to the differences between mammalian and trypanosomal glycolysis this pathway is a potential drug target for drug design against African sleeping sickness (Michels et al., 1998). The first seven glycolytic reactions of glycolysis in trypanosomes are placed in a peroxisome like organelle, the so-called glycosome (Parsons et al., 2004). The presence of a glycosome represents a connection to the plant kingdom similar to the apicoplast in *Apicomplexan* parasites. Accordingly, several plant-like proteins are present in the glycosome.

Under aerobic conditions, in the glycosome glucose is converted to 3-phosphoglycerate which is metabolized into pyruvate in the cytosol. The NADH produced in the glycosome is used to reduce dihydroxyacetone phosphate (DHAP) to glycerol-3-phosphate (Gly-3-P). Further, Gly-3-P is reoxydised by molecular oxygen via glycerol-3-phosphate oxidase in the mitochondria and DHAP is returned into the glycosome. Under anaerobic conditions, equimolar amounts of pyruvate and glycerol are produced. Glycerol has to be rapidly exported out of the glycosome otherwise it has a toxic effect on the parasite. Suppression of glycolysis by inhibiting the release of glycerol or pyruvate is a potential therapeutic approach against sleeping sickness (Bakker et al., 1997).

The aim of this work was to characterise protozoan aquaporins (*P. falciparum*, *T. gondii* and *T. brucei*) in order to obtain information about the water and solute permeability profile, the possible pore size, the similarities and differences between these and other aquaporins. From such functional properties physiological functions may be derived.

2 Materials

2.1 Enzymes, kits and chemicals

Ambion, Austin (USA): mMessage mMachine Transcription Kit

Amersham Pharmacia Biotech, Freiburg: ECL Plus Western Blot Detection System, Hyperfilm ECL, Thermosequenase Fluorescent Labelled Primer Cycle Sequencing Kit with 7-deaza-dGTP

AppliChem, Darmstadt: HEPES, Acrylamide 4K-Solution 30 %

Appligene, Heidelberg: Taq DNA polymerase with 10× reaction buffer

Biogenes, Berlin: C-terminal hexadecapeptid (CPLVDLANNEKDGVDL) from PfAQP, rabbit anti-serum against this peptide

BIO-RAD, München: BIO-RAD Protein-Assay Dye Reagent Concentrate

Celllabs, Brookvale (Australia): Malaria Ag CELISA

Dianova, Hamburg: Goat anti-mouse antibodies horseradish peroxidase conjugated, goat anti-rabbit antibodies horseradish peroxidase conjugated

Macherey-Nagel, Düren: Nucleotrap

Merck, Darstadt: Imidazole, glycine, sodium acetate, glucose, sodium hydrogenphosphate, sodium chloride.

Millipore, Molsheim (France): QTUOO EX, QUANRUM EX

MWG-Biotech, Ebersberg: Oligonucleotides

New England Biolabs, Schwalbach/Taunus: Restriction endonuclease, BSA, T4-Polynucleotide kinase, 10× Kinase buffer.

Peqlab, Erlangen: Agarose, peqGOLD Protein Marker

Promega, Madison: Wizard MiniPreps Plasmid Purification Kit

Qiagen, Hilden: Ni²⁺-NTA-Agarose, pQE Expression vector, purified mouse monoclonal RGS-His antibody (BSA free), QIAamp DNA Blood Mini kit

Roche (Boeinger), Mannheim: Restriction endonucleases, Klenow-polymerase, alkaline phosphatase, Rapid DNA Ligation Kit, dNTP's, Complete Protease Inhibitor Cocktail Tablets

Sartorius, Göttingen: Cellulose acetate filter with pore size 0.2 µm

SERVA Electrophoresis, Heilderberg: Coomassie-Brilliant-blue G250, VISKING dialysis Tubing 8/32 and 27/32 with MW 12000-14000

Sigma, Deisenhofen: Glycerol, TRIS, EDTA, Xgal, IPTG, Ponceau S, Tween 20, TEMED, BSA, dihydroxyacetone, methylglyoxal, RPMI 1640 medium, Giemsa solution, sorbitol

Stratagene, Heidelberg: Plasmid pBluescript II SK (-), *E. Coli* XL1- Blue MRF⁻

2.2 Equipment and materials

Amersham Pharmacia Biotech, Freiburg: Electrophoresis power-supply EPS 3500

Bender and Hobein, Ulm: Vortex Genie 2

Biometra, Göttingen: TRIO-Thermoblock thermocycler

BIO-RAD, München: Trans-Blot SD Semi Dry Transfer Cell

BIO-RAD, München: Trans-Blot SD Semi Dry Transfer Cell

Branson, Danbury (USA): Sonifier B-12

Eberhard-Karls-Universität, Tübingen: Chambers for gel electrophoresis

Eppendorf, Hamburg: Table centrifuges 5410 & 5414, cooling centrifuge 5402,
BioPhotometer

Hybaid, London (GB): Mini Oven MK II

Kähler, Hamburg: *Xenopus laevis* females

Knauer, Berlin: Semi-Micro-Osmometer

Kodak, New Haven (USA): Biomax MR X-ray films

Kontron-Hermle, Gosheim: Centrikon h401 & ZK 401, Rotor SS34

Leica, Germany: Leica MZ6 microscope

Macherey-Nagel, Düren: Porablot PDVF-Blotting membrane (0.2 µm pore size)

Millipore, Eschborn: Water purification system MilliQ UF Plus

MWG-Biotech, Ebersberg: LI-COR DNA sequencer model 4000

Sartorius, Göttingen: Balance BP 2100 S, analytic balance handy

Savant, Farmingdale (USA): Vacuum centrifuge speed vac concentrator SVC100H

Schleicher & Schuell, Dassel: Whatmanpaper 3 MM, Protran BA83 Cellulosenitrate 0.2 µm
Blottingmembrane

Shimadzu, Kyoto (Japan): UV-VIS spectrophotometer UV-1202

Stratagene, Austin (USA): UV Stratalinker 2400

WPI, Sarasota (USA): Nanoliter-Injector, binocular microscope

2.3 Buffers and solutions

2.3.1 Molecular biology

2.3.1.1 DNA electrophoresis

TAE-buffer

40 mM TRIS-acetate, pH 8.0
1 mM Na₂EDTA

TBE-buffer

100 mM TRIS
80 mM Boric acid
25 mM Na₂EDTA

BX-sample buffer

0.5 % Bromphenolblue
0.5 % Xylencyanol
5 % Glycerol

2.3.1.2 Reaction buffers

Klenow buffer (10×)

200 mM TRIS-HCl, pH 7.9
60 mM MgCl₂
10 mM DTT
1 mg/ml BSA

Dephosphrylation buffer

500 mM TRIS-HCl, pH 8.5
1 mM EDTA

2.3.1.3 Media for *E. coli* cultures

LB medium

10 g/l Bacto trypton
10 g/l NaCl
5 g/l Yeast extract

LB medium with antibiotics

100 µg/ml ampicillin and/or
50 µg/ml kanamycin

LB-Agar plates

15 g/l agar in LB medium

LB-Agar plates with ampicillin

100 µg ampicillin/ml LB medium
LB medium with agar

LB-Agar plates with kanamycin

50 µg kanamycin/ml LB medium
LB medium with agar

2.3.1.4 Transformation of *E. coli*

CM-buffer

100 mM CaCl₂
100 mM MgCl₂

Solution was sterilised by sterile filtration (pore size 0.2 µm)

2.3.1.5 DNA precipitation and purification

3 M Na-acetate buffer (stored at room temperature)
98 % EtOH (stored at -25°C)
70 % EtOH (stored at -25°C)

2.3.2 Protein chemistry

2.3.2.1 Protein purification

Lysis buffer

50 mM TRIS-HCl, pH 8.0
10 mM DTT

Washing buffer

50 mM TRIS-HCl, pH 8.0
300 mM NaCl
10 mM Imidazole

30 mM Imidazole
10 mM DTT

Elution buffer

50 mM TRIS-HCl, pH 8.0
300 mM NaCl
150 mM Imidazole
10 mM DTT
1 mM NAD⁺

Hypotonic phosphate buffer

7.5 mM Na₂HPO₄ pH7.5
with protease inhibitors cocktail

2.3.2.2 SDS-Polyacrylamide gel electrophoresis

Running gel buffer

1.5 M TRIS-HCl, pH 8.8
0.4% SDS

Stacking gel buffer

0.5 M TRIS-HCl, pH=6.8
0.4% SDS

Electrophoresis buffer

25 mM TRIS-HCl, pH 8.3
192 mM glycine
0.1% SDS

Protein sample buffer (4×)

130 mM TRIS-HCl, pH 6.8
10% SDS
10% β-mercaptoethanol
20% glycerol
0.06% bromphenolblue
2% LiDS

Coomassie staining solution

0.2% Coomassie Brilliant-Blue G 250
10% acetic acid
50% methanol

Destaining solution

10 % acetic acid
30 % EtOH

2.3.2.3 Western blot

Towbin buffer

25 mM	TRIS-HCl, pH 7.5
192 mM	Glycin
29 %	Methanol
0.0375 %	SDS

TBS-buffer

50 mM	TRIS-HCl
150 mM	NaCl

M-TBS

5%	milk powder in TBS buffer
----	---------------------------

TBS-T

0.1 %	Tween 20 in TBS
-------	-----------------

2.3.2.4 Medium for *Xenopus* oocytes

ND96

96 mM	NaCl
2 mM	KCl
1.8 mM	CaCl ₂
1 mM	MgCl ₂
5 mM	HEPES, pH 7.4

OR-2

82.5 mM	NaCl
2 mM	KCl
1 mM	MgCl ₂
5 mM	HEPES, pH = 7.4

These solutions were sterilised by autoclaving for more than 20 min at 121°C and 1 bar.

2.3.3 Media for *Plasmodium falciparum* cultures

All solutions for parasite cultures were made under sterile conditions, and sterilised by autoclaving or sterile filtration (filter pore size 0.2 µm)

2.3.3.1 Complete RPMI 1640 medium with glucose

RPMI 1640 medium (SIGMA 500 ml)
20 µg/ml gentamicin sulphate
25 mM HEPES
2 mM L-glutamine
10 ml human serum
0.1 µM hypoxanthine
50 ml albumax (Albumax II, Gibco)
store at 4°C

2.3.3.2 Complete RPMI 1640 medium without glucose

RPMI 1640 medium (Gibco 500 ml) without glucose:
20 µg/ml gentamicin sulfate
25 mM HEPES
2 mM L-glutamine
10 ml human serum
0.1 µM hypoxanthine
50 ml albumax II (without glucose)
store at 4°C

2.3.3.3 Albumax II (10× concentrate)

RPMI 1640 medium (with or without glucose)
20 µg/ml gentamicin sulfate
25 mM HEPES
2 mM L-glutamine
10 ml human serum
0.1 µM hypoxanthine
25 g albumax II
pH 7.0-7.4
store at -25°C

2.3.3.4 Solution for parasite synchronization

5% sorbitol

2.3.3.5 Giemsa staining of thin blood films

98% methanol
6.7 mM phosphate buffer pH 7.1
Giemsa stain

2.3.4 Buffers and solutions for enzyme assays

2.3.4.1 GAPDH enzyme assay

50 mM TRIS-HCl buffer, pH 8.0
300 mM NaCl
1 mM NAD⁺
50 mM Na₂HPO₄
10 mM DTT
5 µg/ml GAPDH

2.3.4.2 Assay for ammonia determination

122 mM TEA buffer, pH 8.0
0.56 mM ADP in TEA buffer
6 mM NADPH in TEA buffer
71 mM α-ketoglutarate in TEA buffer
7.4 U/ml enzyme in TEA buffer

2.4 Primer list

primers name	sequence	position	restriction place
PfAQPs	5'-actagatctcaatgcatatgta-3'	-11-12	Bgl II
PfAQPF190Yas	5'ctggatcctaaatctcttgatgggtaagtgc catatcca -3'	564 -602	BamH I
PfGAPDHs	5'- tagcatgcatggcagtaacaaaac ttgg -3'	1-20	Sph I
PfGAPDHEcoRVs	5'-aagatctcgaagtagtgcta ttaacgac-3'	65-86	EcoR V
PfGAPDHas	5'-ggaagcttagtgtagta gtgtac-3'	994-1014	HinD III
Tg1AQPs1	5'-tagaattcgagtgagactgcttctatg-3'	-23-3	EcoR I
Tg1AQPas	5'-ttaagcttccgtgccgccgtca ctctt-3'	1-28	HinD III
Tg1AQPs2	5'-tagaattccgagcatctcatcttcaat-3'	96 -111	EcoR I

3 Methods

3.1 Molecular biology methods

3.1.1 Polymerase chain reaction (PCR)

PCR was used to amplify fragments from plasmid or genomic DNA and for introduction of endonuclease restriction sites or point mutations. The DNA template (1-10 ng) was incubated with DNA polymerase (1-2 U), dNTPs (200 μ M), and two oligonucleotide primers (each 200 nM), whose sequences flank the DNA sequence of interest in a total reaction volume of 50 μ l.

The annealing temperature was calculated as follows:

$$T_m = 60 + 0.41 * \%GC - 600 / n \text{ [for primers } \geq 25 \text{ bp]}$$

%GC represents percent of the GC content of the primer and n is the number of the bases of the primer

$$T_m = 2 * (AT) + 4 * (GC) - 4 \text{ [for primer } \leq 24 \text{ bp]}$$

AT and GC represent the number of A + T and G + C bases, respectively, in the primer sequence.

If the annealing temperature for the two primers of a PCR reaction was different, the lower annealing temperature was used.

The reaction was done in a thermocycler with heatable lids to avoid volume and concentration changes. The temperature program used for the PCR reaction is shown in Table 3.1.

Denaturation		95°C	5 min
20-40 cycles	Denaturation	95°C	50 s
	Annealing	T _m	50 s
	Extension	72°C	50 s
Fill up		72°C	10 min

Table 3.1 Program used for polymerase chain reaction

3.1.2 DNA agarose gel electrophoresis

DNA agarose gel electrophoresis was used to separate and isolate DNA fragments or to analyse the size of DNA fragments.

0.5-1 g of agarose was added to 50 ml of TEA buffer and melted in a microwave oven. DNA samples were mixed with BX buffer (1:10), loaded on the agarose gel (1-2%, TEA buffer) and electrophoresis was performed in TEA buffer at 80-100 V for 1 h at room temperature. The size of the DNA fragments was determined using λ -Marker (EcoR I/HinD III digested λ -phage DNA) and π -Marker (Msp I/Ssp I digested pBluescript II SK(-)-vector). DNA fragment sizes of λ -Marker are 21226, 5184, 4973, 4277, 3530, 2027, 1904, 1584, 1330, 983, 831, 564, 125 bp and π -Marker DNA fragments are: 489, 404, 312, 270, 242, 215, 190, 157, 147, 110, 67, 57, 34, 26 bp. Detection of DNA was done by adding ethidium bromide (10 μ g/100 ml) to

the gel solution. After electrophoresis, DNA was visualised in UV light (302 nm) and photographed.

3.1.3 Plasmid isolation

Plasmid isolation was done from 3-4 ml of bacterial cell (12-16 h at 37°C) using Wizard-Mini preps kits.

3.1.4 Photometric determination of DNA concentration

The absorption of nucleic acid solution was measured at 260 nm. The nucleic acid concentration was calculated using the following equation: $c [\mu\text{g}/\mu\text{l}] = E_{260} * f * (\text{dilution})$, $f = 0.02$ (for oligonucleotides, ss-DNA, RNA), $f = 0.04$ (for ds-DNA, plasmids).

3.1.5 DNA digestion with restriction enzymes

Double stranded DNA molecules were digested with 1-5 U of the restriction enzyme per μg of DNA at the optimal temperature (usually 37°C) in the buffer recommended by the supplier. If digestion was done with two or more enzymes, the most compatible buffer was used. In case that it was not possible to do double digestion, enzymes were used one by one with purification steps in-between. Purification steps were done with the Nucleotrap-Kit.

3.1.6 DNA extraction from agarose gels

DNA bands were cut from the agarose gel with a scalpel. Afterwards DNA was extracted with the Nucleotrap-Kit (Marcherey-Nagel) following the manufacturer's instructions.

3.1.7 Generation of DNA blunt ends

After PCR or restriction digestion, the Klenow fragment of DNA-polymerase I was used to make DNA ends blunt. For one Klenow reaction 7.2 μl DNA (1-2 μg), 0.8 μl Klenow enzyme [1U/ μl], 1 μl 10 \times Klenow buffer and 1 μl dNTPs [1 mM] was used and incubated for 45 min at 37°C. After this reaction DNA was purified using the Nucleotrap-Kit.

3.1.8 5'-DNA-phosphorylation

Treatment of DNA with the Klenow fragment or PCR results in strands without 5'-phosphate groups. For ligation these fragments need to be phosphorylated. One reaction contains 1-2 μg DNA (or all Klenow reaction), 1 mM ATP, 7 U T4-Polynucleotid kinase and 10 \times kinase buffer. The reaction was incubated at 37°C for 45 min.

3.1.9 5'-DNA-dephosphorylation

To avoid recirculation of blunt-ended plasmid DNA after EcoR V digestion, the 5'-phosphates were removed with calf alkaline phosphatase. 1-2 μ g DNA were incubated with 0.2 U alkaline phosphatase in phosphatase buffer at 37°C for 45 min.

3.1.10 Ligation of DNA fragments

DNA fragments were ligated with DNA ligase, using the Rapid DNA Ligation Kit according to the supplier's instructions. The optimal vector/insert ratio was assumed to be 1:3.

3.1.11 Purification of DNA by precipitation with ethanol

To precipitate DNA from solution 1/10 of the total volume 3 M Na-acetate (pH 4.5) and 2 volumes of 98.9% ice-cold ethanol were added and stored at -20°C for 1 h. Afterwards the sample was centrifuged for 15 min at 12000 \times g and 4°C. The supernatant was discarded and the pellet was washed with 750 μ l of 70% ethanol. After centrifugation for 10 min at 12000 \times g and 4°C the supernatant was again discarded and the pellet was dried in a vacuum centrifuge for 5 min.

3.1.12 DNA Sequencing

DNA sequencing was done using the Thermo Sequenase fluorescent labelled primer cycle sequencing kit (Amersham) with 7-deaza-dGTP. The DNA template was cycled together with a 5'-fluorescent sequencing primer. For one sequencing reaction 1 µg plasmid DNA, 2 pmol of primer and 0.7 µl 3% DMSO were used (13 µl total volume). 3 µl of this DNA-primer were added to 2 µl of each G/A/T/C reaction mixture. Finally, one drop of low melting wax was added to each sample. The sequence reaction was done in a PCR block using the following temperature protocol (Table 3.2):

Denaturation		95°C	5 min
30 cycles	Denaturation	95°C	20 s
	Annealing	56°C	20 s
	Extension	70°C	20 s

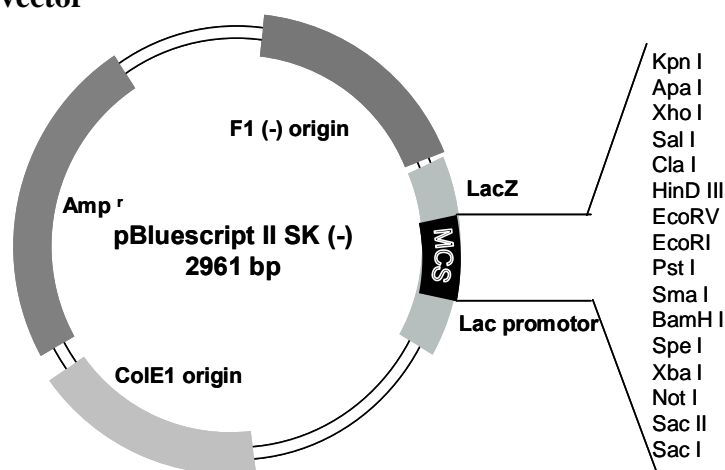
Table 3.2 Temperature program used for DNA sequencing

After adding 5 µl of formamide loading dye provided with the kit the samples were loaded on a 6% polyacrylamide gel. DNA electrophoresis and detection was done with a LI-COR DNA Sequencer model 4000 with TBE as a running buffer. BaselmagelIR V. 4.0 software (MWG-Biotech) was used for analysis.

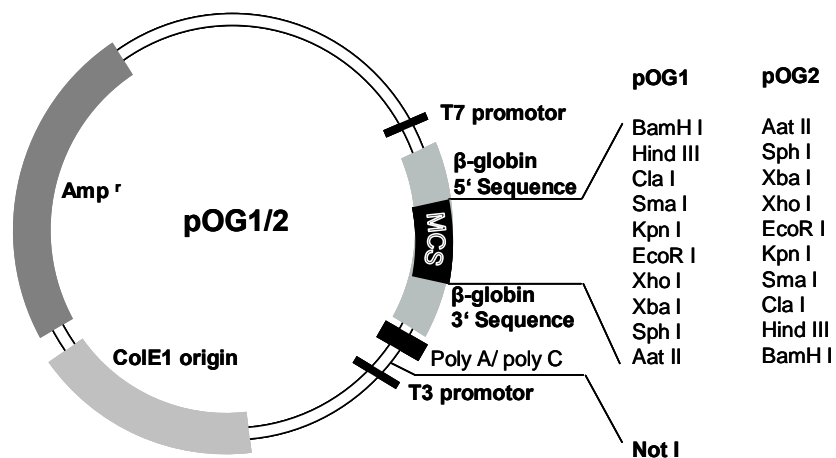
3.2 Cloning strategies

3.2.1 Vectors used

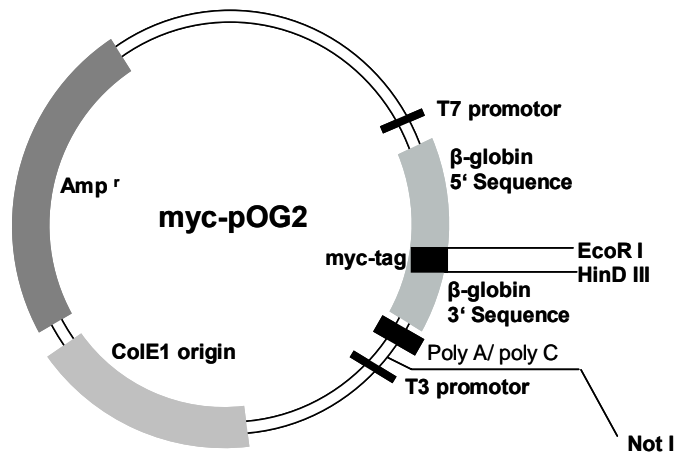
3.2.1.1 pBluescriptII SK (-) vector



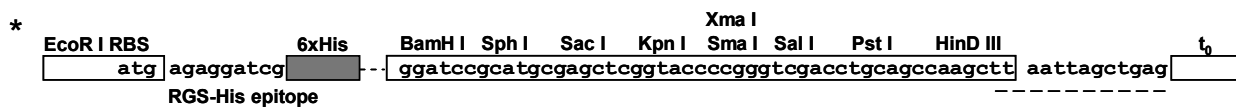
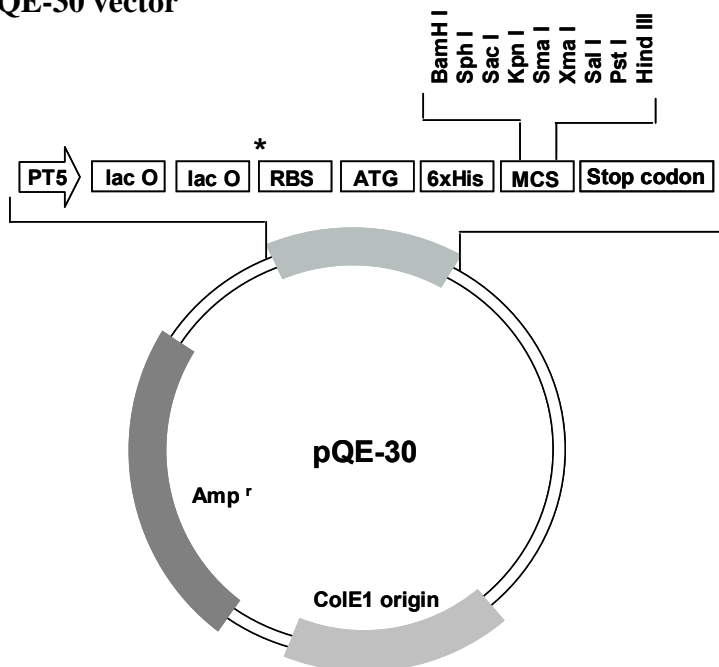
3.2.1.2 pOG1/2 vectors



3.2.1.3 myc-pOG2 vectors



3.2.1.4 pQE-30 vector



3.2.2 Cloning strategy of the PfAQP E₁₂₅S/F₁₉₀Y mutant

The PfAQP E₁₂₅S mutant in the pOG1 vector was used as a template for a PCR reaction, with primer PfAQP F₁₉₀Y as to introduce a F₁₉₀Y mutation. This resulted in a PfAQP E₁₂₅S/F₁₉₀Y mutation. The length of the PCR product was 624 bp. After the purification by agarose gel electrophoresis, the PCR product was purified from the agarose gel, treated with Klenow enzyme and 5' phosphorylated. The purified blunt end PCR product was cloned into pBluescript II (SK-) via the EcoR V site (Fig. 3.1).

Via EcoR I/BamH I restriction sites the PCR product was ligated into the pOG1 vector containing PfAQP mutant (PfAQP M₂₄I). By this procedure, the M₂₄I mutant was replaced by the double mutant PfAQP E₁₂₅S/F₁₉₀Y.

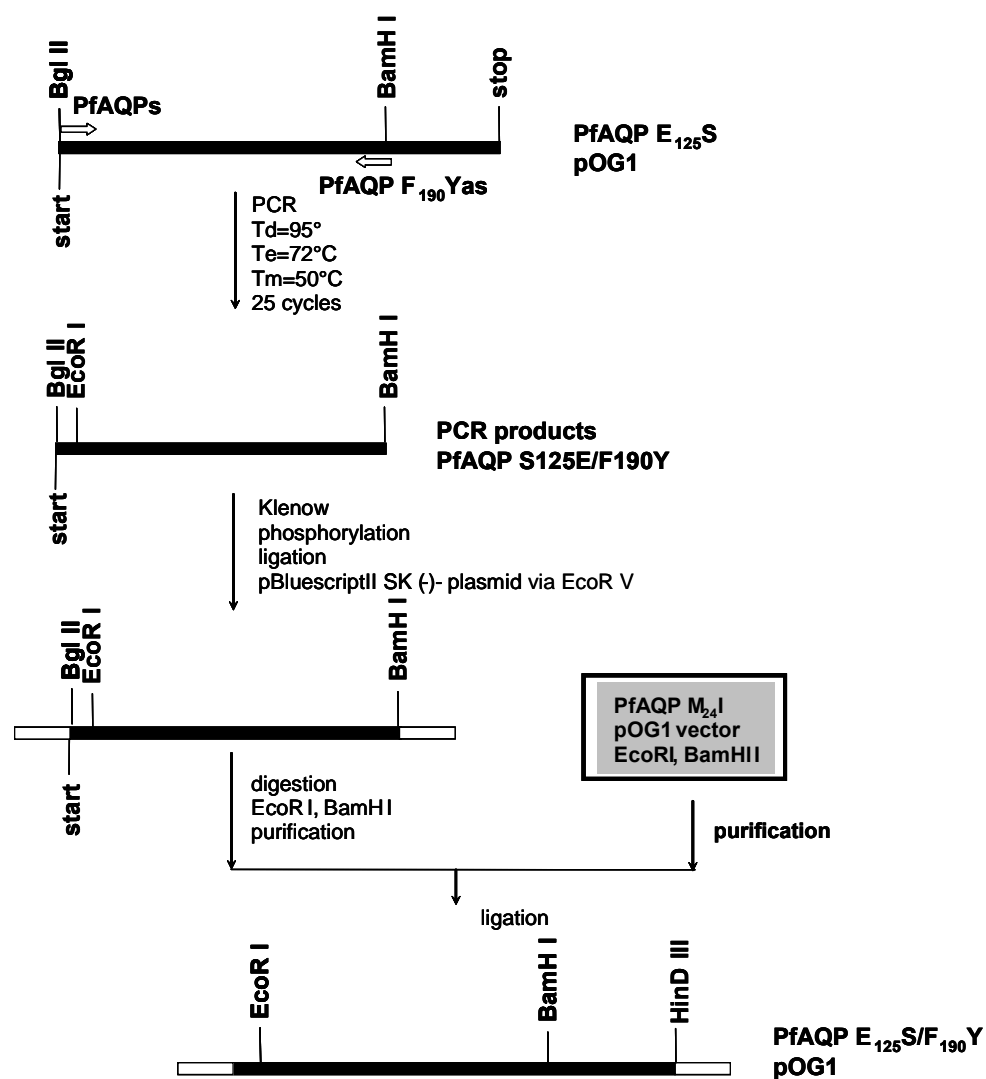


Fig. 3.1. Schematic presentation of cloning strategy of PfaQP E₁₂₅S/F₁₉₀Y mutant

3.2.3 Cloning of the PfGAPDH open reading frame into the pQE-30 expression vector

To amplify the PfGAPDH ORF, *P. falciparum* (strain Binh1) genomic DNA was used (Fig. 3.2). The PfGAPDH ORF contains an intron. To avoid the intron two PCRs were carried out. The first product contained the full length ORF including the intron and the

one the part downstream of the intron. Both PCR products were cloned into pBluescript II SK(-). Afterwards, the PCR product containing the full ORF was cloned into pQE-30 via Sph I/HinD III and was digested afterwards with EcoR V and Hind III restriction enzymes. By this digestion only the first 86 bp PfgAPDH remained in the pQE-30 vector. Finally, the second PCR product (after the intron) was equally digested with EcoR V and Hind III restriction enzymes and ligated into the pQE-30 vector with the first 86 bp of PfgAPDH to complete the full length open reading frame.

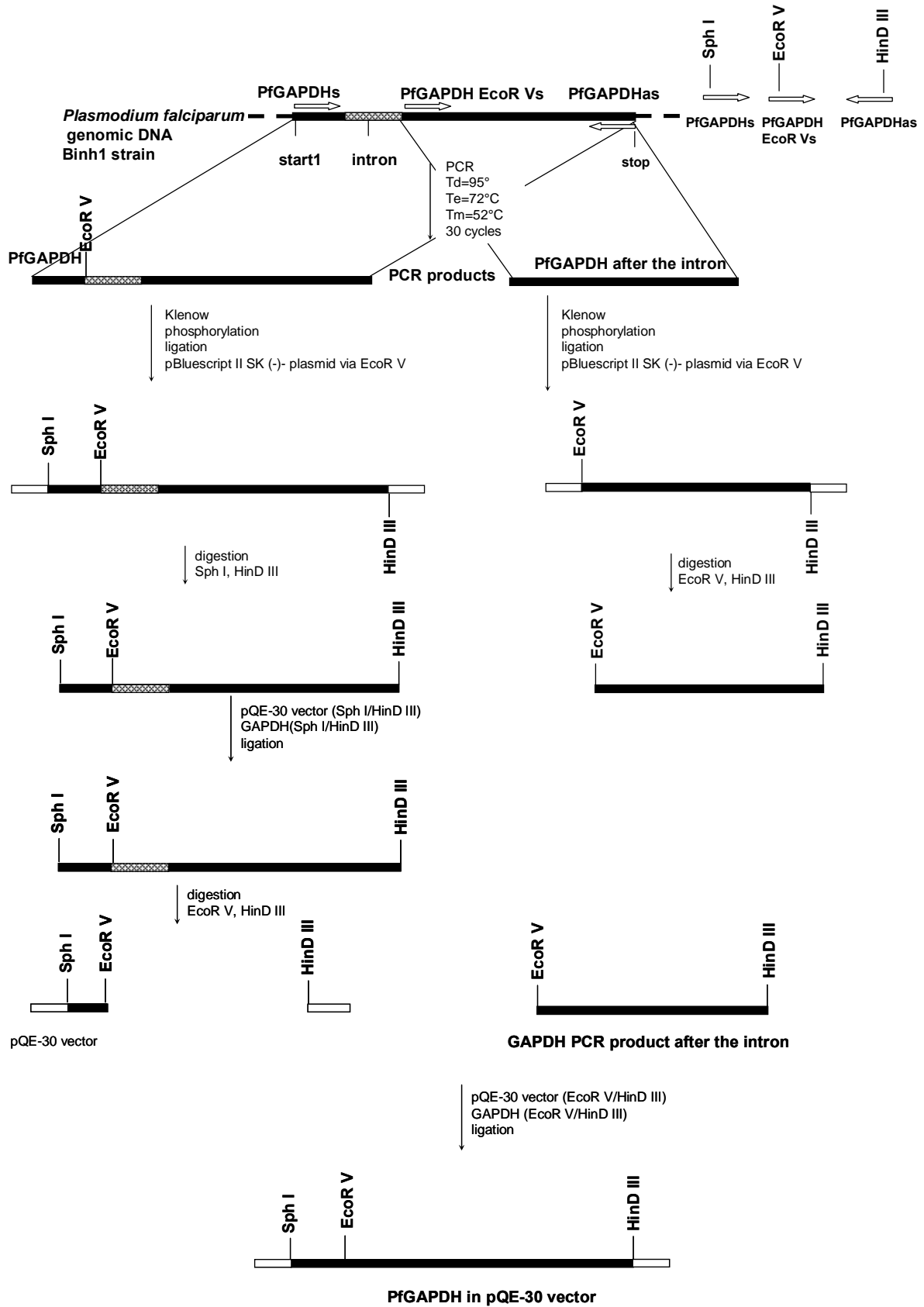


Fig. 3.2. Schematic presentation of cloning strategy of PfGAPDH

3.2.4 Cloning strategy of the *Toxoplasma gondii* aquaporin

The TgAQP open reading frame has two potential start methionines at positions M1 and M39. *T. gondii* genomic DNA was used for TgAQP M1 and TgAQP M39 PCR amplification. Condition for the PCR for both TgAQP M1 and TgAQP M39 were identical (Fig.3.3). The length of the PCR products was 821 bp and 733 bp, respectively. After electrophoresis, the separated fragments were purified, treated with Klenow fragment and finally 5' phosphorylated. The blunt ended fragments were then cloned in pBluescript II SK(-) vector via the EcoR V site. After this first cloning step, cloning into pOG2 vector was done. The pOG2 and myc-pOG2 vectors and TgAQP DNAs were digested with EcoR I/HinD III restriction enzymes and ligated.

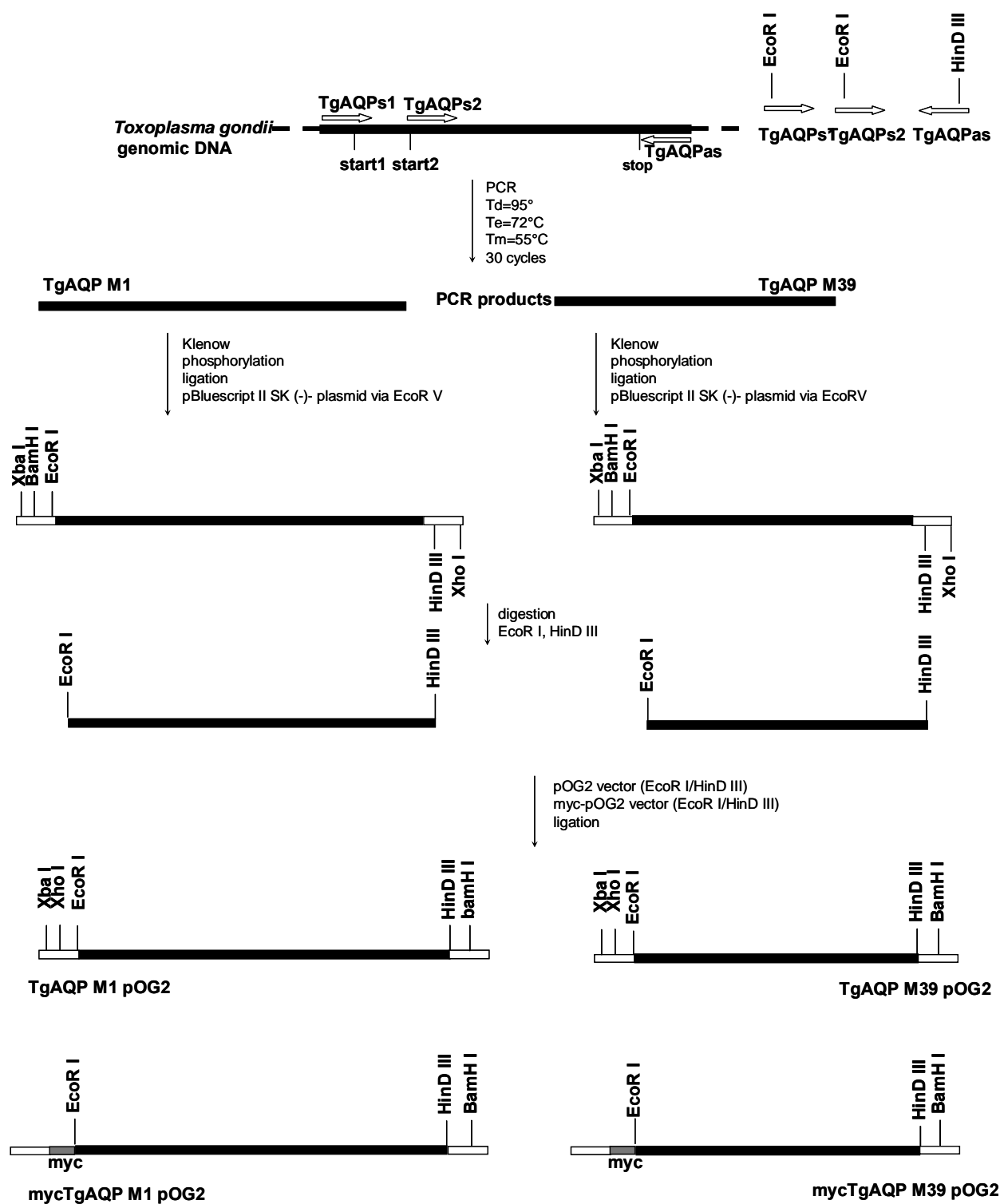


Fig. 3.3. Schematic presentation of cloning strategy of TgAQP M1 and TgAQP M39 open reading frames in pOG2 vector.

3.3 Microbiological methods

3.3.1 Competent cells

5 ml of LB medium were inoculated with a single bacterial colony (XL1-blue MRF^r or BL21 (DE3) [pREP4]) and incubated over night at 37°C at 200 rpm. 1 ml of the culture was transferred into 50 ml fresh LB medium and incubated at 37°C (200 rpm) until an OD₆₀₀ of 0.3-0.4 (approximately 2-3h) was reached. The culture was cooled on ice for 10 min and centrifuged at 2500 × g for 20 min at 4°C. The pellet was re-suspended in 10 ml ice cold CaCl₂ (0.1 M), incubated on ice for 20 min and centrifuged once more (2500 × g, 20 min, 4°C), the pellet was re-suspended in ice cold 0.1 M CaCl₂ supplemented with 20% glycerol and incubated on ice for 2 h. 100 µl aliquots were stored at -80°C.

3.3.2 Transformation of competent *E. coli* cells

The DNA ligation reaction (20 µl) was diluted with 10 µl 10 × CM buffer (100 mM CaCl₂, 100 mM MgCl₂) and 70 µl sterile water. This was added to 100 µl competent cells, mixed gently and then incubated on ice for 25 min. Cells were heat shocked at 42°C for 50 sec. Afterwards, cells were incubated on ice for 10 min and 500 µl of LB medium were added. This mixture was incubated for 45 min at 37°C (200 rpm). 200 µl of the mixture was spread on LB agar plates with appropriate antibiotics. Plates were incubated in an inverted position for 12-16 h at 37°C.

The transformation with the pBluescript II SK (-) vector could be monitored by a blue-white screen by spreading 40 µl of IPTG (0.1 M) and 40 µl of X-Gal (2 %) on the LB agar plate prior to cell plating. Bacteria carrying pBluescript with recombinant DNA formed white colonies, those carrying a plasmid without an insert formed blue colonies.

3.4 Protein expression in *Xenopus laevis* oocytes

3.4.1 Oocyte preparation

A *X. laevis* female frog was anaesthetised in 500 ml Tricain solution (1g/l) and afterwards the oocytes were isolated by making a 1 cm long incision on the left or right ventral side. A part of the ovarian sack was removed and oocytes were placed in ND96 medium. Oocytes were washed in OR-2 medium and incubated in collagenase solution (0.5 mg/ml in OR-2) for 20-30 min (200 rpm). The oocytes were washed in ND96 medium and selected under the microscope (stage V and VI).

3.4.2 cRNA synthesis

The *in vitro* synthesis of cRNA was done with T7 RNA-polymerase using the mMESSEGE m MACHINE-Kit (Ambion). 1-5 µg of Not I linearised pOG1/2 plasmid in a 20

μl reaction mixture was incubated for 2 h at 37°C. After digestion of DNA with 1 μl , 2 U/ μl , DNase I for 15 min at 37°C cRNA was precipitated by addition of 25 μl 7.5 M LiCl for 60 min at -20°C. The precipitate was centrifuged, washed with 70% ethanol, dried in a vacuum centrifuge (5 min) and dissolved in 25 μl RNase free water. The concentration of synthesised RNA was measured photometrically and diluted to a final concentration of 100 ng/ μl .

3.4.3 Oocyte injection

Oocyte injection was performed under the microscope with a nano-liter injector. The oocytes were injected with 50 nl of distilled water or 50 nl of cRNA solution (100 ng/ μl). Injected oocytes were incubated at 15°C for 3-4 days.

3.4.4 Standard oocyte swelling assay

To measure water permeability, oocytes were abruptly placed in 1:3 times diluted ND96 medium. To measure solute permeability 65 mM NaCl in ND96 was exchanged with 130 mM a non-ionic compound (e.g. glycerol, dihydroxyacetone, methylglyoxal). The isosmolality of ND96 medium was checked with a osmometer (Knauer) (± 10 mosm/kg). Oocyte swelling assays were performed under the microscope at room temperature and monitored with a camera connected to a computer, where all calculations were done. From the change in oocyte surface the change in relative volume (V/V_0) was calculated. Using the following formula, water P_f [$\mu\text{m s}^{-1}$] (1) and solute P_s [$\mu\text{m s}^{-1}$] (2) permeability are calculated.

$$P_f = V_0 \cdot d(V/V_0)/dt / [S \cdot V_w \cdot (\text{osm}_{\text{in}} - \text{osm}_{\text{out}})] \quad (1)$$

$V_0 = 9 \cdot 10^{-4} \text{ cm}^3$ (initial oocyte volume), $d(V/V_0)/dt$ (relative volume increase in s^{-1}), $S = 0.045 \text{ cm}^2$ (oocyte surface area), V_w molar water volume ($18 \text{ cm}^3 \text{ mol}^{-1}$) and osmotic gradient ($\text{osm}_{\text{in}} - \text{osm}_{\text{out}}$)

$$P_s = [\text{osm}_{\text{total}} \cdot V_0 \cdot d(V/V_0)/dt] / [S \cdot (\text{sol}_{\text{out}} - \text{sol}_{\text{in}})] \quad (2)$$

$\text{osm}_{\text{total}} = 300 \text{ mOsm}$ (total osmolarity of the system), $V_0 = 9 \cdot 10^{-4} \text{ cm}^3$ (initial oocyte volume), $d(V/V_0)/dt$ (relative volume increase in s^{-1}), $S = 0.045 \text{ cm}^2$ (oocyte surface area), and $(\text{sol}_{\text{out}} - \text{sol}_{\text{in}}) = 130 \text{ mOsm}$ (osmotic solute gradient).

3.5 Protein chemistry methods

3.5.1 Protein expression in *Xenopus laevis* oocytes

P. falciparum aquaporin (PfAQP), *T. gondii* (TgAQP M1, TgAQP M39) aquaporins, *T. brucei* aquaporins (TbAQP1, TbAQP2, TbAQP3), rat AQP3 and rat AQP1 were expressed in *X. laevis* oocytes after injection of 5 ng of cRNA and incubation at 16°C for three days.

3.5.2 Membrane protein preparation from *Xenopus laevis* oocytes

For the preparation of membrane proteins 5 oocytes were lysed in 500 μ l hypotonic phosphate solution and homogenised by pipeting up and down on ice. The homogenate was centrifuged for 5 min at $500 \times g$ at 4°C . Afterwards the supernatant was collected. Further, the supernatant was centrifuged for 30 min on $17000 \times g$ at 4°C , the yolk on the top of the supernatant was soaked away with paper and the rest of supernatant was removed by pipeting. The pellet was resuspended in protein sample buffer and solubilised at 37°C for 1 h and stored at -20°C for later use in Western blots.

3.5.3 *Plasmodium falciparum* glyceraldehyde-3-phosphate dehydrogenase (PfGAPDH) expression in *E. coli*

For expression of PfGAPDH a pre-culture was made with *E. coli* BL21 [rep4] cells containing the plasmid with the PfGAPDH gene. Therefore, 5 ml of LB medium supplemented with 50 $\mu\text{g/ml}$ kanamycin and 100 $\mu\text{g/ml}$ ampicillin were inoculated with *E. coli* BL21 [rep4] cells and incubated over night at 37°C (210 rpm). The overnight culture was inoculated into 200 ml of LB medium supplemented with 50 $\mu\text{g/ml}$ kanamycin and 100 $\mu\text{g/ml}$ ampicillin. Protein expression in *E. coli* BL21 [rep4] cells was induced at an OD_{600} of 0.6 with 1 mM isopropyl- β -D-thiogalactoside (IPTG). After 14 h of incubation at 37°C the cells were harvested at $3000 \times g$ for 10 min. Cell pellets were then stored at -80°C .

3.5.4 Purification of PfGAPDH

The cell pellet from 1 l culture was resuspended in lysis buffer (300 mM NaCl, 50 mM Tris-HCl, pH 8.0) and lysed using a French press. The particulate fraction was removed at 27,000 x g and the soluble, recombinant PfGAPDH protein was bound to 300 µl Ni-NTA agarose (Qiagen) for two hours on ice. After washing with 2 ml 50 mM Tris-HCl buffer pH 8 supplemented with 300 mM NaCl, 10 mM DTT and 1 mM NAD⁺, then with the same buffer (2 ml) supplemented with 10 mM and 30 mM imidazole, respectively, the PfGAPDH protein was eluted in 2 ml (300 mM NaCl, 150 mM imidazole, 10 mM DTT, 1 mM NAD⁺, 50 mM Tris-HCl, pH 8.0) and dialyzed against assay buffer (300 mM NaCl, 1 mM NAD⁺, 50 mM Na₂HPO₄, 10 mM DTT, 50 mM Tris-HCl pH 8.0). Purified PfGAPDH protein was stored at room temperature at a concentration of 3 mg/l.

3.5.5 Determination of protein concentration using the Bradford method

1-10 µg of protein were pipetted to 800 µl distilled water and mixed. 200 µl of Bradford (BioRad) Dye Reagent Concentrate (5×), were added and mixed, and the absorbance was measured at 595 nm. The protein concentration was calculated using a BSA calibration curve.

3.5.6 Preparation of membrane proteins from *Plasmodium falciparum* blood culture

The erythrocytes were collected from 1 ml of blood culture (hematocrit 5%). 50 µl of the erythrocyte pellet were lysed in 4 volumes of phosphate buffer. The mixture was homogenised on ice by gently pipetting up and down. The mixture was centrifuged at 4°C for 30 min at 17000 × g. The supernatant was discarded, the pellet was washed twice with the same buffer and afterwards the pellet was suspended in 100 µl of sample buffer and incubated for 1 h at 37°C.

3.5.7 SDS-polyacrylamide gel electrophoresis (SDS-PAGE)

SDS-PAGE electrophoresis was done using the Hoefer apparatus. In table 3.3 the recipe of polyacrylamide gels are shown:

Stacking gel	4%	Running gel	12.5%
Stacking gel buffer	0.5 ml	Running gel buffer	1.5 ml
Water	1.2 ml	Water	2 ml
AA/Bis (37.5%):(1%)	0.3 ml	AA/Bis 37.5(%) :1(%)	2.5 ml
TEMED	5 µl	TEMED	5 µl
APS 10%	20 µl	APS 10%	40 µl

Table. 3.3. The volumes of ingredients used for SDS-polyacrylamide gel

Protein samples were mixed with sample buffer and heated at 95°C for 5 min (PfgAPDH) or at 37°C for 1h (AQPs) before loading on a 12.5% gel. Electrophoresis was done at a constant current: 20 mA, 200 V for 45-60 min. Gels were stained with Coomassie Blue for 30 min with gentle agitation and afterwards destained or used unstained for electrotransfer for Western blotting.

To estimate protein size peqGold Marker was used Table 3.4:

peqGold Marker	MW (kDa)
Lysozyme	14.4
β -lactoglobulin	18.4
RE Bsp981	25
Lactate dehydrogenase	35
Ovalbumin	45
BSA	66
β -lactoglobulin	116

Table3.4 The list of proteins and their sizes used for SDS-PAGE electrophoresis

3.5.8 Western blot

After SDS-PAGE, Western blot was done using the Semi-Dry-Electrotransfer and a PVDF membrane which was activated in methanol for 5 min. One 3 mm Whatman paper was soaked in Blot buffer, placed on the anode and gently pressed to remove air-bubbles. Then, the activated PVDF membrane was placed on the paper. On top of the PVDF membrane the SDS-PAGE gel was placed. One soaked 3 mm Whatman paper was placed on top. Again,

air-bubbles were removed. At the end, the cathode was placed on the top and transfer was carried out with a current of 2-3 mA/cm² of gel (20 V) for 2-3 h. After the transfer the gel was stained with Coomassie Blue for 30 min. The PVDF membrane was stained with Ponceau S for 5 min. When the proteins were visible the membrane was washed with deionized water and photographed. Afterwards, the membrane was incubated for 1 h in blocking solution (M-TBS buffer). Then, the membrane was incubated for 1 h with the primary antibody diluted in M-TBS buffer. After washing (1 x 15 min, 2 x 5 min) the membrane was incubated with the secondary antibody diluted in M-TBS buffer for 1 h. Washing was repeated. For chemoluminescence a mixture of 2 ml of solution A and 50 µl of solution B of the ECL-Plus Western Blotting Detection Kit was prepared. The mixture was uniformly distributed over the surface of the membrane and incubated for 5 min. Afterwards, a film exposure with Hyperfilm-ECL was taken. Exposure periods varied from 5 sec to 5 min.

3.6 Culture of blood stage *Plasmodium falciparum* and purification of genomic DNA

P. falciparum parasites (strains Binh1 and 3D7) were cultivated at 5% hematocrit (O⁺ bloodtype) and 0.5-5% parasitemia in RPMI 1640 medium supplemented with 25 mM HEPES, 20 µg/ml gentamicin sulphate, 2 mM glutamine, 200 mM hypoxanthine, and 0.5% Albumax II at 37°C in a nitrogen atmosphere (90% N₂, 5% O₂ and 5% CO₂) (Trager et al., 1976).

3.6.1 Synchronisation of erythrocytic stage of *Plasmodium falciparum* parasites

For synchronisation with sorbitol parasites should be in the ring stage (not longer than 10-12 h). Everything was done under sterile conditions.

The parasite culture (10 ml) was centrifuged at $600 \times g$ at room temperature for 5 min. The supernatant was discarded and then 10 ml of 5% sorbitol were added to the red cell pellet. The suspension was mixed gently with a pipette and left for 5 min at room temperature. Afterwards, the cells were collected ($600 \times g$, 5 min), washed twice with complete RPMI 1640 medium. After 6 h the procedure was repeated (Lambros et al., 1979).

3.6.2 Giemsa staining of thin blood films from parasite cultures

The staining of malaria parasites was done by a standard procedure described in “Methods in Malaria Research” (Inger Ljungstöm et al., 2004). Shortly, thin blood films on slides were fixed in methanol for 30 s. After fixation, the slides were dried and stained in 10% Giemsa solution in phosphate buffer (pH 7.1) for 20 min. After staining, the slides were washed and analysed using a microscope at $100\times$ magnification.

3.6.3 *Plasmodium falciparum* culture in medium supplemented with glycerol

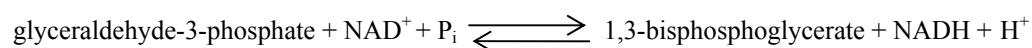
Here, RPMI 1640 medium with and without glucose supplemented with 11 mM glycerol was used for the culture. Starting parasitemia was 0.2%, parasites in the ring stage were synchronized with sorbitol. The total culture volume was 5 ml, hematocrit 5%. Every day a 1 ml sample was taken, the cells were collected (600 × g, 5 min) and frozen at -20°C. Medium was changed every day after taking the samples. Samples cultivated in complete RPMI 1640 medium were used as controls.

3.7 Monitoring of *Plasmodium* proliferation by ELISA

A commercial ELISA based on the quantitation of the *P. falciparum* histidine rich protein 2 (HRP2) was used (Malaria Ag CELISA, Cellabs; Noedl et al., 2002). Briefly, 96-well plates were pre-dosed with 10 µl of dihydroxyacetone, methylglyoxal, glycerol, glucose, chloroquine, fosmidomycin and ammonium chloride dilutions in complete RPMI 1640 medium. Synchronized parasite cultures (80% rings) were diluted to 0.05% of parasitemia at a hematocrit of 1.5%. Then, 90 µl of the diluted cultures were added to each well of the pre-dosed plates. After 72 h of incubation at 37°C in 90 % nitrogen atmosphere the plates were harvested and twice freeze-thawed. The samples were transferred to ELISA plates, and analyzed according to the Cellabs protocol using an ELISA plate reader at 450 nm.

3.8 GAPDH enzyme assay

Glyceraldehyde-3-phosphate dehydrogenase (GAPDH) catalyzes the following reaction:

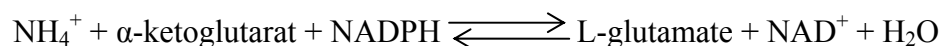


The initial conversion rate of NAD^+ is measured as an increase in absorption at 340 nm. One unit is defined as the amount of enzyme that converts one micromole NAD^+ per minute at 25°C.

The assay was done in Tris-HCl buffer (50 mM, pH 8.0), supplemented with 300 mM NaCl, 50 mM Na_2HPO_4 , 1 mM NAD^+ and recombinantly expressed PfGAPDH (5 $\mu\text{g/ml}$) or commercially available rabbit GAPDH (5 $\mu\text{g/ml}$). The reaction was started at room temperature by the addition of 360 μM DL-glyceraldehyde-3-phosphate.

3.9 Quantification of ammonia in the culture medium

Glutamate dehydrogenase (GLDH) catalyzes the conversion of α -ketoglutarat to L-glutamate in the presence of NH_4^+ and NADPH.



The reaction was followed at 340 nm until the end point was read.

The assay was done in 122 mM TEA buffer pH 8.0 supplemented with 300 μl sample, 0.56 mM ADP, 71 mM α -ketoglutarat, 6 mM NADPH. After 5 min the reaction was started by addition of GLDH to a final concentration of 7.4 U/ml.

From the differences in absorption before and after the reaction the ammonium concentration was calculated based on a calibration curve with known ammonium concentrations.

4 Results

4.1 Modulation of water and glycerol permeability of the *Plasmodium falciparum* aquaglyceroporin by introducing a mutation in the pore constriction region

It has been suggested that the electrostatic environment at the extracellular pore entry of the *P. falciparum* aquaglyceroporin may regulate water permeability (Beitz et al., 2004). An E₁₂₅S mutation introduced in the conserved WET triad in the extracellular C-loop of PfAQP affected water permeability while glycerol permeability was changed only minimally. It was proposed that by removing the charge at position 125 and thus probably disrupting an interaction of Glu125 with Arg196, the polarity of the constriction region would change. The pore layout of PfAQP E₁₂₅S closely resembles that of GlpF, i.e. *E. coli* aquaglyceroporin with high glycerol and low water permeability.

During the course of this work I addressed the question whether the water permeability of PfAQP E₁₂₅S could be improved again by introducing an additional mutation at the pore constriction region. I sought to mimic the AQP3 pore layout which contains a Tyr instead of the Phe present in GlpF (Phe200) and PfAQP (Phe190). AQP3 is an aquaglyceroporin with good glycerol and intermediate water permeability. Mutating Phe190 of PfAQP to tyrosine would introduce an additional hydroxyl group and increase polarity in pore constriction region (Fig. 4.1.).

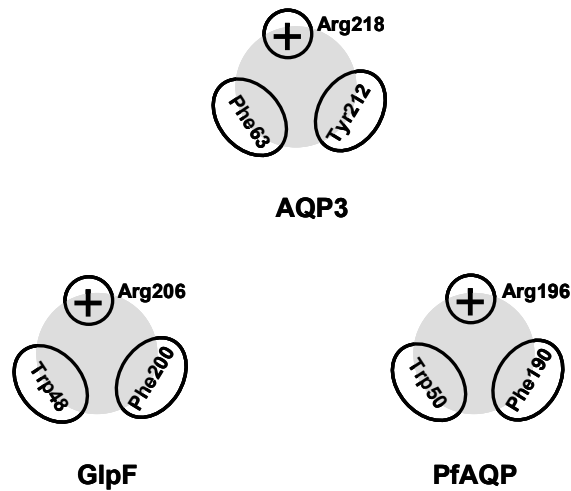


Fig. 4.1. Schematic presentation of the PfAQP, AQP3 and GlpF pore constriction region.

4.1.1 Expression and characterisation of PfAQP E₁₂₅S/F₁₉₀Y

To test this hypothesis I generated the double mutant PfAQP E₁₂₅S/F₁₉₀Y. This variant as well as PfAQP wild type were expressed in oocytes and characterised in standard oocyte swelling assays.

PfAQP E₁₂₅S/F₁₉₀Y cRNA was injected into *X. laevis* oocytes and protein expression was analysed by Western blot using a specific PfAQP antibody (Fig. 4.2.).

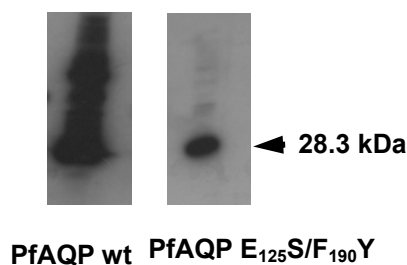


Fig. 4.2. Western blot analysis of PfAQP wt and PfAQP E₁₂₅S/F₁₉₀Y expressed in *X. laevis* oocytes with anti-PfAQP antibody (on the SDS-PAGE gel 1.2 oocyte per line was loaded).

Osmotic swelling assays showed that the PfAQP E₁₂₅S/F₁₉₀Y variant was water permeable. However, compared to wild type PfAQP (316 $\mu\text{m s}^{-1}$) its water permeability (28 $\mu\text{m s}^{-1}$) was 11 times smaller (Fig.4.3. A).

PfAQP E₁₂₅S/F₁₉₀Y (0.55 $\mu\text{m s}^{-1}$) also showed glycerol permeability. Still, glycerol permeability was 3 times smaller than that of PfAQP wt (1.63 $\mu\text{m s}^{-1}$; Fig. 4.3. B).

The expression levels of PfAQP wt and PfAQP E₁₂₅S/F₁₉₀Y were not equal (Fig. 4.2.). To avoid the influence of expression level on oocytes permeability results, the ratios between water and glycerol in wild-type and mutant were calculated. The water/glycerol ratio for PfAQP wt is 194:1, and for the PfAQP E₁₂₅S/F₁₉₀Y it is 51:1 (Fig. 4.3. C). Comparing these data to those of the published PfAQP E₁₂₅S mutation, where water permeability was reduced to background level, with the double mutant water permeability was gained.

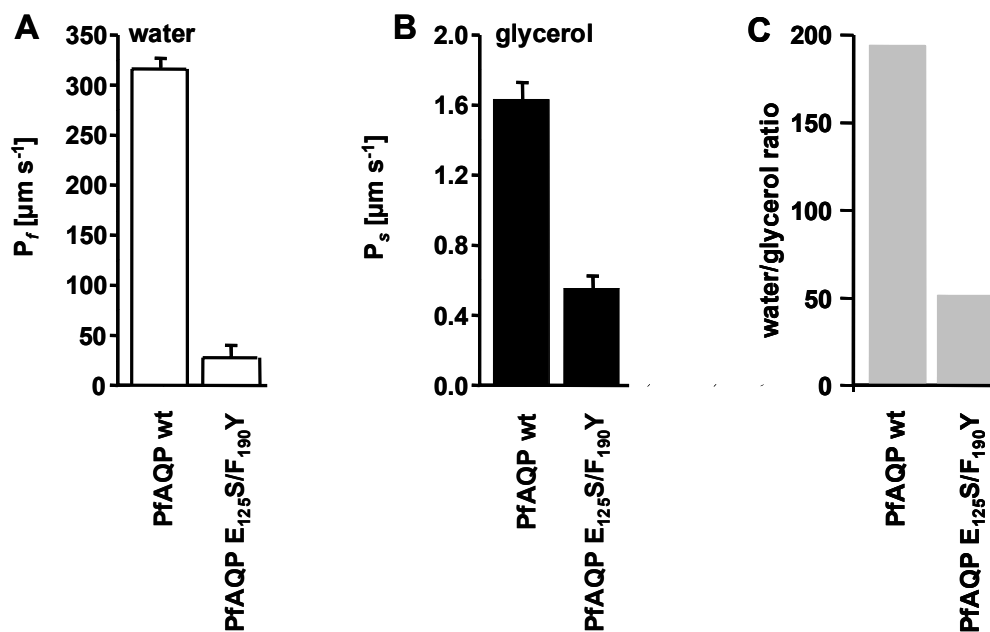


Fig. 4.3. Water and glycerol permeability of PfAQP wt and PfAQP E₁₂₅S/F₁₉₀Y mutant.

A: water permeability P_f [$\mu\text{m s}^{-1}$] of PfAQP wt and PfAQP E₁₂₅S/F₁₉₀Y. B: glycerol permeability P_s [$\mu\text{m s}^{-1}$]. Control values for water (37 $\mu\text{m s}^{-1}$) and glycerol (0 $\mu\text{m s}^{-1}$) were subtracted from the sample values. C: water/glycerol ratio for PfAQP wt and PfAQP E₁₂₅S/F₁₉₀Y. All values are mean \pm S.E.M. (n=5-6).

4.1.2 pH dependency of water permeability in PfAQP

Since a glutamate residue seems to be responsible for the high water permeability of PfAQP I wanted to test for a pH effect on water and glycerol permeability of the PfAQP. Shifts to low pH may change the protonation status of Glu125 and may alter permeability properties. The pKa value of the carboxyl group in glutamic acid is 4.4. As it is known pKa values depend on temperature, ionic strength and microenvironment. Amino acid pKa values in proteins might be different than in solution because of the influence of other amino acids and the environment.

To test water permeability a pH-range of pH 3-7 was used. For glycerol permeability I used a broader range of pH values from pH 3 to pH 9. The basic condition at pH 9 can lead to amino acid deprotonation and may influence the possible interaction between Glu125 and Arg196. Swelling assays at the different pH values were performed with oocytes expressing PfAQP. The data show that water permeability P_f (Fig. 4.4. A) was not dependent on the pH in the range tested. Glycerol permeability was not significantly changed at different pH values, too ($2p > 0.05$; Fig. 4.4. B).

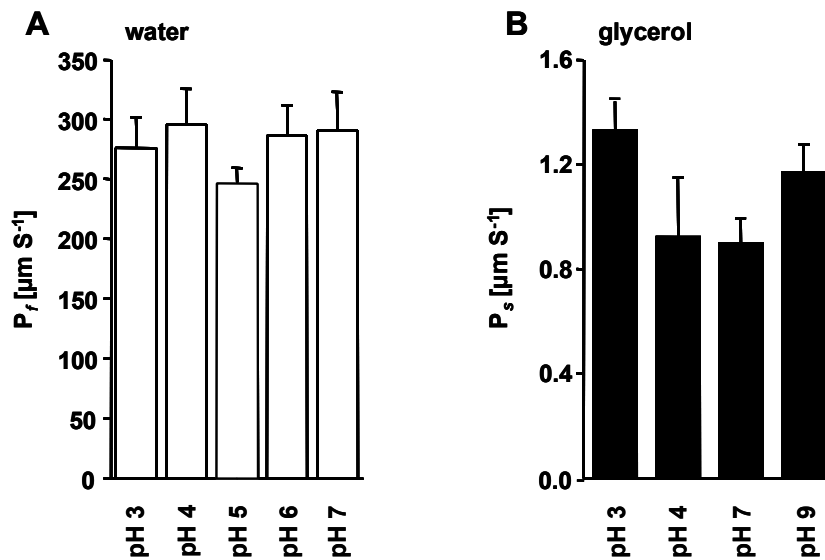


Fig. 4.4. Water and glycerol permeability of PfAQP at different pH values. A: P_f values for water permeability at different pH values. B: P_s values for glycerol permeability different pH values. All values are mean \pm S.E.M. (n=5-6). (control values for water (9, 6, 6,10, 21 $\mu\text{m s}^{-1}$) and glycerol (-0.018, -0.01, 0.024, 0.141 $\mu\text{m s}^{-1}$) at different pH values were subtracted from sample values. Two control values for glycerol have negative values because of oocyte shrinking).

4.2 Glycerol induction of PfAQP expression in *Plasmodium falciparum*

blood culture

The physiological functions of PfAQP are unknown. It has been reported that parasites utilize serum glycerol to synthesise glycerolipids (Vial et al., 1975). Hansen *et al.* proposed that glycerol may be used as a backup energy source in *P. falciparum* in hypoglycaemia states when glucose uptake is restricted (Hansen et al., 2002).

After phosphorylation and oxidation glycerol could enter glycolysis. Further, glycerolipid synthesis using glycerol from the host should be favoured by the parasite over generating

glycerol from glucose due to the resulting shift in the NAD^+/NADH ratio towards the oxidized form.

There are examples that glycerol content in the serum regulates aquaporin expression in humans (Carbrey et al., 2003). Expression of AQP9 in the hepatocyte plasma membrane is induced up to 20 fold when glycerol levels rise. AQP9 is permeable to glycerol and urea and to a wide range of different solutes including polyols, carbamides, purines, pyrimidines, nucleosides and monocarboxylates (Tsukaguchi et al., 1998).

After *in vitro* characterisation of PfAQP I moved to an *in vivo* parasite system and tested for glycerol induction of PfAQP expression in *P. falciparum* blood culture.

Parasite growth and expression levels of two cultures were analysed, one without glycerol and one with 11 mM glycerol supplementation (Fig. 4.5. A). Starting parasitemia was 0.2% with the parasites in the ring stage. After two days, parasitemia increased 4-5 fold and after five days 25-30 fold. Addition of glycerol led to an 8 fold increase of the PfAQP protein expression (Fig. 4.5. B). However, parasites did not survive in medium where glucose was replaced by glycerol. Apparently, plasmodia cannot use glycerol as the only energy source (Fig. 4.6).

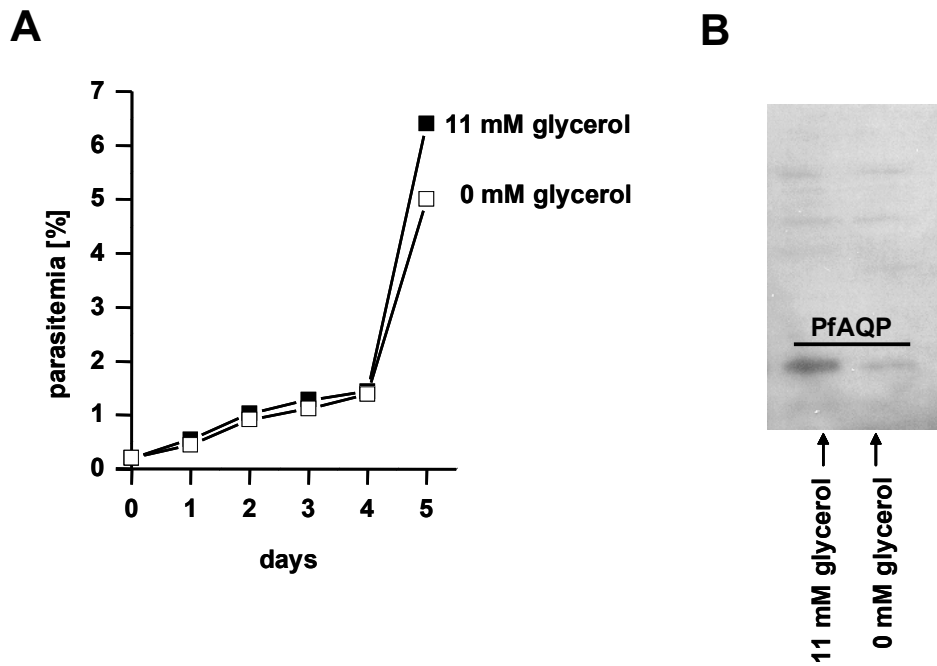


Fig. 4.5. Influence of glycerol on parasite proliferation and PfAQP expression. A. Growth curves of *P. falciparum* parasites in medium without (open squares) and with 11 mM (filled squares) glycerol addition. B. Western blot with samples taken after three days of parasite culture with and without glycerol (control).

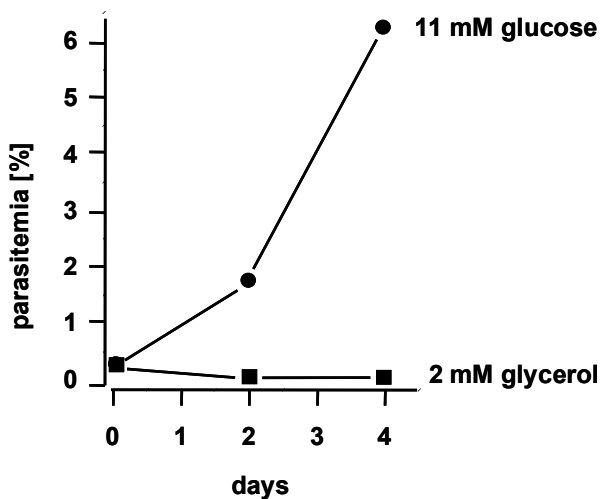


Fig. 4.6. Growth curves of *P. falciparum* parasites in medium supplemented with glucose (filled circles) or glycerol (filled squares) as an energy source.

4.2.1 Ammonia permeability of PfAQP

One of the central features in malaria metabolism is digestion of the host cell cytosolic proteins (predominantly haemoglobin) to be used as a source of amino acids for protein biosynthesis (Francis et al., 1997).

Protein biosynthesis and degradation is accompanied by the production of cytotoxic ammonia. Further, *P. falciparum* deaminates and oxidises glutamine to gain reduced NADH. One biochemical way of detoxification is to convert ammonia to urea. This detoxification process is accomplished in the urea cycle by most terrestrial vertebrates. In the plasmodia genomes, none of the enzymes of the urea cycle, except arginase, have been detected.

Alternatively, ammonia could be exported from a cell by ammonium transporters but these do not seem to be present in the *Plasmodium* genome. Ammonia diffusion through the membrane could occur, but the question is, would it be sufficient?

It was reported that a yeast strain lacking ammonium transporters could not grow if the only nitrogen source is ammonium chloride (5 mM). When the ammonium ion concentration is increased to 20 mM then yeast cells grow (Marini et al., 1997). Some aquaporins like plant aquaporins and human AQP8 were characterised as ammonia channels (Janh et al., 2004; Holm et al., 2005).

PfAQP as an aquaglyceroporin is also a good candidate for an ammonia channel. A yeast strain lacking all ammonia transporters and the endogen aquaporin Fps1 was used as an assay system to test ammonia permeability and indeed, it turned out that PfAQP facilitates ammonia permeation (Wu, personal communication).

4.2.2 Ammonia production in *Plasmodium falciparum* parasites

To test ammonia production in parasites I used standard culturing conditions (Trager et al., 1976) with highly synchronised parasites (more than 85% were in ring stage). Starting parasitemia was 5%, total culture volume was 20 ml. Samples (1 ml) were taken at 0, 16, 24, 38, 48 and 64 h and ammonia was quantified. After each time point, bottles were gassed and again incubated at 37°C until the next sample was taken.

Non-infected erythrocytes were used as a control. Ammonia production in non-infected erythrocytes was absent, but in culture with parasites ammonia production was detected after 16 h. (Fig. 4.7).

Between 16 and 24 h there is a sudden increase in ammonia production in parasites. This time interval corresponds to the trophozoites developmental stage of *P. falciparum*. After 16 h parasites were in the trophozoite stage.

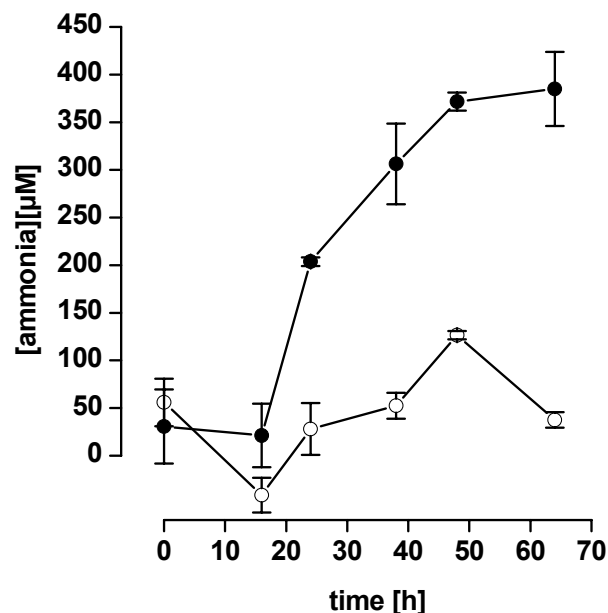


Fig. 4.7. Ammonia production in *P. falciparum* clone 3D7 culture (filled circles) and in non-infected erythrocytes (open circles). Ammonia levels in RPMI 1640 medium were subtracted from ammonia levels in parasite and erythrocytes samples. (n=3 ± S.E.M.)

The parasitemia between 16 and 24 h was 5%, hematocrit 5%. Ammonia production at this time point was 175 $\mu\text{mol/l}$ corresponding to 2.75×10^{10} infected red blood cells (IRBC). The amount of ammonia produced by one parasite per hour was 0.8 fmol/parasite. Accordingly, one litre of IRBC produce 8.8 mmoles of ammonia per liter of triphozoite infected cells per hour whereas lactate production is 220 mmoles (one litre of packed erythrocytes contains 1.1×10^{13} cells). Thus, there is 20 times less ammonia production than lactate production in plasmodia (Ginsburg et al., 2002).

4.2.3 Effect of ammonia on growth of *Plasmodium falciparum* parasites

An ELISA was used to test growth of *P. falciparum* 3D7 in medium supplemented with various concentrations of NH_4Cl . Ammonium chloride was toxic for plasmodia 3D7 clone with an IC_{50} of 2.8 mM (Fig. 4.8.).

The parasite volume is 20 fl in the trophozoite stage. If ammonia is not transported out from the cell in 4.2 min the concentration of ammonia in the parasite cell might reach 2.8 mM. Thus, parasites live on the edge of death.

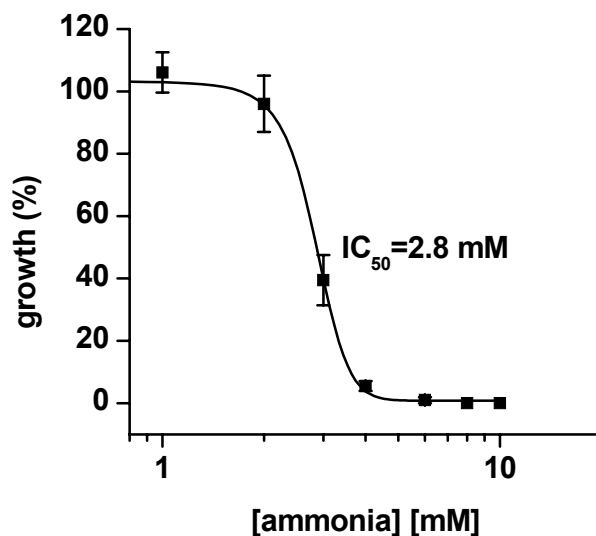
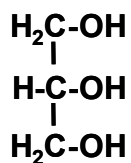


Fig. 4.8. Effect of ammonium chloride on growth of *P. falciparum* 3D7 clone. The IC₅₀ for ammonium is 2.8 mM (n=2 ± S.E.M.).

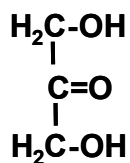
4.3 Dihydroxyacetone and methylglyoxal permeability of PfAQP and AQP3

Except for water and glycerol, PfAQP is permeable for other uncharged solutes, such as polyols of up to five carbon-hydroxyls in length (Hansen et al., 2002).

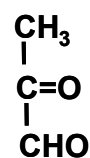
Carbonyl containing compounds have not been tested before. Dihydroxyacetone (DHA) is a three carbon sugar with one keto group at the C-2 atom and methylglyoxal (MG) is a three-carbon compound with a keto and an aldehyde group.



glycerol



dihydroxyacetone



methylglyoxal

Dihydroxyacetone can be metabolised in glycolysis after phosphorylation to dihydroxyacetone phosphate. Non-phosphorylated DHA is cytotoxic as shown with a yeast strain that lacks both endogenous DHA kinases. Non-enzymatic and enzymatic elimination of phosphate from dihydroxyacetone phosphate leads to formation of methylglyoxal. Methylglyoxal is a physiological substrate of the glyoxalase system which catalyses the conversion of methylglyoxal to D-lactate (Phyllips et al., 1993). Efficient conversion of methylglyoxal to D-lactate via the glyoxalase system protects the cell from the highly reactive and toxic methylglyoxal.

PfAQP and the red cell aquaglyceroporin, AQP3, were tested for dihydroxyacetone and methylglyoxal permeability. Isosmotic swelling assays with oocytes expressing PfAQP and AQP3 were done in isosmotic glycerol, DHA or MG solution (130 mM; Fig. 4.9. A and B). Oocytes expressing water specific AQP1 were used as controls. From the swelling curves the solute permeability coefficients P_s were calculated. The glycerol permeability of PfAQP ($0.49 \mu\text{m s}^{-1}$) was two times higher compared to that of AQP3 ($0.29 \mu\text{m s}^{-1}$), DHA permeability was similar for both aquaglyceroporins, (PfAQP $0.32 \mu\text{m s}^{-1}$, AQP3 $0.28 \mu\text{m s}^{-1}$). PfAQP showed permeability for MG ($0.29 \mu\text{m s}^{-1}$) in the same range as with DHA, but AQP3 was not permeable for MG (Fig. 4.9. C).

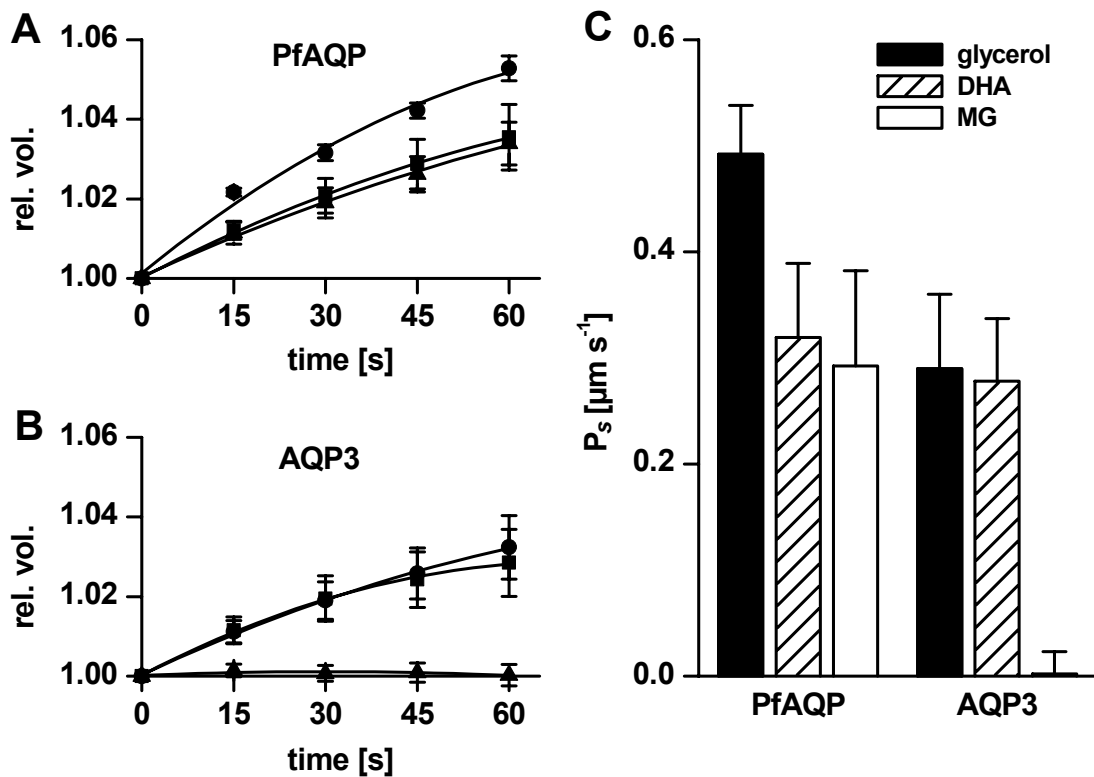


Fig. 4.9. Permeability of PfAQP and AQP3 for glycerol, dihydroxyacetone and methylglyoxal. A: The relative oocyte volume increase in oocytes expressing PfAQP in a 130 mM glycerol (circles) or dihydroxyacetone (squares) or methylglyoxal (triangles) gradient. B: Swelling curves of oocytes expressing AQP3 in a isosmotic chemical gradient (130 mM) for glycerol (circles) or dihydroxyacetone (squares) or methylglyoxal (triangles) gradient. C: Solute permeability (P_s) calculated from the initial slope of the oocytes swelling curves ($n=4-10 \pm$ S.E.M.). Control oocytes were injected with AQP1 cRNA and control values for glycerol ($-0.077 \mu\text{m s}^{-1}$), DHA ($-0.034 \mu\text{m s}^{-1}$) and MG ($-0.03 \mu\text{m s}^{-1}$) were subtracted from measured values.

4.4 Influence of dihydroxyacetone and methylglyoxal on parasite growth

Erythrocytes can use DHA as an energy source (Taguchi et al., 2002). Triose kinase phosphorylates one hydroxyl group of dihydroxyacetone. As a phosphorylated compound it can enter glycolysis. Using BLAST search I could not identify any triose kinase in *P. falciparum* genome.

To test the influence of DHA on parasite growth the Binh1 strain was used. Culturing was done in standard medium supplemented with different concentration of DHA (0, 1, 2.5, 5, 10 mM). Parasite cultures were synchronised with sorbitol (Lambros et al., 1979), starting parasitemia was 0.5% and parasites were in ring stage.

Parasitemia was counted every day for four days and for each DHA concentration. To estimate parasitemia 5000 erythrocytes of each sample were counted. Cultures which had been treated with 5 and 10 mM DHA, did not proliferate at all. A culture which had been treated with 2.5 mM DHA, showed 20% lower parasitemia than the untreated control (Fig. 4.10. B).

Using the parasitemia values after four days I determined an IC_{50} of 3.3 mM DHA (Fig. 4.10. C).

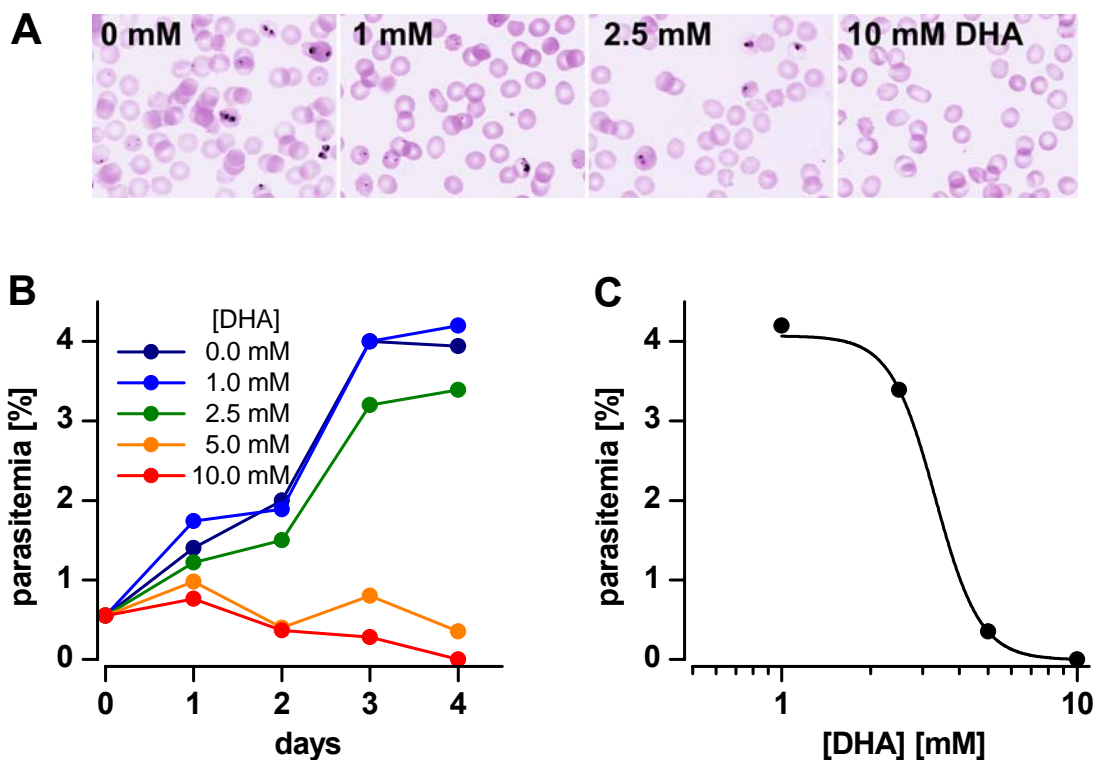


Fig. 4.10. Effect of DHA on *P. falciparum* (Binh1) proliferation. A: Giemsa stained parasites after four days of treatment with DHA. B: Growth curves of *P. falciparum* cultured with DHA. C: Parasitemia values after four days are plotted as a growth inhibition curve. The IC_{50} for DHA is 3.3 mM.

The DHA effect on parasites was confirmed by an ELISA based on quantification of the constitutively expressed plasmodial histidine rich-protein II (Noedl et al., 2002).

Starting parasitemia was 0.02%, hematocrit 1.5% and the samples were incubated at 37°C for three days. At the beginning of the experiment parasites were more than 85% in ring stage. It is important to have highly synchronised parasites because different compounds affect different developmental stages of parasites and by synchronization the effect of a compound can be followed easier.

The DHA influence on parasite proliferation was tested on the Binh1 and the 3D7 strains. The 3D7 clone is chloroquine sensitive contrary to Binh1. I tested the parasite proliferation of different DHA concentrations (0-10 mM). The IC₅₀ for the Binh1 strain was 3.0 mM and for the 3D7 clone it was 2.6 mM. Parasite growth in samples which were treated with 5 and 10 mM DHA, was fully inhibited (Fig. 4.11. A: open and closed circles).

Both, Binh1 and 3D7 were also treated with MG (0-10 mM) and it turned out that this compound was 10-20 times more toxic to both parasite strains than DHA. The IC₅₀ value for the 3D7 clone was 128 μM MG and for the Binh1 strain 223 μM MG (Fig. 4.11. B)

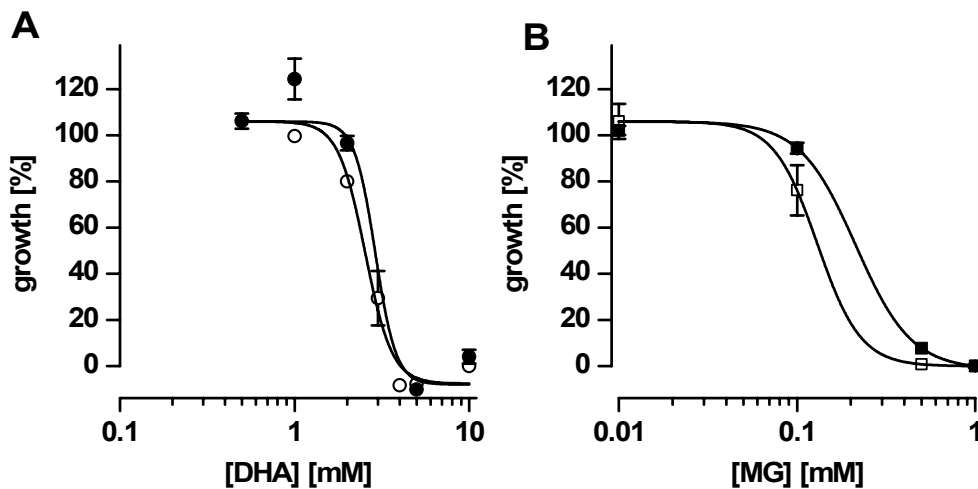


Fig. 4.11. Growth inhibition curves of *P. falciparum* clone 3D7 and Binh1 strain treated with dihydroxyacetone and methylglyoxal A: Growth inhibition curves of Binh1 (filled circles) and 3D7 (open circles) treated with DHA. IC₅₀ values based on these curves are 3.0 mM (Binh1) and 2.6 mM (3D7 clone). B: Inhibitory effect of methylglyoxal on Binh1 and 3D7 clone growth. The IC₅₀ values are 223 μM (Binh1, filled squares) and 128 μM (3D7, open squares; n=2-3, ± S.E.M.).

To exclude the possibility that DHA and MG interact with erythrocyte membranes causing a decrease in parasite invasion or disturbing parasite intracellular metabolism I treated erythrocytes with up to 10 mM DHA and up to 2 mM MG. I observed them for three days.

However, presence of DHA and MG in the media did neither change the morphology of erythrocytes nor increase cell lysis. Pre-treated erythrocytes were washed to remove residual DHA and MG and then infected with plasmodia parasites. Growth and proliferation of parasites using these erythrocytes were not affected. This suggested that the mechanism of DHA and MG toxicity is not via host cell disturbance, but through direct interaction with the parasites.

4.5 Co-treatment of *Plasmodia* with dihydroxyacetone plus chloroquine and fosmidomycin

Having found that DHA is toxic to parasite cells I became interested in the mode of toxicity. Since the early 1950s chloroquine has been widely used as an antimalarial drug. Chloroquine inhibits heme polymerisation in the food vacuole of plasmodia. Fosmidomycin has been used in clinical trials. Its mode of action is inhibition of the isoprenoid synthesis in the apicoplast. Co-treatment of parasites with DHA plus chloroquine or fosmidomycin may give hints on the mode of DHA toxicity.

First the 3D7 clone was treated with DHA (0, 0.5, 1, 2, 5, 10 mM) in combination with chloroquine (0, 0.1, 0.3, 1, 3, 10, 30, 100 nM). The IC_{50} was 5 nM for chloroquine and 2.2 mM for DHA with or without co-treatment. This indicates that both compounds act independently (Fig. 4.12. A and B)

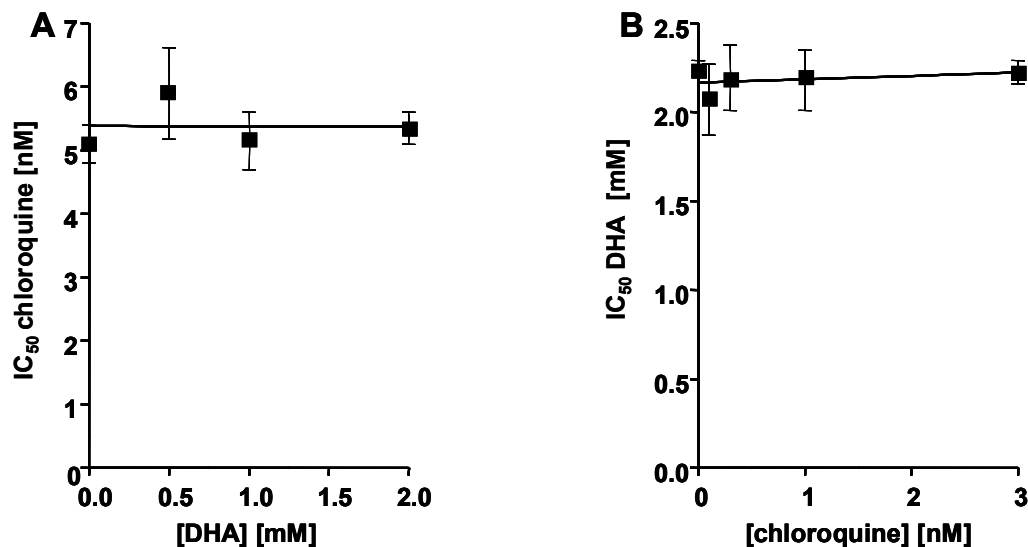


Fig. 4.12. A: Influence of different concentrations of dihydroxyacetone on chloroquine IC_{50} values. B: Effect of different concentrations of chloroquine on dihydroxyacetone IC_{50} values. (n=3, \pm S.E.M.).

To test DHA-fosmidomycin combinations DHA was used at 0, 0.5, 1, 2, 5, 10 mM and fosmidomycin at 10, 30, 100, 300, 1000, 3000, 10000 nM. The IC_{50} for DHA was 2 mM and for fosmidomycin 240 nM with or without co-treatment, indicating independent modes of action (Fig. 4.13. A and B).

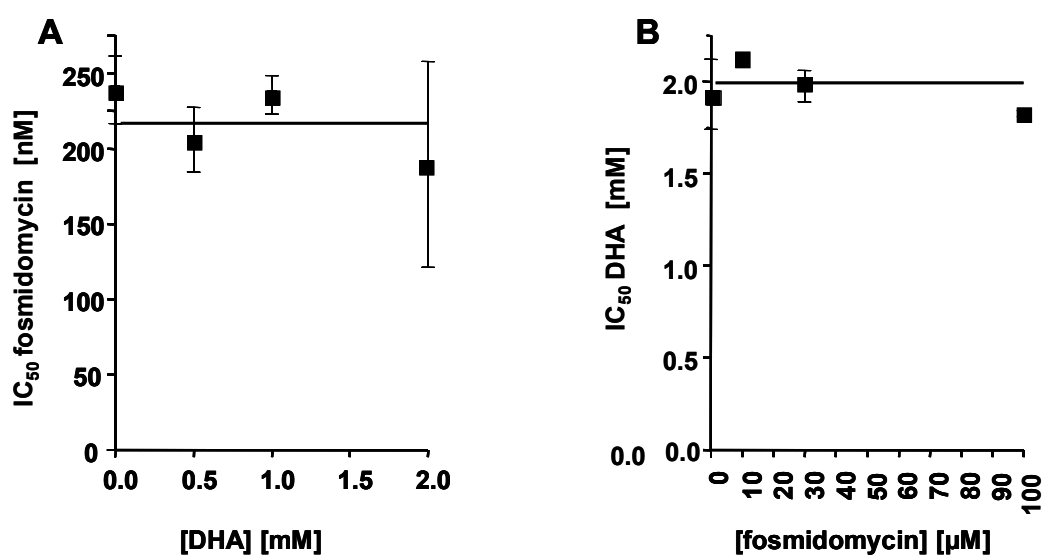


Fig. 4.13. A: Influence of different concentrations of dihydroxyacetone on fosmidomycin IC_{50} values. B: Effect of different concentrations of fosmidomycin on dihydroxyacetone IC_{50} values (n=3, \pm S.E.M.).

Various low-molecular-weight aldehydes and carbonyl compounds, including DHA and MG, can modify proteins by irreversible modification of cysteine, lysine and arginine groups (Oya et al., 1999). It was suggested that MG might selectively react with lysine and arginine groups near the active site of GAPDH and that these modifications lead to the inhibition of enzyme activity (Lee et al., 2005).

4.6 Cloning and characterisation of PfGAPDH from *Plasmodium falciparum* strain Binh1

P. falciparum glyceraldehyde-3-phosphate (PfGAPDH) dehydrogenase was cloned and expressed before (Daubenberger et al., 2000). I amplified the open reading frame from genomic DNA of *P. falciparum* strain Binh1. Sequencing of the complete open reading frame resulted in a single, probably strain specific mutation (C₄₁₈A) compared to the published genome (www.plasmoDB.org; gene_ID 140598) leading to a Q₁₄₀K change, but comparing with the sequence published by Daubenberger *et al.* there are two additional differences, P₂₇₂L and I₂₇₆V.

4.6.1 Expression and purification of PfGAPDH

The PfGAPDH gene was subcloned into the pQE30 vector with an N-terminal RGS-His₆ tag and then expressed in *E. coli*. Expression yield was 3 mg of enzyme/litre cell culture. Coomassie staining was used to detect the purified protein (Fig. 4.14.).

The PfGAPDH protein was unstable at 4°C and precipitation occurred within 24 h at 4°C, while at room temperature it was stable for one week.

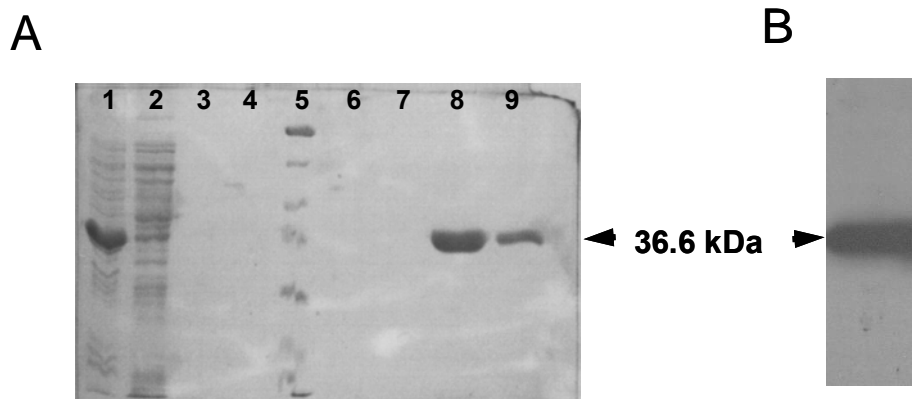


Fig. 4.14. A: Ni²⁺-NTA purification of PfGAPDH. 1-pellet, 2-flow through, 3-wash with without imidazole, 4-marker (12.5, 18, 25, 35, 45, 66, 116 kDa), 5-wash with 10 mM imidazole, 6-wash with 30 mM imidazole, 7-elution with 150 mM imidazole, 8-elution with 600 mM imidazole. SDS-PAGE gel 12.5%. B: Western blot analysis of recombinant PfGAPDH. His-tagged protein detected with anti-RGS-His₆ antibody.

4.6.2 GAPDH inhibition assay with dihydroxyacetone and methylglyoxal

For inhibition assays PfGAPDH was incubated with 2.5 mM DHA and 200 μ M MG, i.e. the IC₅₀ values obtained in growth inhibition experiments. 200 μ M MG did not have an influence on PfGAPDH activity. Thus, PfGAPDH and rabbit GAPDH were incubated at 37°C with 2.5 mM MG and DHA. With DHA, rabbit GAPDH activity was instantly reduced to 60%, after 3 h enzyme was fully inhibited. With MG, rabbit GAPDH activity decreased to 50% after 3 h and after 20 h the enzyme was fully inhibited (Fig. 4.15. A). PfGAPDH was more resistant to DHA and MG inhibition. After 3 h of incubation with DHA, activity was around 30% and after 6 h enzyme activity was fully inhibited. Incubation with MG did not have any inhibitory effect on PfGAPDH even after 20 h of incubation (Fig. 4.14. B).

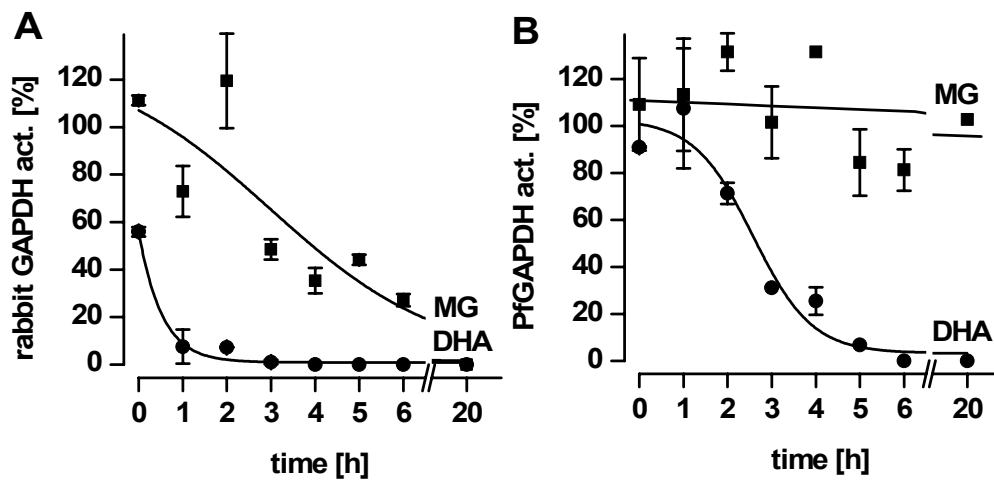


Fig. 15. Influence of dihydroxyacetone and methylglyoxal on rabbit GAPDH (A) and on PfGAPDH (B) activity. Relative activity of enzymes treated with 2.5 mM DHA (circles) and 2.5 mM MG (squares) were plotted. ($n=2 \pm$ S.E.M.)

4.7 *Toxoplasma gondii* aquaporin (TgAQP)

Besides *P. falciparum*, another human pathogenic parasite, i. e. *T. gondii*, belongs to the phylum Apicomplexa. *P. falciparum* multiplies exclusively in erythrocytes, whereas *T. gondii* invades various cell types.

4.7.1 Identification of TgAQP

Using BLAST searches I identified a single putative aquaporin gene in the *T. gondii* genome (TgAQP). The longest open reading frame is 792 bp. In the same reading frame two start codons are present, at nucleotide positions 1 and 115 which could translate into proteins TgAQP M₁ (29.9 kDa) and TgAQP M₃₉ (26.3 kDa) (Fig. 4.16. A). At position 13-99 an in-frame intron with classical GT/AG boundaries may be located (gray shading in Fig. 4.16. A). Surprisingly, the TgAQP aquaporin had only 28% sequence similarity to PfAQP. Instead, TgAQP showed highest similarity to water-specific plant tonoplast intrinsic proteins (e.g. TIP 2;1, 47%, *Arabidopsis thaliana*). The level of similarity between TgAQP, γ -TIP, AQP1 and GlpF is reflected by “Expected” (E) values from the BLAST analysis which vary by four orders of magnitude (Fig. 4.16. B). The pore forming residues around the canonical NPA motifs are highly conserved between TgAQP and γ -TIP channels including a valine at the pore constriction region where other aquaporins including AQP1 and GlpF almost exclusively have a positively charged arginine (Fig. 4.16. B).

A

```

atggaccaatttgttttttcaggagggttctgaaggaggaggcgagttaggcggagaccga 60
M D Q F V F S G G S E G G G E L G G D R
1
gagcgcgactccttgacgccagagctcggaaggttcgagcatctcatcttcaatatgcaa 120
E R D S L T P E L G R F E H L I F N M Q
39
aagtatttttgtgagttcttcgcagcactcgttatcgtcagtgagttgcctttggttta 180
K Y F C E F F A A L V I V S A V A F G L

gcgaaggaaggcgggtgccagggcagcgcactgtctatcacgagcaccatttttgccttg 240
A K E G G A Q A A P L S I T S T I F A L

attacgttgttcaaagatatcagcgggtgcacatttcaatccggcgggtatcatgtacaatt 300
I T L F K D I S G A H F N P A V S C T I

tatatgacagatcctcgttttactctggtagatcttttatgctacgtagctgctcaactg 360
Y M T D P R F T L V D L L C Y V A A Q L

ataggaggtagctgctcggagcgtttattggatattggaatcatgggaaaggccctggatattc 420
I G G T V G A F I G Y G I M G K A L D I

ctccccttagatccgggtatgagcgcgaagccgcccagctgttccacgaagtcattcctaca 480
L P L D P G M S A S R Q L F H E V I P T

atggttatgatctacgctgtcctcgtttctcgttttcggatatggggtaatgtgggagttg 540
M V M I Y A V L V L V F G Y G V M W E L

acgggtccctttcgtcgtcggcgcgctgcgtcttggcggggcggtttgcggggcgacgatg 600
T V P F V V G A C V L A G A F A G A T M

aaccagcaggtcacatttgggtattatttttcaaacatctgtacaaagaacacaaatatt 660
N P A V T F G I I I S N I C T K N T N I

gatgttgctgcactgctggtaacggtatttgggcccgtttttgggtgccatggttcgcattc 720
D V A A L L V T L F G P F L G A M F A F

ctgggttacgctcgggacgcatgcctatcacaaatcctgtcccactacgcttcttgaacttc 780
L G Y V G T H A Y H N P V P L R F L N F

agggggctctga 792
R G L .

```

B

						E value
TgAQP	88	SGAHFNPAVS	. . .	AGATMNPAVT	205	
γ -TIP	80	SGGHVNPAVT	. . .	SGASMNPAVA	203	$3 \cdot 10^{-9}$
AQP1	71	SGAHLNPAVT	. . .	TGCGINPARS	196	$7 \cdot 10^{-7}$
glpF	64	SGAHLNPAVT	. . .	TGFAMNPARD	207	$3 \cdot 10^{-1}$

Fig. 4.15. Sequence analysis of TgAQP. A: The open reading frame is shown with two potential ATG start codons. The canonical NPA sequences are shaded in black. An in-frame intron is possibly located at position 13-99 (grey shaded). B: Part of the protein sequence alignment of prototypical aquaporins. In γ -TIP and in TgAQP the highly conserved arginine is exchanged by valine (marked with a star). The expected (E) value from a BLAST search with TgAQP as a query is indicated on the right.

4.7.2 Expression and functional characterisation of TgAQP transcripts

Both TgAQP M1 and TgAQP M39 constructs were expressed in oocytes to determine whether they form functional pores.

Initially, protein expression was checked in *X. laevis* oocytes. As shown by Western blots constructs of TgAQP M1 and TgAQP M39 with an N-terminal c-myc epitop tag were equally expressed (Fig. 4.16. A). Protein migration was lower than expected from the molecular weight calculation which is supposed to be 30 kDa and 26 kDa, respectively, but they were 27.7 and 20.1. The blot further shows TgAQP dimers (arrows Fig. 4.17. A).

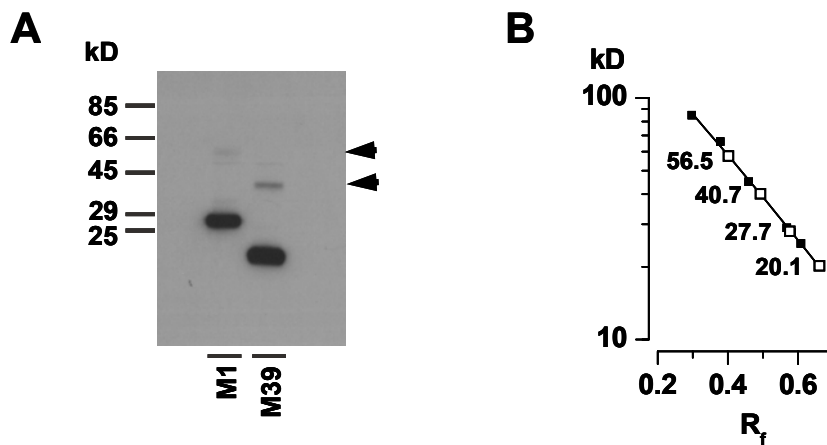


Fig. 4.17. Immunoblots of myc-TgAQP M1 and myc-TgAQP M39 constructs expressed in *X. laevis* oocytes. A: The oocytes membranes were probed with anti-c-myc antiserum. Arrows show myc-TgAQP M1 and myc-TgAQP M39 dimers. B: MW calculation curve, filled squares represent MW of marker and open squares represent MW of TgAQP M1 (27.7 kDa), TgAQP M39 (20.1) and dimers.

For functional characterisation, the amount of cRNA for injection and the incubation time was optimised.

4.7.2.1 Optimisation of cRNA amount and incubation time

X. laevis oocytes were injected with 1-10 ng of TgAQP M1 cRNA. During the course of four days oocytes were daily tested for water permeability. Expectedly, permeability was dependent on the amount of injected cRNA and increased with longer incubation time. After three days maximal water permeability was reached and only a minor difference between 5 ng and 10 ng of cRNA was noted. Thus, injecting 5 ng of cRNA and incubation for three days was used in the following for TgAQP M1 expression in the oocyte system (Fig. 4.18.).

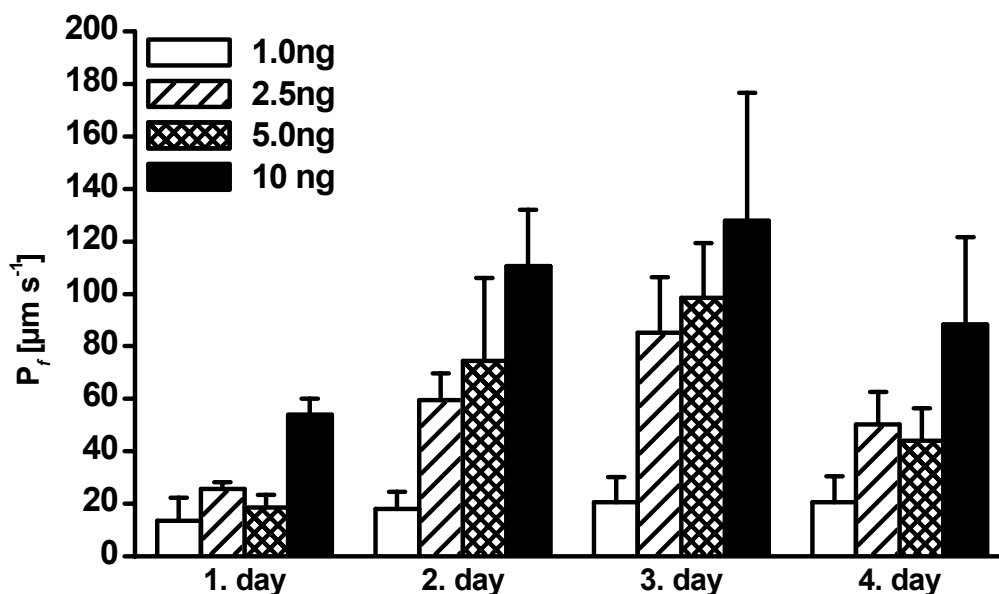


Fig. 4.18. Water permeability in oocytes injected with different amounts of TgAQP M1 cRNA during four days of incubation. Bars represent P_f values. Control values were subtracted from the sample values (15, 14, 18, 18 $\mu\text{m s}^{-1}$; $n=5$, \pm S.E.M.).

4.7.3 Water and glycerol permeability of TgAQP M1 and TgAQP M39

TgAQP M1 and TgAQP M39 water and solute permeability was compared to the previously characterised PfAQP.

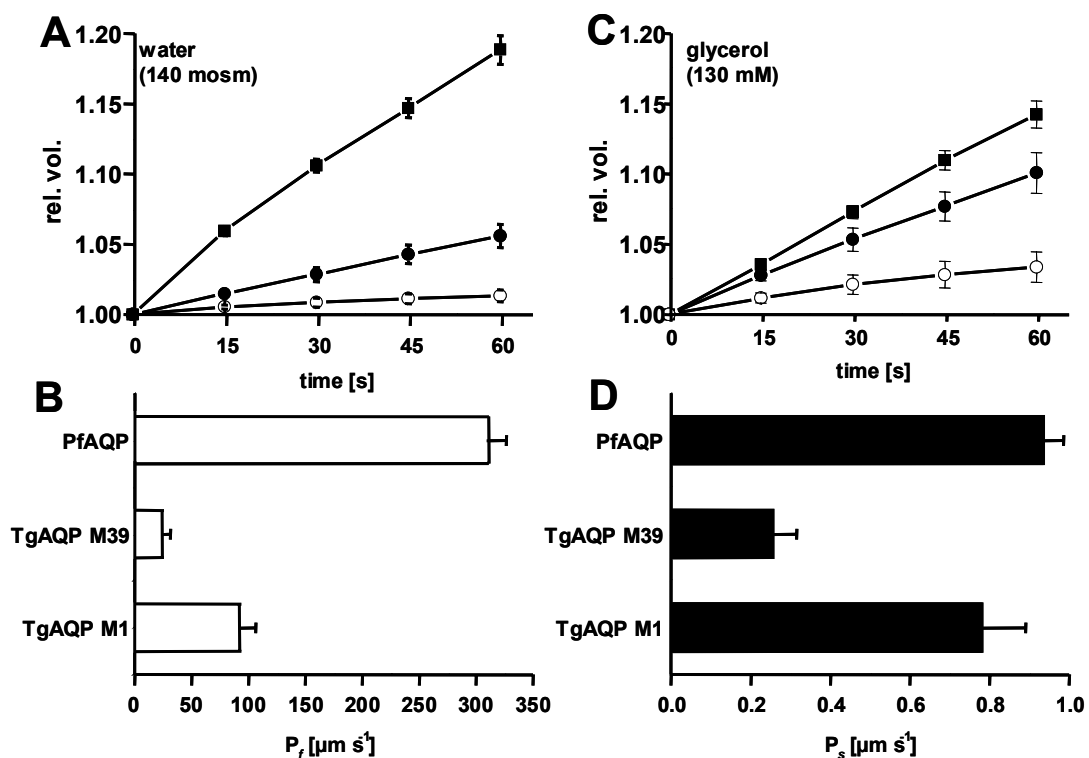


Fig. 4.19. Water and glycerol permeability of *X. laevis* oocytes expressing TgAQP M1, TgAQP M39 and PfAQP.

A: Relative volume increase of *X. laevis* oocytes injected with cRNA for TgAQP M1 (filled circles), TgAQP M39 (open circles), PfAQP (squares) in 1:3 diluted medium during the first minute of swelling. B: P_f values (mean \pm S.E.M) were calculated from the swelling curves. C: Relative volume increase of *X. laevis* oocytes (co-)injected with cRNA for TgAQP M1/AQP1 (filled circles) PfAQP/AQP1 (filled squares), TgAQP M1/AQP1 (open circles). Relative volume change is shown for 1 min, in isotonic medium with 130 mM glycerol instead of 65 mM NaCl. D: P_s values were calculated from swelling curves. All values are mean \pm S.E.M. The number of oocytes is 5-8 in osmotic and 5 in isosmotic swelling assays. Control values for water ($14 \mu\text{m s}^{-1}$) and glycerol ($0.025 \mu\text{m s}^{-1}$) were subtracted from measured values.

Swelling curves taken after hypotonic shock of TgAQP M1, TgAQP M39 and PfAQP (Fig. 4.19. A) showed that oocytes injected with PfAQP cRNA swelled faster compared to oocytes injected with TgAQP M1 and TgAQP M39 cRNA. The P_f value for TgAQP M1 ($98.7 \mu\text{m s}^{-1}$) was three times smaller than that of PfAQP ($311.2 \mu\text{m s}^{-1}$), and 3.5 times higher than TgAQP M39 ($25.2 \mu\text{m s}^{-1}$; Fig. 4.19. B). Compared to the water permeability of PfAQP, the *T. gondii* aquaporin is a channel with intermediate water permeability. Given that PfAQP is a bi-functional channel with both, high water and glycerol permeability (Hansen et al., 2002), TgAQP was tested for glycerol permeability. Swelling curves of TgAQP M1, TgAQP M39 and PfAQP showed that oocytes injected with PfAQP and TgAQP M1 cRNA had a similar swelling rate ($0.98 \mu\text{m s}^{-1}$, $0.77 \mu\text{m s}^{-1}$ respectively), but oocytes injected with TgAQP M39 cRNA swell three times slower ($0.25 \mu\text{m s}^{-1}$; Fig. 4.19. C and D).

In summary, TgAQP M1 is a good glycerol channel with intermediate water permeability.

4.7.4 Solute permeability of TgAQP

As a characteristic of aquaglyceroporins, the solute permeability profile of TgAQP M1 was determined. Besides urea which passed the pore as well as glycerol, only erythritol and D-arabitol led to reasonable swelling rates of about 25% compared to glycerol glycerol permeability. Larger compounds hardly passed the pore and *myo*-inositol and charged compounds did not pass at all (Fig. 4.20. A).

It has been reported that proliferation of *T. gondii* parasites was inhibited by hydroxyurea. Thus I tested whether TgAQP may be involved in hydroxyurea delivery into the cell. Further,

I compared TgAQP hydroxyurea permeability to that of PfAQP. Indeed, the drug passed through both aquaglyceroporins with rates 75% of the glycerol permeability (Fig. 4.19. B).

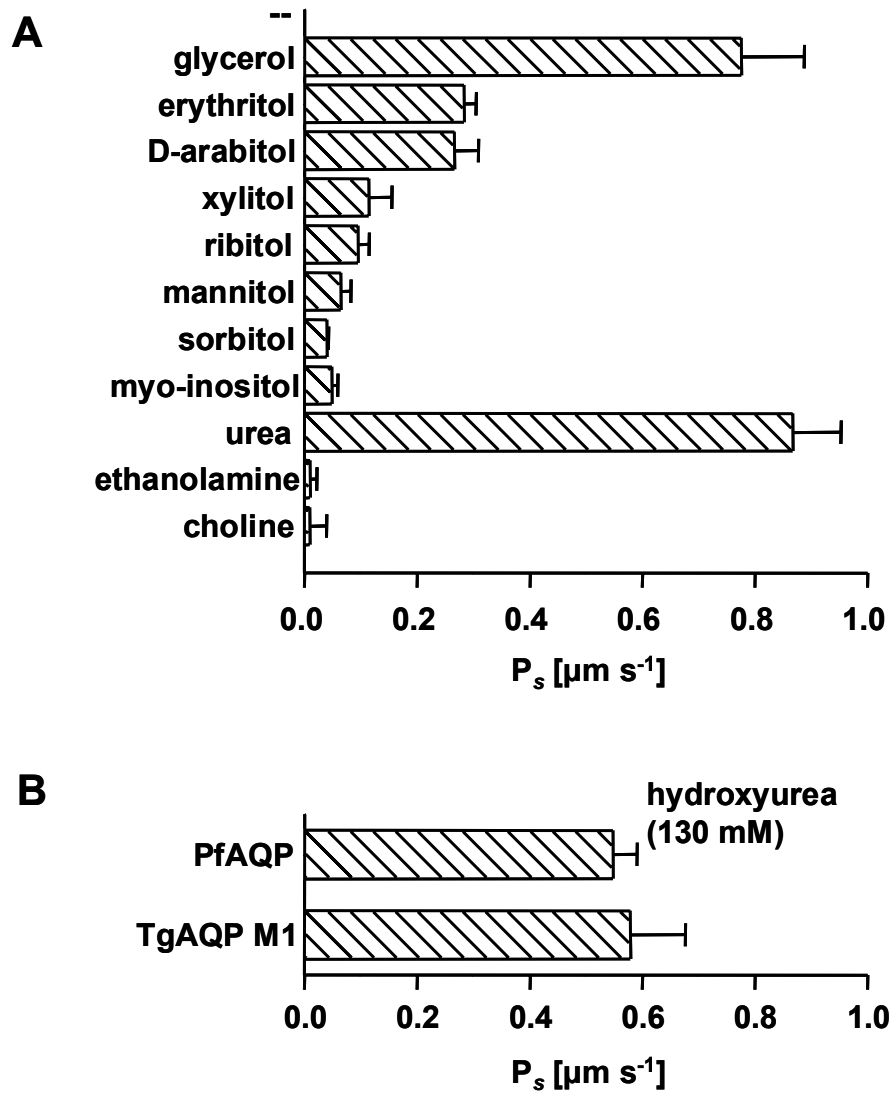


Fig. 4.20. Solute permeability of TgAQP M1 and PfAQP. Bars present P_s values calculated from swelling curves. For each calculation 5-6 oocytes were used. The error bars are \pm S.E.M.

4.8 *Trypanosoma brucei* aquaporins (TbAQPs)

T. brucei, the causative agent of sleeping sickness transmitted by the tsetse fly is a member of the genus Kinetoplastida. Effective drugs against sleeping sickness have not been found yet.

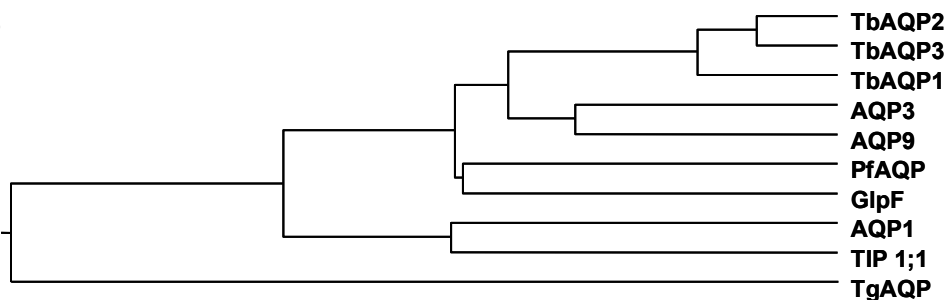
4.8.1 Identification of *Trypanosoma brucei* aquaporins

In collaboration with N. Uzcategui and M. Duszenko (Physiological Chemistry, Tübingen) three aquaporins were identified in the expressed sequence tags (ESTs) database of *T. brucei*. These three aquaporins were named TbAQP1, TbAQP2 and TbAQP3. TbAQP1 and TbAQP3 have the canonical triads NPA/NPA and the highly conserved arginine after the second NPA motif. The TbAQP2 has some differences. The first canonical motif is NSA and the second is NPS and instead of the highly conserved arginine at the constriction site, leucine was found (Fig. 4.21. A). Sequence alignment and phylogenetic tree analyses suggested that these three aquaporins have more similarity to aquaglyceroporins (AQP3, AQP9, PfAQP, GlpF) than to aquaporins (AQP1, AQPZ) (Fig. 4.21. B). Prediction of amino acid content in the pore constriction region of TbAQPs was done using the crystal structure of *E. coli* GlpF. The only difference in TbAQP1 and TbAQP3 pore constriction region compared to GlpF are Tyr267(258) instead of Phe200 (Fig. 4.21. C). The predicted pore constriction region of TbAQP2 contains Ile109, Leu258 and Leu264 and the presence of un-polar amino acids suggests that the pore is wider than in GlpF and that it has similar composition as the pore constriction region of TgAQP (Fig. 4.21. C).

A

	*	20	*	40	*	60	
TbAQP1 :	MSDEKINVHOYPS	EADVRGLKARN	CGACEVPPFE	ENNEPIPN	RSANPQEK	NENELVGD	NAD : 60
TbAQP2 :	MQSOPDNV	-AYPMELQA	----	VNKDGTVEV	RVQGNVDN	SSNERWDAD	VQKH-----EVAE : 50
TbAQP3 :	MQSOPDNV	-AYPMELQA	----	VNKDGTVEV	RVQGNDDSSN	-----	RKH-----EVAE : 42
	*	80	*	100	*	120	
TbAQP1 :	NEAHDAVDV	VNYWAPRQL	RLDYRNYM	GEFLGTFV	LLFMGN	GVVATV	ILDKDILGFLSIAFGW : 120
TbAQP2 :	AQEKPVGG	INFWAPREL	RRLNYR	DYVAEFLG	NEVLLI	YIAKCAV	ITSLLVDELGILLCLTIGI : 110
TbAQP3 :	AQEKPVGG	INFWAPREL	RRLNYR	DYMGELLG	TFVLL	FMGN	GVVATVILIDGKLGFLSITIGW : 102
	*	140	*	160	*	180	
TbAQP1 :	GIAVTMGLY	ISLGIS	CGHLNPA	AVTLANAV	FGCFP	PWRRVPGY	IAAQMLGAFVGAACAYGVY : 180
TbAQP2 :	GVAVTMALY	VSLGIS	CGHLNSA	VTVGNAV	FGDFP	WRKVP	GYIAAQMLGTEFLGAACAYGVF : 170
TbAQP3 :	GIAVTMALY	VSLGIS	SSGHLNPA	VTVGNAV	FGDFP	WRKVP	GYIAAQMLGAFVGAACAYGVF : 162
	*	200	*	220	*	240	
TbAQP1 :	ADLLKQHS	GG-LVGF	GDKGFAG	MSTYP	REGNRL	FYCFE	SEFICTAILLFCVCGIFDPNN : 239
TbAQP2 :	ADLLKAH	GGGELI	AFGEK	GIWV	FAMYP	AEENG	IFYPFAELISTAVILLFCVCGIFDPNN : 230
TbAQP3 :	ADLLKAH	GGGELI	AFGEK	GTAG	VFSTY	PRDSN	GLFSCIFGEFICTAMLLFCVCGIFDPNN : 222
	*	260	*	280	*	300	
TbAQP1 :	SPAKGHE	PLAVGAL	VFAIGN	NIGYAS	GYAIN	PARDF	GPRVFSAILFGSEVFTIGNYYFWV : 299
TbAQP2 :	SPAKGYE	TVAGAL	VFVMV	NNEGLAS	PLAMN	PSIDF	GPRVFGAILLGGEVFSSHANYFWV : 290
TbAQP3 :	SPAKGHE	PLAVGAL	VFAIGN	NIGYST	GYAIN	PARDF	GPRVFSSELYGGEVFSHANYFWV : 282
	*	320					
TbAQP1 :	PLFIPFL	GGI	GLFLY	KYFV	PY		: 321
TbAQP2 :	PLVVP	FFGAIL	GLFLY	KYFL	PH		: 312
TbAQP3 :	PLVIP	PLFGGI	GLFLY	KYFV	PH		: 304

B



C

	●	—	●	—	●		
TbAQP1 :	119	WGIAVTMGLYISLGIS	CGHLNPAV	...	NNIGYASGYAINPAR	273	
TbAQP2 :	109	IGVAVTMALYVSLGIS	CGHLNSAV	...	NNEGLASPLAMNPSL	264	
TbAQP3 :	102	WGIAVTMALYVSLGIS	SSGHLNPAV	...	NNIGYSTGYAINPAR	256	
GlpF :	48	WGI	VAMAIYLTAGV	SGAHLNPAV	...	ASMGPLTGFAMNPAR	206

Fig. 4.21. Sequence analysis of *T. brucei* aquaporins. A: Alignment of amino acid sequence of *T. brucei* aquaporins. Red shaded parts represent canonical NPA (TbAQP1 and 3)/NSA (TbAQP2), and second NPA (TbAQP1 and 3) /NPS (TbAQP2) regions. The blue shaded region represents the conserved arginine in TbAQP1 and 3 and leucine in TbAQP2. B: Phylogenetic tree analysis of TbAQPs. C: The part of protein sequence alignment of TbAQPs and GlpF, in purpose to predict the structure of pore constriction region, based on crystal structure of *E. coli* GlpF. Underlined parts represent NPA/NSA and NPA/NPS regions, and red dots label possible amino acids in pore constriction region.

4.8.2 Water and glycerol permeability of TbAQPs

After sequence analysis which suggested that these three aquaporins might be aquaglyceroporins, TbAQPs were tested for water and glycerol permeability. Oocytes expressing TbAQP1-3 swelled when exposed to hypotonic shock (Fig. 4.22. A). From the calculated P_f values for TbAQP1 ($139 \mu\text{m s}^{-1}$), TbAQP2 ($109 \mu\text{m s}^{-1}$), TbAQP3 ($129 \mu\text{m s}^{-1}$), these channels can be characterised as channels with intermediate water permeability between TgAQP M1 ($98.7 \mu\text{m s}^{-1}$) and PfAQP ($311 \mu\text{m s}^{-1}$; Fig. 4.22. B).

The swelling rate in 130 mM glycerol gradient was similar among the TgAQPs (Fig. 4.22. C). The P_s values were in the range of $0.9\text{-}1.2 \mu\text{m s}^{-1}$ which is comparable to the swelling rate of PfAQP (Fig. 4.22. D).

In conclusion, all three TbAQPs are channels with intermediate water and excellent glycerol permeability.

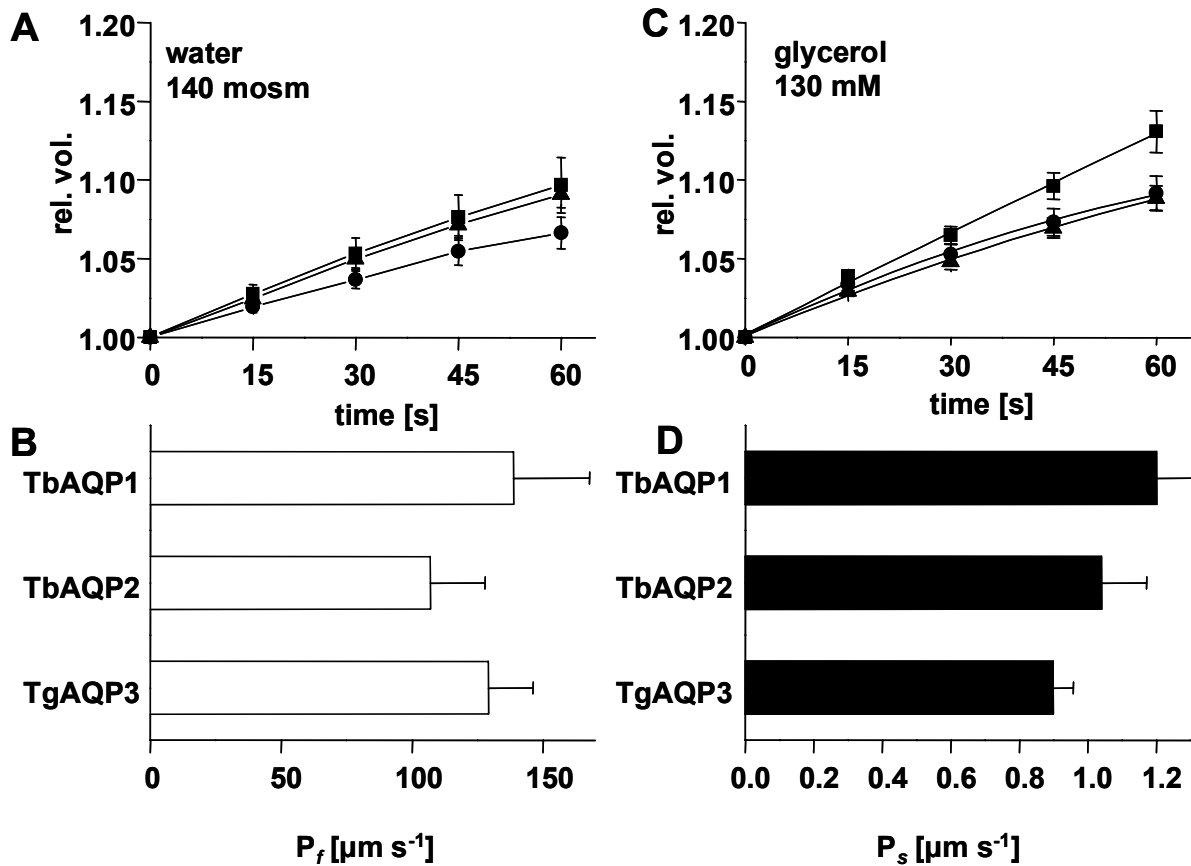


Fig. 4.22. Water and glycerol permeability of *X. laevis* oocytes expressing TbAQPs.

A: Relative volume increase of *X. laevis* oocytes injected with cRNA for TbAQP1 (squares), TbAQP2 (circles), TbAQP3 (triangles) in 1:3 diluted medium during the first minute of swelling. B: P_f values (mean \pm S.E.M.) were calculated from the swelling curves. C: Relative volume increase of *X. laevis* oocytes (co-)injected with cRNA for TbAQP1/AQP1 (squares) TbAQP2/AQP1 (circles), TbAQP3/AQP1 (triangles). Relative volume change is shown for 1 min, in isotonic medium with 130 mM glycerol instead of 65 mM NaCl. D: P_s values were calculated from swelling curves. All values are mean \pm S.E.M. The number of oocytes is 5 in osmotic and 5 in isosmotic swelling assays. Control values for water ($34 \mu\text{m s}^{-1}$) and glycerol ($0.087 \mu\text{m s}^{-1}$) were subtracted from measured values.

4.8.3 Solute permeability profile of TbAQPs

The swelling rate of TbAQP expressing oocytes was measured in the presence of a variety of polyols, dihydroxyacetone, urea, pyruvate and alanine. Oocytes expressing TbAQPs were hardly permeable for longer polyols. Only erythritol and ribitol permeated through TbAQP3

with about half the rate of glycerol. All TbAQPs were highly permeable for DHA, especially TbAQP2 with a swelling rate double that of glycerol. TbAQP1 showed a 1.5 fold higher swelling rate than for glycerol and TbAQP3 exhibited an equal swelling rate as glycerol. Urea passed the pores of TbAQP2 and TbAQP3 somewhat slower than glycerol but less well that of TbAQP1. Only TbAQP3 transported erythritol and ribitol. Pyruvate passed only TbAQP2 at a 8 times slower rate compared to glycerol (Fig. 4.23.).

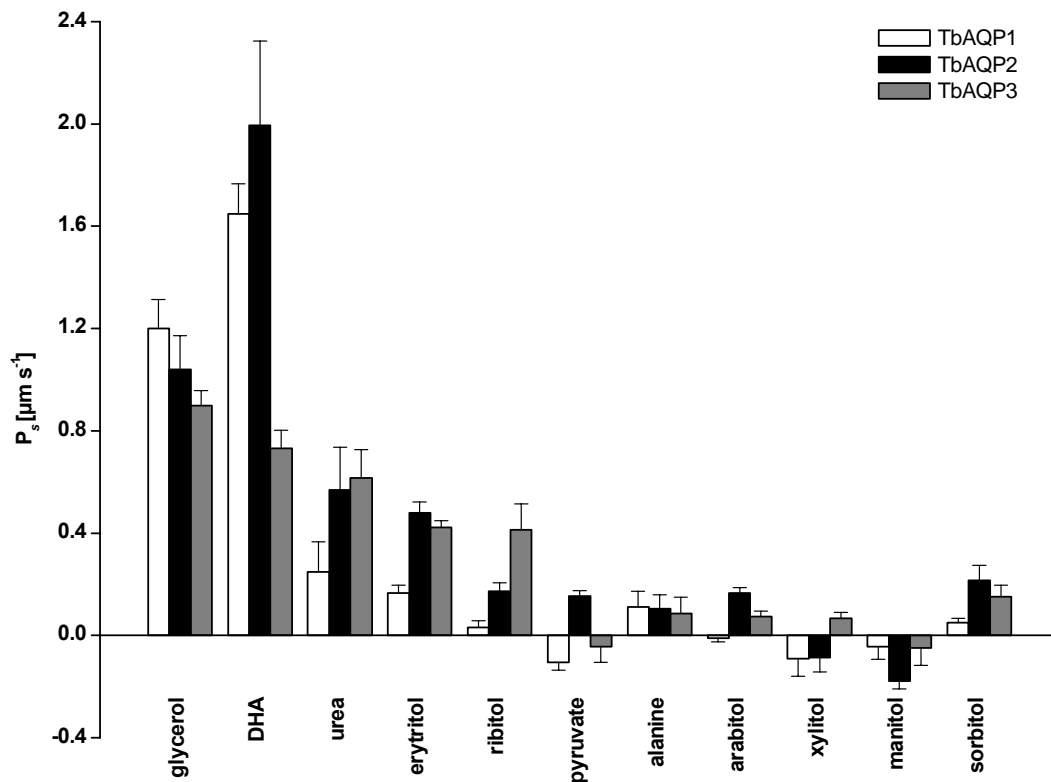


Fig. 4.23. Substrate permeability of *X. laevis* oocytes injected with TbAQPs cRNA. The bars represent P_s values calculated from swelling curves. (n=4-5, \pm S.E.M.).

5 Discussion

5.1 Importance of the C-loop in water permeability

As a complementary study to the already published data on molecular dissection of water and glycerol permeability of the PfAQP by mutational analysis (Beitz et al., 2004), here, additional mutants were generated.

Although there is an equal amino acid composition in the pore constriction region in PfAQP and GlpF of *E. coli*, they have different water permeability. Both aquaglyceroporins are glycerol permeable, but PfAQP additionally has a high water permeability.

The PfAQP as an extraordinary aquaglyceroporin was used to study water permeability in aquaglyceroporins. This work showed that the C-loop has an important role in water permeability, precisely Glu125 (Beitz et al., 2004). The mutation E₁₂₅S dramatically reduces water permeability. I succeeded in improving the relative water permeability by making the double mutant PfAQP E₁₂₅S/F₁₉₀Y. By introducing F190Y mutation the polarity in the pore constriction region was increased. Composition of the pore constriction now resembled the aquaglyceroporin AQP3. The presented data suggest that the polarity in the pore constriction region and the possible interaction of C-loop with arginine at the same region might be important for water permeability.

5.2 The influence of different pH values on water and glycerol permeability

The results show that pH shifts between 3 and 7 have no influence on water and glycerol permeability of PfAQP. The idea that low pH values might influence the protonation of Glu125 in the C-loop could not be demonstrated. An explanation can be that the Glu125 is not solvent exposed.

5.3 PfAQP as a conductor for dihydroxyactone and methylglyoxal

Except for water and glycerol aquaporins can be permeable to many other solutes such as C3-C6 polyols and urea (Hansen et al., 2002), ammonia (Jahn et al., 2004), carbon dioxide (Cooper et al., 1998), arsenite (Liu et al., 2002). In mammals, aquaporins are expressed in many epithelia involved in water transport, as well as in cell types which are not predominantly involved in water transport such as skin, or in glycerol transport in hepatocytes and adipocytes.

The complete energy metabolism in *Plasmodium* parasites relies on glucose utilisation. The end product of glucose consumption under anaerobic condition is lactate. Parasitized red blood cells produce 30 times more lactate than uninfected erythrocytes (Vander Jagt et al., 1990). The metabolism of glucose is accompanied to D-lactate production. D-lactate production of the parasites appears to be a defence mechanism to protect the parasite from the toxic methylglyoxal. Formation of methylglyoxal via dihydroxyacetone 3-phosphate as a spontaneous side-reaction of glycolysis becomes physiologically relevant (Vander Jagt et al., 1990). Methylglyoxal as a compound with a keto and an aldehyde group (4.3) is highly reactive and can covalently modify many proteins or even DNA.

DHA can be used as an energy source in erythrocytes after phosphorylation but in its dephosphorylated form it can be toxic. Apparently, plasmodia cannot utilize DHA, possibly due to the lack of a triose kinase.

I showed that PfAQP is permeable to DHA and MG, i.e. two new potentially cytotoxic compounds that permeate aquaporins. They are added to the list of other cytotoxic permeants like arsenite and ammonia.

The permeability of PfAQP for cytotoxic metabolites hints at multiple roles of this aquaglyceroporin possibly in the disposal of compounds which might be harmful for the parasite cell.

Human AQP3, a member of the erythrocyte cell membrane is permeable to DHA but not to MG. DHA is a more polar and more flexible compound compared to MG due to specific structural differences in carbon atom hybridization. In DHA, only C₂ is sp²-hybridized whereas in MG there are two vicinal sp²-hybridized carbons which makes MG a strict hydrogen bond acceptor. DHA might be both, donor and acceptor. This may explain different permeabilities of these compounds which are similar in size, but carry different structural properties.

DHA and MG have an inhibitory effect on parasite growth (**4.4**). Both compounds are highly reactive, and the mode of action might be due to modification of a broad range of proteins.

The obligate dependence of plasmodia on glycolysis for ATP production suggests that the enzymes of the glycolytic pathway can be used as drug targets (Roth et al., 1988; Dobeli et al., 1990).

It was reported that after prolonged treatment of rabbit GAPDH, the key enzyme in glycolysis, with MG in the micromolar range might be inhibited (Lee et al., 2005). The

function of PfGAPDH was fully inhibited after 6 h of treatment with 2.5 mM DHA at 37°C, but MG did not have influence on PfGAPDH activity. An explanation for this might be hidden in differences in the molecular flexibility of these two compounds. DHA, as a more flexible one, might be able to approach a lysine near the active centre of PfGAPDH better than the rigid structure of MG. The active site of PfGAPDH seems to be more protected than that of rabbit GAPDH because of an insertion of two amino acids Lys194-Gly195. The treatment of rabbit GAPDH with 2.5 mM DHA and MG turned out to be different compared to PfGAPDH. Rabbit GAPDH was inhibited by both compounds. Inhibition with DHA was immediate, and slower with MG (complete after 20 h).

Due to the high metabolic flux in plasmodia, there is a high production of MG. Additional supplementation of this compound might overwhelm the defence mechanism and thus be lethal for the parasites. DHA may preferentially act on GAPDH. When the concentration of DHA rises too high this compound might enter the parasite cell and modify GAPDH. Consequently, glycolysis is stopped.

Further, the modification of PfGAPDH by DHA may lead to a rise in glyceraldehyde phosphate concentration, then the accumulation of this compound may increase the spontaneous formation of cytotoxic MG.

In conclusion, small compounds might be used as potential drugs against malaria. However, DHA needs to be used in a concentration which is most likely to high to be applied as the possible drug.

5.4 Characterisation of the *Toxoplasma gondii* aquaglyceroporin

In the *T. gondii* genome I found only one aquaporin. According to sequence analysis, TgAQP has similarity to plant TIP aquaporins. The layout of the pore constriction region is similar to TIP 1;1, especially the presence of a valine instead of the highly conserved arginine.

Inspection of the genome of *T. gondii* showed the presence of plant derived genes in it. TgAQP may be additional evidence for the hypothesis that the phylum *Apicomplexa* originated from an eukaryotic ancestor which acquired a plastid by secondary endosymbiosis probably from an alga.

TgAQP has intermediate water permeability, and rather surprisingly good glycerol permeability. The plant TIP aquaporins are exclusive water channels. Obviously, TgAQP glycerol permeability was gained afterwards.

In the TgAQP open reading frame a possible intron was identified (4.8.1) with classical GT/AG boundaries. The water/glycerol permeability ratio of both possible ORFs TgAQP M1 and TgAQP M39 is the same. The length of the C-terminal part of TgAQP did not influence the water/glycerol ratio. Testing the permeability of different solutes to estimate the size of the TgAQP pore region, TgAQP was mainly permeable for C3 polyols and barely for myo-inositol which is a C₆ cyclic compound. This aquaporin has also high permeability for urea. This information led to idea to test hydroxyurea, an anti-neoplastic compound. TgAQP had good permeability to this anti-neoplastic and toxic agent and may thus represent a path through which parasites take up this drug. Hydroxyurea is a new compound added to the list which pass aquaporins.

5.5 Characterisation of *Trypanosoma brucei* aquaglyceroporin

The characterisation of *T. brucei* aquaporins (TbAQP1-3) showed that the TbAQPs are glycerol transporters with intermediate water permeability in the range of TgAQP and good glycerol permeability in the range of AQP3 and PfAQP. The permeability for different solutes was tested too, an intriguing finding is that all three aquaporins have good permeability for DHA which is even better than the permeability for glycerol.

TbAQPs are differently expressed (Uzcategui et al., 2004) in different life cycle stages. The TbAQP1 is expressed in all phases (logarithmic, static phase in the host blood and in the insect procyclic form). Highest expression of TbAQP1 is during the static phase and it is the only aquaporin expressed in the procyclic form. TbAQP2 is scarcely expressed in all developmental phases where TbAQP2 was detectable only in the blood stream forms of the parasite.

One characteristic of the static phase is glycerol production, and glycerol needs to be exported out of the glycosome because it suppresses ATP production. TbAQP1 is the best glycerol conductor of the three aquaporins expressed in *T. brucei*. Its physiological function might thus be in protection of parasites from detoxification.

Further, DHA turned out to be toxic for *T. brucei* parasites as it is for plasmodia parasites.

5.6 Comparison of the constriction regions of parasite aquaporin pores

Functional characterisation of *T. gondii* and *T. brucei* aquaporins showed that these channels are water and glycerol permeable. Comparing water and glycerol permeability of these aquaporins to PfAQP, glycerol permeability is similar for all of them but PfAQP has strikingly high water permeability. The amino acid composition at the pore entry determined pore selectivity for water and glycerol (solutes) (Tajkhorshid et al., 2002; Beitz et al., 2004). According to the crystal structures of aquaglyceroporin GlpF (Fu et al., 2000) and orthodox aquaporin1 (Walz et al., 1997), the narrowest pore constriction is located in the pore entry region. Thus the amino acid composition in the pore constriction region of TgAQP1 and TbAQP3 is similar to GlpF. The only difference is some additional polarity introduced by the p-hydroxy group of Tyr267 and Tyr250, respectively, in TgAQP1 and TbAQP3 instead of Phe200 in GlpF (Fig. 5.1). The introduction of a polar hydroxyl group in the pore constriction region of TbAQP1 and TbAQP3 might allow water to enter the channel better whereas GlpF has low water permeability (Borgnia et al., 2001). The pore layout of TgAQP1 and TgAQP3 is thus identical to the human AQP3, i.e. an aquaglyceroporin with intermediate water and good glycerol permeability.

The amino acid composition in the pore constriction region of TgAQP and TbAQP2 is similar to the plant TIP1;1 aquaporin. The main characteristic of these plant aquaporins is the presence of a valine instead of a highly conserved arginine. TgAQP and TbAQP2 are both water and glycerol permeable aquaporins whereas the TIP1;1 has only water permeability. The presence of His55 in the pore constriction region of TIP1;1 might be responsible for the exclusion of glycerol permeability by rendering the pore smaller and more polar. In TbAQP2

an isoleucine is present at this position which might make more room for a glycerol molecule to pass.

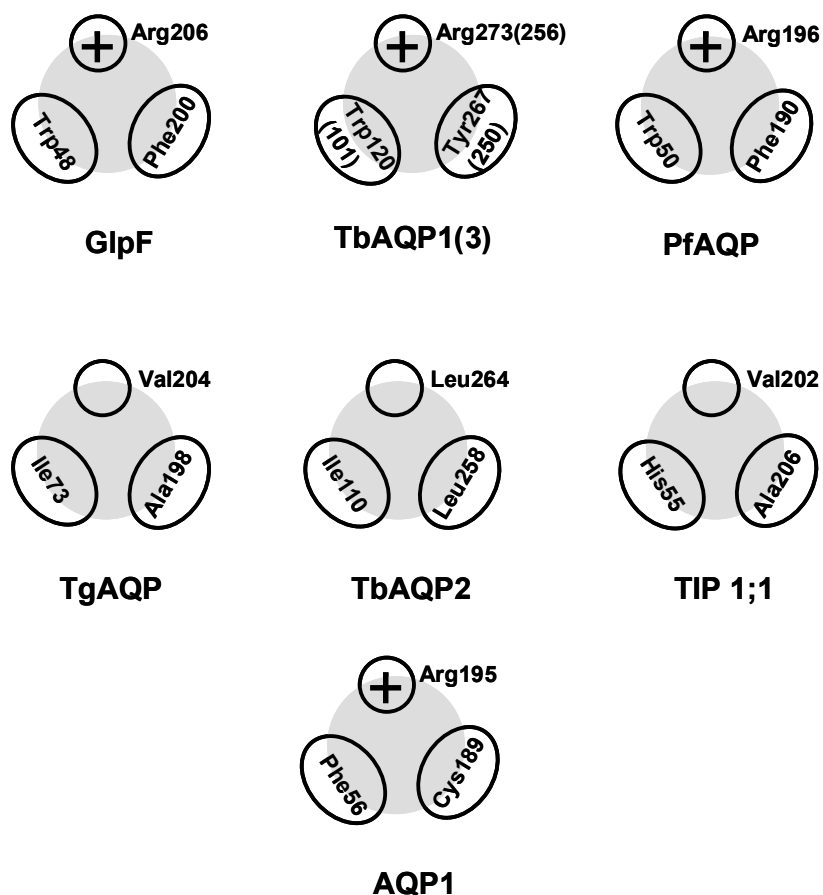


Fig. 5.1 Schematic presentation of the GlpF, TbAQP1-3, PfAQP, TgAQP, TIP 1;1 and human AQP1 pore constriction region

It appears that PfAQP has the widest pore. It allows polyols up to 5 C atoms in back bone to pass. On the first sight, TgAQP aquaporin pore looks wide, it contains Leu204, Ile73 and Ala198 in the pore narrowest region but C₅ polyols barely pass the pore. Similar results were obtained with TbAQPs. Surprisingly, even in the case of TbAQP2, the permeability to urea is very low compared to the other protozoan aquaporins.

However, a simple size selection mechanism cannot explain the differences in water permeability observed within the orthodox aquaporins. The distribution of polarity at the pore constriction region might be responsible for the rate of water flux through an aquaporin channel. The polarity at the pore mouth region of the *E. coli* GlpF is strongly concentrated on Arg206, in PfAQP the polarity of the Arg196 may be neutralised by Glu125 and in orthodox aquaporins such as in AQP1 the polarity of the pore is enhanced by the histidine residue (Beitz et al., 2004).

5.7 Possible physiological functions of protozoan aquaporins

The *Toxoplasma*, *Trypanosoma* and *Plasmodium* parasites are exposed to a high selective pressure and need to adapt to different environments. The transmission of the parasite from the vector to the mammalian host and passage through the kidneys are situations in which the osmotic stress might be coped by water-passing aquaporins.

Aquaglyceroporins may be linked to glycolysis, i.e. the main energy source in protozoan parasites.

During the aerobic stage of the *Trypanosoma* life cycle, glycerol can be used as an energy source (Ryley et al., 1962). In the anaerobic phase glycerol is formed from the glycerol-3-phosphate by glycerol kinase and one ATP molecule is made. Glycerol molecules have to be quickly removed from the cytosol otherwise the production of ATP is decreased or stopped. Addition of 5 mM glycerol to the medium fully inhibits the glycerol growth (Bakker,

2000). This approach was tried as a treatment against *T. brucei*, however unsuccessful. When the treatment with glycerol was stopped, it came to a rebound.

During infection with *P. falciparum* serum glycerol levels in the host rise from 20-60 μM to more than 200 μM (Pukrittayakamee et al., 1994). One fifth of the infected persons develop hypoglycaemia. Here, glucose levels drop down to 2.2 mM what is less than half compared to normal glucose levels (4-6 mM).

It was shown that serum glycerol is used by plasmodia for lipid biosynthesis (Vial, et al., 1989). Hansen et al. (2002) hypothesized that the glycerol which enters the parasite cell through the PfAQP, becomes phosphorylated by glycerol kinase and is used for glycerolipid synthesis. Glycerol-3-phosphate might be oxidised to dihydroxyacetone phosphate and further be used in glycolysis.

My results showed that parasites cannot use the glycerol as the sole energy source. But the addition of glycerol in 11 mM concentration into the medium induced PfQAP expression, probably the glycerol was used for lipid biosynthesis.

In the liver, glycerol 3-phosphate is generated by direct phosphorylation of glycerol while in the muscles and adipocytes, it is generated by reducing dihydroxyacetone phosphate with NADH. In adipocytes and muscles, glycerol-3-phosphate dehydrogenase (GPDH) (EC.1.1.1.8) is found in the cytosol and another GPDH (EC. 1.1.99.5) using FAD as a coenzyme is responsible for the reverse reaction of glycerol 3-phosphate to dihydroxyacetone phosphate in mitochondria (Kozak et al., 1974; Kuri-Harcuch et al.; Garrib et al., 1986). The *Arabidopsis thaliana* contains both NAD^+ and FAD^+ dependent GPDH. However, the NAD^+ dependent GPDH is less likely to play a role in glycerol dissimilation as the equilibrium constant favours the synthesis of glycerol 3-phosphate (Eastmond et al., 2004). *P. falciparum* GPDH is still not characterised, but it might be that the reduction of

DHAP is favoured by the GPDH and it might be the reason why glycerol cannot be used as an energy source.

Due to the high protein degradation in the parasite food vacuole, high level of toxic ammonia might be produced. Secondly, the parasite medium is in reached with 2 mM L-glutamine, which might be source of ammonia too. The rate of ammonia production in 1 l parasite culture is 0.022 mmoles per hour. In 4.2 min parasites can reach IC_{50} value of ammonium toxic concentration and further production without excretion of toxic compounds might lead parasites to death.

The possible causes of ammonia toxicity might be in changing the pH value in food vacuole, as the weak base it can rise, the pH value and inhibit the proteases. Rapid export of toxic ammonia is needed. Thus, PfAQP is a good candidate for ammonia export from the cell.

5.8 Remaining questions

The physiological function of characterised *Plasmodium*, *Toxoplasma* and *Trypanosoma* aquaporins is still uncertain. Knocking-out the genes of aquaporins in these parasites might give an answer whether these aquaporins are important for parasite survival or whether they are needed under stress. Immunochemical localisation of protozoan aquaporins might be helpful too.

The crystallisation of these protozoan aquaporins can give a better picture of the structural impact in water and glycerol permeability and this may ultimately lead to novel approaches in anti-protozoan therapy.

6 Summary

P. falciparum, *T. gondii* and *T. brucei* parasites cause infectious diseases that affect more than 300-400 million people world-wide and, thus, represent a major health problem. The rapid spreading of drug resistant parasite strains initiated the search for new drug targets. Aquaporins at the parasite host interface have the potential to be used as a novel targets.

I characterised biochemically a single *T. gondii* aquaporin (TgAQP) which has only 28% sequence similarity to the *P. falciparum* aquaporin (PfAQP) and 47% sequence similarity to water specific plant aquaporins (TIP 1;1) and three *T. brucei* aquaporins (TbAQP1-3) which show 40-45% similarity to mammalian AQP3.

The pore constriction region of TgAQP has a valine instead of a highly conserved arginine. This exchange is rather typical for above-mentioned plant aquaporins. Thus, it supports the hypothesis that apicomplexans have plant ancestors. TbAQP1 and 3 have a similar amino acid composition in the pore constriction as AQP3. TbAQP2, however, has a leucine instead of the pore arginine, and NSA and NPS motifs instead of the canonical NPA motifs.

I established that TgAQP and the TbAQPs are bifunctional pores with high glycerol and intermediate water permeability whereas in PfAQP both, water and glycerol permeability are high.

Further testing of TgAQP permeability showed that besides urea, which passes the pore equally well as glycerol, only erythritol and D-arabitol reasonably permeate TgAQP. Other larger and/or charged compounds do not pass. Strikingly, hydroxyurea, an anti-neoplastic

agent with an inhibitory effect on parasite proliferation, could be identified as a permeant of TgAQP.

Solute permeability TbAQPs is more restricted. Only TbAQP3 passed erythritol and ribitol well. TbAQP2 showed permeability for pyruvate. All TbAQPs passed urea.

The TbAQPs and PfAQP were further highly permeable for dihydroxyacetone (DHA). I could show that DHA is toxic for plasmodia parasites (IC_{50} 2.5 mM). PfAQP was also tested for methylglyoxal (MG) permeability. MG is a side product of glycolysis and has a similar structure as DHA. MG was conducted by PfAQP and showed a toxic effect on malaria parasites (IC_{50} 200 μ M). *P. falciparum* glyceraldehydes phosphate dehydrogenase (PfGAPDH) was fully inhibited by 2.5 mM DHA after 6 h whereas MG did not have an inhibitory effect. Rabbit GAPDH as a control was fully inhibited by DHA after 3 h and by MG after 20h.

In addition, PfAQP is permeable for ammonia. I showed that one liter of packed plasmodia red cells produces 8.8 mmol of ammonia of ammonia per hour. PfAQP may thus be vital for malaria parasites as a pathway for ammonia release.

7 Zusammenfassung

P. falciparum, *T. gondii* und *T. brucei* Parasiten verursachen Infektionskrankheiten, die mehr als 300-400 Millionen Menschen auf der Welt betreffen und stellen ein großes Gesundheitsproblem dar. Die schnelle Ausbreitung von resistenten Stämmen löste die Suche nach neuen Angriffspunkten für Medikamente aus. Aquaporine im Membransystem zwischen Parasit und Wirt könnten als neue Angriffspunkte für Medikamente genutzt werden.

In der vorliegenden Arbeit wurden ein Aquaporin aus *T. gondii* (TgAQP) sowie drei Aquaporine aus *T. brucei* (TbAQP1-3) biochemisch charakterisiert.

TgAQP zeigt 28% Sequenzähnlichkeit zu dem Aquaglyceroporin aus *P. falciparum* (PfAQP) und 47% Sequenzähnlichkeit zu wasserspezifischen Pflanzenaquaporinen (TIP 1;1). TbAQP1-3 weisen 40-45% Ähnlichkeit zu AQP3 aus Säugern auf.

In der Porenregion von TgAQP, befindet sich ein Valin anstelle eines hochkonservierten Arginins. Dieser Aminosäureaustausch ist typisch für die TIPs der Pflanzen und stützt die Hypothese, dass Apicomplexa pflanzliche Vorfahren haben. TbAQP1 und 3 haben eine ähnliche Aminosäurezusammensetzung der Porenregion wie AQP3 und NPA Motive in der Region, die den Porenengpass bildet. TbAQP2 bildet eine Ausnahme, da es ein Leucin anstelle des Arginins hat und NSA und NPS Motive aufweist.

Es wurde gezeigt, dass TgAQP und TbAQPs bifunktionale Poren sind, die durch eine hohe Permeabilität für Glycerin und eine mittlere Wasserpermeabilität gekennzeichnet sind. PfAQP hingegen hat eine hohe Permeabilität für sowohl Glycerin als auch Wasser.

Die weitere Untersuchung der Permeabilität von TgAQP ergab, dass neben Harnstoff, der die Pore ebenso gut wie Wasser passiert, auch Erythritol und D-Arabitol eine gewisse

Durchgängigkeit besitzen. Für andere Verbindungen, die größer und/oder geladen sind, ist TgAQP nicht durchlässig. Interessanterweise kann Hydroxyharnstoff, ein anti-neoplastischer Wirkstoff, der die Parasitenproliferation inhibiert, durch die Pore dringen.

Die Soluteleitfähigkeit der TbAQPe ist eingeschränkt. Nur TbAQP3 lässt Erythritol und Ribitol passieren. TbAQP2 hat eine geringe Permeabilität für Pyruvat. Alle TbAQPe sind permeabel für Harnstoff.

Sowohl die TbAQPs als auch PfAQP haben eine hohe Durchlässigkeit für Dihydroxyaceton (DHA). Es wurde nachgewiesen, dass DHA für die Plasmodienparasiten toxisch ist (IC_{50} 2,5 mM). PfAQP wurde positiv auf Permeabilität von Methylglyoxal (MG) getestet. MG ist ein Nebenprodukt der Glykolyse und hat eine ähnliche Struktur wie DHA. Das von PfAQP eingeschleuste DHA wirkte toxisch auf die Malariaparasiten (IC_{50} 200 μ M). Des Weiterem wurde die Auswirkung von 2,5 mM DHA bzw. MG auf *P. falciparum* Glycerolaldehyd-Dehydrogenase (PfGAPDH) untersucht. PfGAPDH wird nach 6 h vollständig von DHA inhibiert, wohingegen MG keinen inhibitorischen Effekt zeigt. Als Kontrolle wurde GAPDH aus dem Kaninchen verwendet, das von DHA nach 3 h und von MG nach 20 h vollständig inhibiert wird.

PfAQP ist auch durchlässig für Ammoniak. Es wurde gezeigt, dass ein Liter gepackter malariainfizierter Erythrozyten 8,8 mmol Ammoniak pro Stunde produzieren. PfAQP könnte demnach überlebenswichtig für *Plasmodien* sein und als Anlass für Ammoniak fungieren.

8 References

Bakker, B. M., Michels, P. A., Opperdoes, F. R., Westerhoff, H. V. (1997). "Glycolysis in bloodstream form *Trypanosoma brucei* can be understood in terms of the kinetics of the glycolytic enzymes." J Biol Chem **272**(6): 3207-15.

Bakker, B. M. W., H. V., Opperdoes, F. R., Michels, P. A. (2000). "Metabolic control analysis of glycolysis in trypanosomes as an approach to improve selectivity and effectiveness of drugs." Mol Biochem Parasitol **106**(1): 1-10.

Baldauf S.L., R. A. J., Wenk-Siefert I., Doolittle W.F. (2000). "A kingdom-level phylogeny of eukaryotes based on combined protein data." Science **290**(5493): 972-7.

Beitz, E. (2005). "Aquaporins from pathogenic protozoan parasites: structure, function and potential for chemotherapy." Biol Cell **97**(6): 373-83.

Beitz, E., Pavlovic-Djuranovic, S., Yasui, M., Agre, P., Schultz, J. E. (2004). "Molecular dissection of water and glycerol permeability of the aquaglyceroporin from *Plasmodium falciparum* by mutational analysis." Proc Natl Acad Sci U S A **101**(5): 1153-8.

Borgnia, M., Nielsen, S., Engel, A., Agre, P. (1999). "Cellular and molecular biology of the aquaporin water channels." Annu Rev Biochem **68**: 425-58.

Borgnia, M. J., Agre, P. (2001). "Reconstitution and functional comparison of purified GlpF and AqpZ, the glycerol and water channels from *Escherichia coli*." Proc Natl Acad Sci U S A **98**(5): 2888-93.

Carbrey, J. M., Gorelick-Feldman, D. A., Kozono, D., Praetorius, J., Nielsen, S., Agre, P. (2003). "Aquaglyceroporin AQP9: solute permeation and metabolic control of expression in liver." Proc Natl Acad Sci U S A **100**(5): 2945-50.

d

Clayton, C. E., Michels, P. (1996). "Metabolic compartmentation in African trypanosomes." Parasitol Today **12**(12): 465-71.

D

Cooper, G. J., Boron, W. F. (1998). "Effect of PCMBs on CO₂ permeability of *Xenopus oocytes* expressing aquaporin 1 or its C189S mutant." Am J Physiol **275**(6 Pt 1): C1481-6.

Cowan-Jacob, S. W., Kaufmann, M., Anselmo, A. N., Stark, W., Grutter, M. G. (2003). "Structure of rabbit-muscle glyceraldehyde-3-phosphate dehydrogenase." Acta Crystallogr D Biol Crystallogr **59**(Pt 12): 2218-27.

- Daubenberger, C. A. P.-F., F. Jiang, G. Lipp, J. Certa, U. Pluschke, G.** (2000). "Identification and recombinant expression of glyceraldehyde-3-phosphate dehydrogenase of *Plasmodium falciparum*." Gene **246**(1-2): 255-64.
- Dobeli, H., Trzeciak, A., Gillessen, D., Matile, H., Srivastava, I. K., Perrin, L. H., Jakob, P. E., Certa, U.** (1990). "Expression, purification, biochemical characterization and inhibition of recombinant *Plasmodium falciparum* aldolase." Mol Biochem Parasitol **41**(2): 259-68.
- Dzierszinski, F., Popescu, O., Tourse, C., Slomianny, C., Yahiaoui, B., Tomavo, S.** (1999). "The protozoan parasite *Toxoplasma gondii* expresses two functional plant-like glycolytic enzymes. Implications for evolutionary origin of apicomplexans." J Biol Chem **274**(35): 24888-95.
- Eastmond, P. J.** (2004). "Glycerol-insensitive Arabidopsis mutants: gli1 seedlings lack glycerol kinase, accumulate glycerol and are more resistant to abiotic stress." Plant J **37**(4): 617-25.
- Engel, A., Fujiyoshi, Y., Agre, P.** (2000). "The importance of aquaporin water channel protein structures." EMBO J **19**(5): 800-6.
- Francis, S. E., Sullivan, D. J., Jr., Goldberg, D. E.** (1997). "Hemoglobin metabolism in the malaria parasite *Plasmodium falciparum*." Annu Rev Microbiol **51**: 97-123.
- Fu, D., Libson, A., Miercke, L. J., Weitzman, C., Nollert, P., Krucinski, J., Stroud, R. M.** (2000). "Structure of a glycerol-conducting channel and the basis for its selectivity." Science **290**(5491): 481-6.
- Garrig, A. and W. C. McMurray** (1986). "Purification and characterization of glycerol-3-phosphate dehydrogenase (flavin-linked) from rat liver mitochondria." J Biol Chem **261**(17): 8042-8.
- Ginsburg, H.** (2002). "Abundant proton pumping in *Plasmodium falciparum*, but why?" Trends Parasitol **18**(11): 483-6.
- Hansen, M. K., J. F. Schultz, J. E. Beitz, E.** (2002). "A single, bi-functional aquaglyceroporin in blood-stage *Plasmodium falciparum* malaria parasites." J Biol Chem **277**(7): 4874-82.
- Heymann, J. B., Engel, A.** (1999). "Aquaporins: Phylogeny, Structure, and Physiology of Water Channels." News Physiol Sci **14**: 187-193.
- Holm, L. M., Jahn, T. P., Moller, A. L., Schjoerring, J. K., Ferri, D., Klaerke, D. A., Zeuthen, T.** (2005). "NH₃ and NH₄⁺ permeability in aquaporin-expressing *Xenopus oocytes*." Pflugers Arch **450**(6): 415-28.
- Inger Ljungström, H. P., Martha Schlichtherle, Arthur Scherf, Mats Wahlgren** (2004). Methods in Malaria Research. Manassas.

- Jahn, T. P. M., A. L. Zeuthen, T. Holm, L. M. Klaerke, D. A. Mohsin, B. Kuhlbrandt, W. Schjoerring, J. K.** (2004). "Aquaporin homologues in plants and mammals transport ammonia." FEBS Lett **574**(1-3): 31-6.
- Jung, J. S., Preston, G. M., Smith, B. L., Guggino, W. B., Agre, P** (1994). "Molecular structure of the water channel through aquaporin CHIP. The hourglass model." J Biol Chem **269**(20): 14648-54.
- Kozak, L. P. and J. T. Jensen** (1974). "Genetic and developmental control of multiple forms of L-glycerol 3-phosphate dehydrogenase." J Biol Chem **249**(24): 7775-81.
- Kuri-Harcuch, W., L. S. Wise, Green, H.** (1978). "Interruption of the adipose conversion of 3T3 cells by biotin deficiency: differentiation without triglyceride accumulation." Cell **14**(1): 53-9.
- Lambros, C. V., J. P.** (1979). "Synchronization of *Plasmodium falciparum* erythrocytic stages in culture." J Parasitol **65**(3): 418-20.
- Lee, H. J. H., S. K. Sanford, R. J. Beisswenger, P. J.** (2005). "Methylglyoxal can modify GAPDH activity and structure." Ann N Y Acad Sci **1043**: 135-45.
- Liu, Z., Shen, J., Carbrey, J. M., Mukhopadhyay, R., Agre, P., Rosen, B. P.** (2002). "Arsenite transport by mammalian aquaglyceroporins AQP7 and AQP9." Proc Natl Acad Sci U S A **99**(9): 6053-8.
- Marini, A. M., Soussi-Boudekou, S., Vissers, S., Andre, B.** (1997). "A family of ammonium transporters in *Saccharomyces cerevisiae*." Mol Cell Biol **17**(8): 4282-93.
- Michels, P. A.** (1988). "Compartmentation of glycolysis in trypanosomes: a potential target for new trypanocidal drugs." Biol Cell **64**(2): 157-64.
- Noedl, H. W., W. H. Miller, R. S. Wongsrichanalai, C.** (2002). "Histidine-rich protein II: a novel approach to malaria drug sensitivity testing." Antimicrob Agents Chemother **46**(6): 1658-64.
- Oya, T., Hattori, N., Mizuno, Y., Miyata, S., Maeda, S., Osawa, T., Uchida, K.** (1999). "Methylglyoxal modification of protein. Chemical and immunochemical characterization of methylglyoxal-arginine adducts." J Biol Chem **274**(26): 18492-502.
- Parsons, M.** (2004). "Glycosomes: parasites and the divergence of peroxisomal purpose." Mol Microbiol **53**(3): 717-24.
- Phillips, S. A., Thornalley, P. J.** (1993). "Formation of methylglyoxal and D-lactate in human red blood cells in vitro." Biochem Soc Trans **21**(2): 163S.
- Preston, G. M., Carroll, T. P., Guggino, W. B., Agre, P.** (1992). "Appearance of water channels in *Xenopus oocytes* expressing red cell CHIP28 protein." Science **256**(5055): 385-7.

- Pukrittayakamee, S., White, N. J., Davis, T. M., Supanaranond, W., Crawley, J., Nagachinta, B., Williamson, D. H.** (1994). "Glycerol metabolism in severe falciparum malaria." Metabolism **43**(7): 887-92.
- Roos, D. S.** (2005). "Genetics. Themes and variations in apicomplexan parasite biology." Science **309**((5731)): 72-3.
- Roth, E. F., Jr., Calvin, M. C., Max-Audit, I., Rosa, J., Rosa, R.** (1988). "The enzymes of the glycolytic pathway in erythrocytes infected with *Plasmodium falciparum* malaria parasites." Blood **72**(6): 1922-5.
- Ryley, J. F.** (1962). "Studies on the metabolism of the protozoa. 9. Comparative metabolism of blood-stream and culture forms of *Trypanosoma rhodesiense*." Biochem J **85**: 211-23.
- Satchell, J. F., Malby, R. L., Luo, C. S., Adisa, A., Alpyurek, A. E., Klonis, N., Smith, B. J., Tilley, L., Colman, P. M.** (2005). "Structure of glyceraldehyde-3-phosphate dehydrogenase from *Plasmodium falciparum*." Acta Crystallogr D Biol Crystallogr **61**(Pt 9): 1213-21.
- Sirover, M. A.** (1999). "New insights into an old protein: the functional diversity of mammalian glyceraldehyde-3-phosphate dehydrogenase." Biochim Biophys Acta **1432**(2): 159-84.
- Taguchi, T. M., S. Miwa, I.** (2002). "Glyceraldehyde metabolism in human erythrocytes in comparison with that of glucose and dihydroxyacetone." Cell Biochem Funct **20**(3): 223-6.
- Tajkhorshid, E., Nollert, P., Jensen, M. O., Miercke, L. J., O'Connell, J., Stroud, R. M., Schulten, K.** (2002). "Control of the selectivity of the aquaporin water channel family by global orientational tuning." Science **296**(5567): 525-30.
- Trager, W. J., J. B.** (1976). "Human malaria parasites in continuous culture." Science **193**(4254): 673-5.
- Tsukaguchi, H., Shayakul, C., Berger, U. V., Mackenzie, B., Devidas, S., Guggino, W. B., van Hoek, A. N., Hediger, M. A.** (1998). "Molecular characterization of a broad selectivity neutral solute channel." J Biol Chem **273**(38): 24737-43.
- Uzcategui, N. L., Szallies, A., Pavlovic-Djuranovic, S., Palmada, M., Figarella, K., Boehmer, C., Lang, F., Beitz, E., Duszenko, M.** (2004). "Cloning, heterologous expression, and characterization of three aquaglyceroporins from *Trypanosoma brucei*." J Biol Chem **279**(41): 42669-76.
- Vander Jagt, D. L., Hunsaker, L. A., Campos, N. M., Baack, B. R.** (1990). "D-lactate production in erythrocytes infected with *Plasmodium falciparum*." Mol Biochem Parasitol **42**(2): 277-84.

- Vial, H. J. A., M. L. Thuet, M. J. Philpott, J. R.** (1989). "Phospholipid metabolism in Plasmodium-infected erythrocytes: guidelines for further studies using radioactive precursor incorporation." *Parasitology* **98 Pt 3**: 351-7.
- Walz, T., Hirai, T., Murata, K., Heymann, J. B., Mitsuoka, K., Fujiyoshi, Y., Smith, B. L., Agre, P., Engel, A.** (1997). "The three-dimensional structure of aquaporin-1." *Nature* **387(6633)**: 624-7.
- Yayon, A., Cabantchik, Z. I., Ginsburg, H.** (1984). "Identification of the acidic compartment of *Plasmodium falciparum*-infected human erythrocytes as the target of the antimalarial drug chloroquine." *Embo J* **3(11)**: 2695-700.
- Zardoya, R.** (2005). "Phylogeny and evolution of the major intrinsic protein family." *Biol Cell* **97(6)**: 397-414.

Meine akademischen Lehrer neben PD Dr. E. Beitz und Prof. Dr. J.E. Schultz waren die Damen und Herren Professoren und Doktoren:

Vuckovic, G.	Anorganische Chemie I
Pavlovic, V.	Organische Chemie I/ Organische Chemie II
Tesic, Z.	Analytische Chemie I
Bukvic, S.	Physik
Vrecica, S.	Mathematik
Popovic, O.	Englisch I/ Englisch II
Serban, N.	Biologie
Konjevic, R.	Physikalische Chemie
Niketic, S.	Anorganische Chemie II
Micovic, Lj.	Organische Chemie III
Jankov, R.M.	Naturstoff-Chemie/Immunochemie
Niketic, V.	Biochemie I
Todorovic, M.	Analytisch Chemie II
Vajs, V.	Strukturaufklärung
Matic, G.	Biochemie II
Petrovic, Dj.	Enzymatik I
Spasic, M.	Biochemie III
Vucetic, J.	Mikrobiologie und Mikrobiologische Chemie/Biothechnologie
Soskic, V.	Experimental biochemistry
Romac, S.	Molekularbiologie
Tomic, M.	Enzymatik II
Davidovic, V.	Physiologie
Kataranovska, M.	Immunobiologie
Nedic, O.	Pathobiochemie
Vasiljevic, B.	Molekulare Genetik/Molecularbiologie von Krebszellen
Milojkovic-Opsenica, D.	Statistik
Milosavljevic, S.	Chemie der Sekundärmetaboliten
Duscenko, M.	Biochemie

LEBENS LAUF

Zur Person		Slavica Pavlovic-Djuranovic Geboren am 5. Januar 1974 in Prokuplje Serbien und Montenegro
Schulbildung	9/1981-6/1989 9/1989-6/1993	Grundschule Rados Jovanovic-Selja, Gymnasium, Kursumlija, Serbien und Montenegro
Studium	10/1993- 23.11/1999	Studium der Biochemie an der Fakultät für Chemie der Universität Belgrad in Serbien und Montenegro
	11/1999- 02.07/2001	Vertiefungsfach Organische Chemie an der Fakultät für Chemie der Universität Belgrad in Serbien und Montenegro
Praktische Ausbildung	11/2001-10/2002	gearbeitet in der Kinderklinik in Podgorica, Serbien und Montenegro
Promotion	10/2002 - 03/2004	Durchführung des experimentellen Teils der vorliegenden Arbeit „ <i>Funktionelle Charakterisierung von Aquaporinen aus Plasmodium falciparum, Toxoplasma gondii und Trypanosoma brucei</i> “ am Pharmazeutisches Institut der Eberhard- Karls-Universität Tübingen unter der Anleitung von PD Dr. Eric Beitz und Prof. Dr. J.E. Schultz.